

Julius-Maximilians-Universität Würzburg



**Studies on the role of calcium channels and the kinase domain of
transient receptor potential melastatin-like 7 (TRPM7) in platelet
function**

**Studien über die Rolle von Calcium Kanälen und der Kinase
Dömane von *transient receptor potential melastatin-like 7* (TRPM7)
für die Thrombozytenfunktion**

**Doctoral thesis for a doctoral degree
at the Graduate School of Life Sciences,
Julius-Maximilians-Universität Würzburg,
Section Biomedicine**

submitted by

Wenchun Chen

from

Fujian, China

Würzburg, 2014

Submitted on:

Members of the *Promotionskomitee*:

Chairperson:

Primary Supervisor: Prof. Dr. Bernhard Nieswandt

Supervisor (Second): Prof. Dr. Guido Stoll

Supervisor (Third): Prof. Dr. Manfred Gessler

Date of Public Defence:

Date of Receipt of Certificates:

SUMMARY

Platelet activation and aggregation are essential processes for the sealing of injured vessel walls and preventing blood loss. Under pathological conditions, however, platelet aggregation can lead to uncontrolled thrombus formation, resulting in irreversible vessel occlusion. Therefore, precise regulation of platelet activation is required to ensure efficient platelet plug formation and wound sealing but also to prevent uncontrolled thrombus formation. Rapid elevations in the intracellular levels of cations are a core signaling event during platelet activation. In this thesis, the roles of Ca^{2+} and Mg^{2+} channels in the regulation of platelet function were investigated.

Orai1, the major *store-operated calcium* (SOC) channel in platelets, is not only vital for diverse signaling pathways, but may also regulate *receptor-operated calcium entry* (ROCE). The coupling between the Orai1 signalosome and *canonical transient receptor potential channel* (TRPC) isoforms has been suggested as an essential step in the activation of *store-operated calcium entry* (SOCE) and ROCE in human platelets. However, the functional significance of the biochemical interaction between Orai and TRPC isoforms still remains to be answered. In the first part of this thesis, the functional crosstalk between Orai1 and TRPC6 was addressed. Orai1-mediated SOCE was found to enhance the activity of *phospholipases* (PL) C and D, to increase *diacylglycerol* (DAG) production and finally to regulate TRPC6-mediated ROCE via DAG, indicating that the regulation of TRPC6 channel activity seems to be independent of the physical interaction with Orai1. Furthermore, Orai1 and TRPC6 double deficiency led to a reduced Ca^{2+} store content and basal cytoplasmic Ca^{2+} concentrations, but surprisingly also enhanced ATP secretion, which may enhance Ca^{2+} influx via P2X_1 and compensate for the severe Ca^{2+} deficits seen in double mutant platelets. In addition, Orai1 and TRPC6 were not essential for *G protein-coupled receptor* (GPCR)-mediated platelet activation, aggregation and thrombus formation.

Transient receptor potential melastatin-like 7 (TRPM7) contains a cytosolic serine/threonine protein kinase. To date, a few *in vitro* substrates of the TRPM7 kinase have been identified, however, the physiological role of the kinase remains unknown. In the second part of this thesis, mice with a point mutation which blocks the catalytic activity of the TRPM7 kinase (*Trpm7^{Kl}*) were used to study the role of the TRPM7 kinase in platelet function. In *Trpm7^{Kl}* platelets *phosphatidylinositol-4,5-bisphosphate* (PIP_2) metabolism and Ca^{2+} mobilization were severely impaired upon *glycoprotein* (GP) VI activation, indicating that the TRPM7 kinase regulates PLC function. This signaling defect in *Trpm7^{Kl}* platelets resulted in impaired aggregate formation under flow and protected animals from arterial thrombosis and ischemic brain infarction. Altogether, these results highlight the kinase domain of TRPM7 as a pivotal signaling moiety implicated in the pathogenesis of thrombosis and cerebrovascular events.

Zusammenfassung

Die Aktivierung und Aggregation von Thrombozyten sind zwei elementare Prozesse für das Abdichten verletzter Gefäßwände und damit zur Verhinderung von exzessivem Blutverlust. Unter pathologischen Bedingungen kann die Thrombozytenaggregation jedoch zur unkontrollierten Thrombusbildung und folglich zum irreversiblen Gefäßverschluss führen. Daher ist eine präzise Regulation der Thrombozytenaktivierung wichtig, um effizient Gefäßverletzungen zu schließen aber gleichzeitig eine unkontrollierte Thrombusbildung zu verhindern. Schnelle Veränderungen der zytoplasmatischen Konzentration von Kationen stellen ein Kernelement der Signaltransduktion während der Plättchenaktivierung dar. In dieser Arbeit wurden die Rolle von Ca^{2+} und Mg^{2+} Kanälen in der Regulation der Thrombozytenfunktion untersucht.

Orai1, der bedeutendste *store-operated calcium* (SOC) Kanal in Thrombozyten, ist nicht nur entscheidend für verschiedene Signalwege, sondern reguliert möglicherweise auch *receptor-operated calcium entry* (ROCE). Die Kopplung zwischen dem Orai1-Signalkomplex und *canonical transient receptor potential channel* (TRPC) Isoformen wurde als entscheidender Schritt in der Aktivierung von *store-operated calcium entry* (SOCE) und ROCE in humanen Thrombozyten vermutet. Die Frage nach der funktionellen Relevanz der Interaktion zwischen Orai und TRPC Isoformen blieb jedoch unbeantwortet. Im ersten Teil dieser Arbeit wurde der funktionelle *Crosstalk* zwischen Orai1 und TRPC6 adressiert. Hierbei zeigte sich, dass Orai1-vermittelter SOCE die Aktivität der Phospholipasen (PL) C und D steigert, die *Diacylglycerol* (DAG) Produktion verstärkt und schließlich TRPC6-vermittelten ROCE via DAG reguliert, was darauf hindeutet, dass die Regulation der TRPC6 Kanalaktivität unabhängig von einer direkten Interaktion mit Orai1 zu sein scheint. Darüber hinaus führte die Doppeldefizienz von Orai1 und TRPC6 zu verringerten Ca^{2+} Konzentrationen in intrazellulären Ca^{2+} -Speichern und im Zytoplasma der Thrombozyten. Überraschenderweise war auch die ATP-Sekretion erhöht, was eventuell den Ca^{2+} -Einstrom durch P2X_1 verstärkt und möglicherweise das starke Ca^{2+} -Defizit in den doppeldefizienten Thrombozyten kompensiert. Außerdem wurde gezeigt, dass Orai1 und TRPC6 nicht für die Aktivierung und Aggregation von Thrombozyten sowie für die Thrombusbildung mittels *G protein-gekoppelter Rezeptoren* (GPCR) benötigt werden.

Transient receptor potential melastatin-like 7 (TRPM7) enthält eine zytosolische Serin/Threonin-Kinase Domain. Bislang wurden zwar wenige *in vitro* Substrate der TRPM7 Kinase identifiziert, jedoch ist die physiologische Rolle dieser Kinase immer noch unbekannt. Im zweiten Teil dieser Arbeit wurden Mäuse mit einer Punktmutation, welche die katalytische Aktivität der TRPM7 Kinase blockiert (*Trpm7^{K1}*) eingesetzt um die Rolle der TRPM7 Kinase für die Funktion von Thrombozyten zu untersuchen. In *Trpm7^{K1}*

Thrombozyten war der Metabolismus von *phosphatidylinositol-4,5-bisphosphat* (PIP₂) und die Ca²⁺-Mobilisierung nach Aktivierung des Rezeptors Glykoprotein (GP) VI schwer beeinträchtigt, was darauf hindeutet, dass die Aktivität der TRPM7 Kinase die Funktion der PLC reguliert. Aus diesem Signaltransduktionsdefekt in *Trpm7^{KI}* Thrombozyten resultierte eine verringerte Aggregatbildung unter Flussbedingungen und ein Schutz der Tiere vor arteriellen Thrombosen und ischämischem Schlaganfall. Zusammenfassend heben diese Ergebnisse die Kinasedomäne von TRPM7 als einen ausschlaggebenden Bestandteil in Signalkaskaden hervor und implizieren eine Rolle dieser Domäne in der Pathogenese von ischämischen Kardio- und zerebrovaskulären Erkrankungen.

TABLE OF CONTENTS

1	INTRODUCTION	1
1.1	Platelets	1
1.2	Platelet activation and thrombus formation	1
1.3	Signaling events during platelet activation	3
1.4	Calcium signaling in platelets	5
1.4.1	Store-operated calcium entry.....	7
1.4.1.1	STIM1	7
1.4.1.2	Orai1	8
1.4.1.3	Coupling machinery of STIM1 and Orai1	8
1.4.1.4	Orai1 is the major SOC channel in mouse platelets	9
1.4.2	Receptor-operated calcium entry.....	10
1.4.2.1	Phospholipase-mediated DAG production.....	10
1.4.2.2	TRPC6.....	10
1.4.2.3	P2X ₁	11
1.4.3	Crosstalk between Orai1 and TRPC6.....	11
1.5	The role of magnesium in platelets.....	12
1.5.1	Mechanisms of Mg ²⁺ influx	12
1.5.2	The role of TRPM6 and TRPM7 channels in Mg ²⁺ homeostasis.....	14
1.5.3	TRPM7	15
1.5.3.1	The physiological role of TRPM7 protein	15
1.5.3.2	The kinase domain of TRPM7	16
1.6	AIM OF THE STUDY	17
2	MATERIALS AND METHODS	18
2.1	Materials.....	18
2.1.1	Chemicals and reagents.....	18
2.1.2	Antibodies.....	21
2.1.2.1	Purchased primary and secondary antibodies.....	21
2.1.2.2	Monoclonal antibodies (mAbs) used for flow cytometry.....	22
2.1.3	Mice	22
2.1.4	Buffers and media	23

2.2	Methods	26
2.2.1	RNA isolation and reverse transcription PCR (RT-PCR).....	26
2.2.2	Mouse Genotyping	28
2.2.2.1	Mouse DNA isolation	28
2.2.2.2	Detection of the <i>Trpc6</i> ^{-/-} by PCR	28
2.2.2.3	Detection of the <i>Orai1</i> ^{-/-} by PCR	29
2.2.2.4	Detection of the <i>Trpm7</i> ^{KI} by PCR.....	31
2.2.3	Fetal liver cell or bone marrow transplantation	31
2.2.4	Tyrosine phosphorylation assay	32
2.2.5	Cell cultures, transient expression.....	32
2.2.6	Electrophysiology	32
2.2.7	Determination of Mg ²⁺ levels in the serum and bones	33
2.2.8	<i>In vitro</i> analysis of platelet function.....	33
2.2.8.1	Platelet preparation and washing	33
2.2.8.2	Platelet counting	33
2.2.8.3	Flow cytometry	33
2.2.8.4	Determination of phosphatidylserine exposure by flow cytometry	35
2.2.8.5	Aggregometry	35
2.2.8.6	Adhesion under flow conditions	35
2.2.8.7	Determination of PS exposing platelets after perfusion	36
2.2.8.8	Intracellular Ca ²⁺ measurements	36
2.2.8.9	Measurement of ATP release	36
2.2.8.10	Measurement of <i>inositol 1 phosphate</i> (IP ₁).....	36
2.2.8.11	Measurement of <i>thromboxane B₂</i> (TxB ₂) release	37
2.2.8.12	Measurement of serotonin release	37
2.2.8.13	Measurement of PLD activity.....	37
2.2.8.14	Spreading assay.....	37
2.2.8.15	Fluorescence microscopy of platelets.....	38
2.2.9	<i>In vivo</i> analysis of platelet function	38
2.2.9.1	Platelet life span	38
2.2.9.2	Tail bleeding time assay	38
2.2.9.3	Intravital microscopy of thrombus formation in FeCl ₃ -injured mesenteric arterioles.....	39
2.2.9.4	Mechanical injury of the abdominal aorta	39

2.2.9.5	<i>Transient middle cerebral artery occlusion (tMCAO) model</i>	39
2.2.9.6	<i>Magnetic resonance imaging (MRI)</i>	40
2.2.9.7	Platelet transfusion	40
2.3	Data analysis.....	40
3	RESULTS.....	41
3.1	Functional crosstalk between Orai1 and TRPC6.....	41
3.1.1	TRPC6 contributes to TG-induced SOCE and regulates Ca ²⁺ store content together with Orai1	41
3.1.2	Orai1 regulates TG-induced phospholipase activity	43
3.1.3	Platelet agonists can activate PLC and PLD independently of Orai1	45
3.1.4	TxA ₂ -induced second phase of Ca ²⁺ signaling is controlled by Orai1	46
3.1.5	Normal platelet count, size and glycoprotein expression in <i>Orai1^{-/-}/Trpc6^{-/-}</i> platelets	47
3.1.6	Defective platelet activation in response to the GPVI agonists, but normal responses to the GPCR agonists in <i>Orai1^{-/-}/Trpc6^{-/-}</i> platelets	48
3.1.7	Defective aggregation in response to the GPVI agonists in <i>Orai1^{-/-}/Trpc6^{-/-}</i> platelets	49
3.1.8	<i>Orai1^{-/-}/Trpc6^{-/-}</i> platelets display normal spreading on fibrinogen.....	50
3.1.9	Normal <i>in vivo</i> thrombus formation in <i>Orai1^{-/-}/Trpc6^{-/-}</i> mice.....	51
3.1.10	Enhanced <i>ex vivo</i> thrombus formation, but reduced PS exposure in <i>Orai1^{-/-}/Trpc6^{-/-}</i> platelets	52
3.1.11	Enhanced ATP secretion in <i>Orai1^{-/-}/Trpc6^{-/-}</i> platelets in response to GPCR agonists	53
3.2	The role of the TRPM7 kinase in mouse platelets	55
3.2.1	Impaired Ca ²⁺ homeostasis in the presence of high levels of extracellular Mg ²⁺	55
3.2.2	Inhibiting effects of high extracellular Mg ²⁺ concentrations on platelet activation	56
3.2.3	TRPM7 is expressed in mouse platelets	58
3.2.4	Generation of TRPM7 "kinase-dead" mice <i>Trpm7^{KI}</i>	58
3.2.5	Normal TRPM7 channel activity in <i>Trpm7^{KI}</i> mice	59
3.2.6	TRPM7 kinase function is dispensable for platelet generation	60
3.2.7	Impaired PLC γ 2-ITAM-mediated and partially defective PLC β -GPCR-	

mediated activation in <i>Trpm7^{Kl}</i> platelets	62
3.2.8 <i>Trpm7^{Kl}</i> platelets display normal spreading on fibrinogen	63
3.2.9 Impaired dense granule secretion in <i>Trpm7^{Kl}</i> platelets	64
3.2.10 The TRPM7 kinase regulates PL-mediated Ca ²⁺ responses in platelets	65
3.2.11 Normal GPVI-induced tyrosine phosphorylation in <i>Trpm7^{Kl}</i> platelets.....	67
3.2.12 <i>Trpm7^{Kl}</i> platelets exhibit impaired procoagulant activity	68
3.2.13 Impaired thrombus formation of <i>Trpm7^{Kl}</i> platelets on collagen under flow conditions	68
3.2.14 Impaired arterial thrombus formation and hemostasis in <i>Trpm7^{Kl}</i> mice ...	69
3.2.15 The TRPM7 kinase plays an important role in ischemic stroke	71
4 DISCUSSION	73
4.1 Functional crosstalk between Orai1-mediated SOCE and TRPC6-mediated ROCE in mouse platelets	73
4.1.1 Orai1-mediated SOCE indirectly regulates TRPC6-mediated ROCE	73
4.1.2 Orai1 together with TRPC6 regulates store content	76
4.1.3 Enhanced ATP secretion in response to the GPCR agonists in <i>Orai1^{-/-}</i> <i>/Trpc6^{-/-}</i> platelets	77
4.2 The role of the TRPM7 kinase in mouse platelets	78
4.2.1 Normal Mg ²⁺ homeostasis and TRPM7 channel activity in <i>Trpm7^{Kl}</i> mice	78
4.2.2 The TRPM7 kinase regulates the enzymatic activity of phospholipase ...	78
4.2.3 The TRPM7 kinase plays an important role in thrombosis, hemostasis and stroke.....	80
4.3 Concluding remarks	81
4.4 Perspective.....	82
5 REFERENCES	83
6 APPENDIX	100
6.1 Abbreviation	100
6.2 Curriculum vitae	103
6.3 Publications.....	104
6.3.1 Original articles.....	104
6.3.2 Posters	104

6.4 Acknowledgement.....105

6.5 Affidavit.....107

1 INTRODUCTION

1.1 Platelets

At the end of the eighteenth century, platelets were first described as particles smaller than leukocytes and erythrocytes in the blood system. In the years 1881-1882, Giulio Bizzozzero for the first time discovered the activity of platelets and their physiological function in hemostasis and thrombosis. Over the last 130 years, the understanding of platelets and their important role in hemostasis and thrombosis has remarkably increased.

Platelets are anuclear and discoid-shaped cells, deriving from megakaryocytes. In human blood, the platelet number is about 150,000-350,000 platelets/ μ L and the platelet size is 3-4 μ m in diameter, whereas in mouse blood the platelet count is approximately 1,000,000 platelets/ μ L and the platelet diameter is 1-2 μ m. Platelets have a limited life span in the blood stream. Platelets circulate for about ten and five days in human and mouse, respectively, before they are cleared by the reticulo-endothelial system in spleen and liver. Platelets play an important role in hemostasis. After vessel wall injury, exposed components of the *extracellular matrix* (ECM) trigger platelet activation and adhesion. Activated platelets subsequently release soluble mediators, which together with locally produced thrombin lead to the recruitment of further platelets, thus resulting in the rapid formation of a platelet plug. Platelet plug formation is essential for sealing injured vessel walls and preventing excessive blood loss. However, under pathological conditions, platelet aggregation may lead to uncontrolled thrombus formation, which causes vessel occlusion or embolism, which may result in severe diseases such as myocardial infarction and stroke. These two diseases are the leading causes of death in developed nations.¹

Since platelets have this double-edge sword function, their activation has to be precisely regulated to ensure efficient platelet plug formation and wound sealing but to prevent uncontrolled thrombus formation as well. To maintain this equilibrium, platelets possess various receptors and regulation mechanisms.

1.2 Platelet activation and thrombus formation

After injury of the vessel wall, platelets are activated and thrombi are formed at the sites of injury. This process involves multiple signaling events, which can be divided into three distinct steps: (1) tethering, (2) activation and (3) firm adhesion and thrombus growth (Figure 1-1).

In the first step, platelets initially get in contact with the exposed ECM, which comprises adhesive molecules like collagens, laminins, fibronectin and *von Willebrand Factor* (vWF). This contact is mediated by the interaction between the platelet *glycoprotein* (GP)Ib-IX-V

complex and vWF, which is immobilized on collagen of the ECM.² Under high shear conditions, the GPIb-vWF interaction is insufficient to allow stable adhesion, however it slows the platelets down, resulting in platelets “rolling” on the vessel wall at the site of injury.

Due to the tethering step, platelets have the opportunity to interact with the ECM protein collagen via the platelet-specific immunoglobulin superfamily receptor GPVI.³⁻⁵ This interaction triggers intracellular signaling via the *immunoreceptor tyrosine-based activation motif* (ITAM) and induces an intracellular Ca^{2+} signal, thereby inducing the release of “second wave” mediators, such as *thromboxane A₂* (TxA₂), *adenosine diphosphate* (ADP) and epinephrine. In addition, thrombin is locally produced from the zymogen prothrombin. These “second wave” mediators and thrombin can bind to *G protein-coupled receptors* (GPCRs) and contribute to the full activation of platelets. In addition, the hemITAM receptor *C-type lectin-like receptor 2* (CLEC-2) can trigger platelet activation as well. Recently, podoplanin was proposed to directly bind and activate CLEC-2,⁶ but the physiological ligand of CLEC-2 inducing intravascular platelet activation and thrombus formation still remains largely unknown.⁷ The GPVI-collagen interaction and the GPCR activation trigger an “inside-out” activation of the integrins $\alpha IIb\beta 3$, $\alpha 2\beta 1$, $\alpha 5\beta 1$ and $\alpha 6\beta 1$, which turn from a low- into a high-affinity binding state.

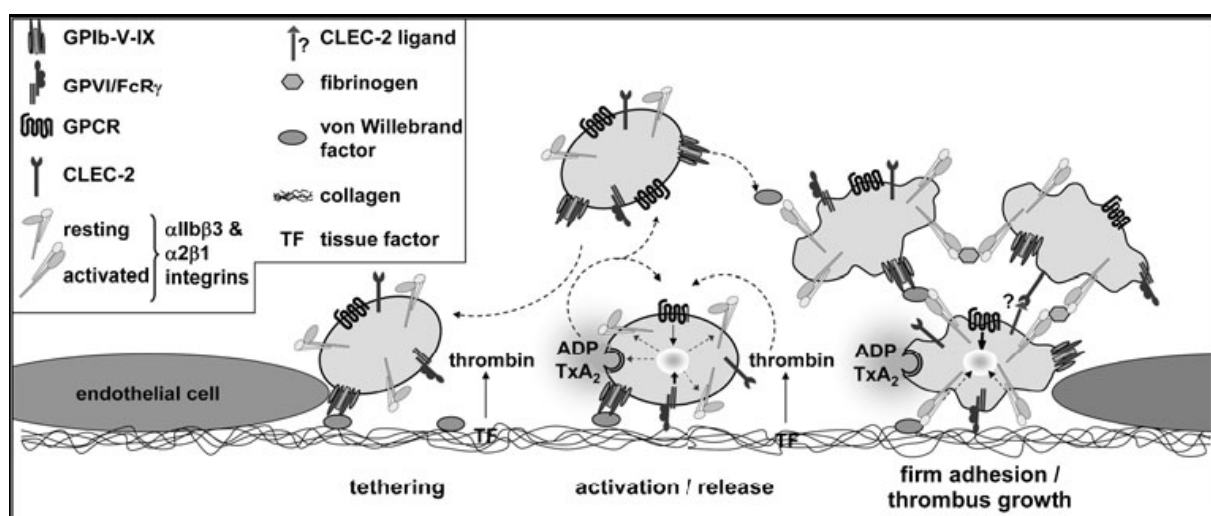


Figure 1-1: Platelet activation and aggregation on the ECM. At sites of vessel wall injury, the GPIb-vWF interaction triggers platelet tethering and enables the close contact of platelets with the ECM. GPVI subsequently binds to collagen, resulting in the release of secondary mediators ADP and TxA₂ and the shift of integrins from a low-affinity state to an activated high-affinity state. Secondary mediators, as well as locally produced thrombin, further enhance platelet activation and thrombus growth. In addition, CLEC-2-mediated signaling contributes to platelet activation as well. High-affinity integrins mediate firm adhesion of platelet by binding to ligands on the ECM ($\alpha 2\beta 1$, $\alpha IIb\beta 3$) and thrombus growth by bridging platelets via fibrinogen and vWF ($\alpha IIb\beta 3$). (Picture is taken from: Stegner and Nieswandt, *J Mol Med*, 2011).⁸

In the third step, the high-affinity integrins bind to their ligands and induce firm platelet adhesion and thrombus growth. Platelets express three $\beta 1$ integrins, $\alpha 2\beta 1$, $\alpha 5\beta 1$ and $\alpha 6\beta 1$,

which bind to collagen, fibronectin and laminin, respectively, whereas the most abundant integrin α IIb β 3 (GPIIb/IIIa) binds to fibrinogen and collagen-bound vWF on the ECM.⁹ Ligand-bound integrins in turn transduce “outside-in” signals which induce platelet shape change, spreading and clot retraction.^{10,11} Finally, thrombus growth is reinforced by recruitment and activation of additional platelets from the blood stream by the released mediators ADP and TxA₂ and subsequent clustering of platelets via plasma fibrinogen and vWF.

1.3 Signaling events during platelet activation

In platelets, two principal signaling pathways induce platelet activation. First, soluble agonists, like thrombin, ADP, TxA₂ and epinephrine bind to GPCRs and induce the downstream signalings via G proteins (G_q, G_{12/13}, G_i, G_z).¹² G_q proteins activate *phospholipase* (PL) C β ,¹³ leading to intracellular Ca²⁺ mobilization via *inositol-1,4,5-trisphosphate* (IP₃) and *protein kinase C* (PKC) activation via *diacylglycerol* (DAG). G_{12/13} proteins stimulate *Ras homolog gene family* (Rho)-GTPase activity, which is critical for platelet cytoskeletal rearrangement, shape change and cell spreading.¹⁴⁻¹⁷ The $\beta\gamma$ complex of G_i proteins regulates various effectors, such as *phosphatidylinositol 3-kinase* (PI3K), contributing to α IIb β 3 integrin activation,^{18,19} and the α -subunit of G_i proteins and G_i-type G protein G_z inhibit *adenylyl cyclase* (AC), which leads to the decrease of *cyclic adenosine monophosphate* (cAMP) levels, facilitating platelet activation (Figure 1-2).^{12,20,21}

The other pathway involves platelet adhesion receptors, such as GPVI and CLEC-2. GPVI is non-covalently associated with a disulfide-linked *Fc receptor* (FcR) γ chain homodimer, which bears ITAMs.²² Activation of GPVI by collagen binding results in the recruitment of two Src-family kinases (SFKs) Fyn and Lyn to the FcR γ chain ITAM, leading to the tyrosine phosphorylation of the ITAMs and *spleen tyrosine kinase* (Syk).^{23,24} Subsequently, a downstream tyrosine phosphorylation is initiated, which involves several adapter proteins, such as *linker of activated T cells* (LAT) and *SH2 domain-containing leukocyte protein of 76 kDa* (SLP-76), leading to the activation of effector proteins, most notably PLC γ 2. PLC γ 2 activation triggers the generation of DAG and IP₃, leading the activation of PKC and intracellular Ca²⁺ mobilization. Similarly, CLEC-2, the receptor for the snake venom toxin rhodocytin,²⁵ bears a YXXL motif with a single tyrosine residue termed hemITAM, which resembles the ITAM. Activation of CLEC-2 triggers a tyrosine phosphorylation cascade and subsequently induces activation of PLC γ 2 (Figure 1-2).

In both signaling pathways, PLC isoforms are activated, and consequently IP₃ and DAG are generated by the cleavage of *phosphatidylinositol-4,5-bisphosphate* (PIP₂). IP₃ triggers Ca²⁺ release from the intracellular Ca²⁺ stores and subsequent Ca²⁺ influx through *store-operated calcium* (SOC) channel in the *plasma membrane* (PM).²⁶ On the other hand, DAG activates

PKC and contributes to *receptor-operated calcium entry* (ROCE) in platelets.²⁷ The elevation of the *intracellular Ca²⁺ concentrations* ($[Ca^{2+}]_i$) is essential for platelet activation, firm adhesion and stable aggregation, as well as granule secretion. In platelets, there are two major types of secretory granules: α -granules and dense granules. As the largest and most abundant secretory granules, α -granules contain a large number of proteins including platelet factor 4, β -thromboglobulin, coagulation factor V, thrombospondin, fibronectin, vWF and P-selectin. In contrast, dense granules contain high concentrations of small molecules, such as ADP, *adenosine triphosphate* (ATP), serotonin and Ca^{2+} . These small molecules, released from α -granules and dense granules, amplify platelet activation, aggregation and thrombus growth.

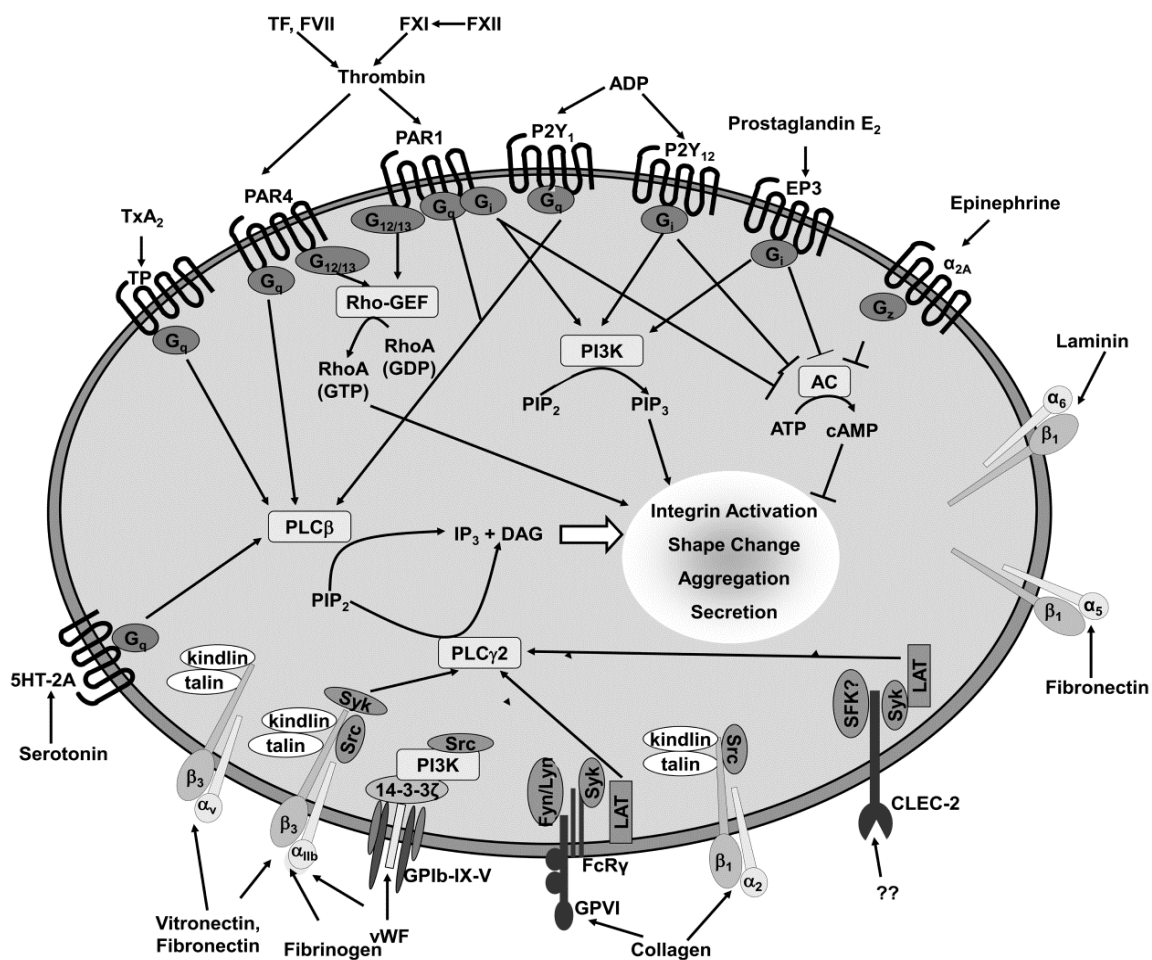


Figure 1-2: Major signaling pathways in platelets. Two principal signaling pathways exist in platelets. Soluble agonists, such as thrombin, ADP, TxA_2 and epinephrine induce various intracellular signaling pathways via GPCRs, leading to the activation of PLC β , Rho-GTPases, PI3K and inhibition of AC. Adhesion receptors, such as GPVI, CLEC-2 and active integrins induce PLC γ 2 activation upon ligand binding. In both pathways, the activation of PLC isoforms leads to IP $_3$ and DAG production. IP $_3$ and DAG induce the elevation of the intracellular Ca^{2+} concentrations, which is critical for full platelet activation. Abbreviations: TF, *tissue factor*; TP, *TxA₂ receptor*; PAR, *protease-activated receptor*; Rho-GEF, *Rho-specific guanine nucleotide exchange factor*; PIP $_2$, *phosphatidylinositol-4,5-bisphosphate*; PIP $_3$, *phosphatidylinositol-3,4,5-trisphosphate*; (Picture is taken from: Stegner and Nieswandt, *J Mol Med*, 2011).⁸

1.4 Calcium signaling in platelets

Ca^{2+} is an ubiquitous second messenger in virtually every cell, which regulates a broad spectrum of cellular functions including gene transcription, exocytosis, cell motility, cell cycle and apoptosis.²⁸ The increase of the cytoplasmic Ca^{2+} concentrations can be achieved by the following two ways: release from the intracellular Ca^{2+} stores or Ca^{2+} influx into the cell via Ca^{2+} channels located in the PM. In eukaryotic cells, it is firmly established that the *endoplasmic/sarcoplasmic reticulum* (ER/SR)-like structure termed *dense tubular system* (DTS) and mitochondria are the major intracellular Ca^{2+} stores.^{29,30} However, growing evidence indicates that additional organelles like the Golgi apparatus, lysosomes, the nuclear envelope and secretory granules play a role in intracellular Ca^{2+} mobilization.^{31,32} Regarding to Ca^{2+} channels in the PM, a variety of different Ca^{2+} -permeable channels have been identified. The main channels are: (1) voltage-gated Ca^{2+} channels, which are found in electrically excitable cells like nerve and muscle cells, but are largely excluded from electrically nonexcitable cells; (2) *receptor-operated Ca^{2+}* (ROC) channels, operated by extracellular and intracellular ligand binding, are found mainly in excitable cells and some in nonexcitable cells; (3) store-operated Ca^{2+} channels, which are widespread, almost existing in all eukaryotes from yeasts to humans.^{33,34} In nonexcitable cells, SOC channels are the major Ca^{2+} channels mediating *store-operated calcium entry* (SOCE), in which the depletion of intracellular Ca^{2+} stores activates SOC channels and induces subsequent Ca^{2+} influx across the PM.²⁸

In platelets, Ca^{2+} plays a central role for several processes. The elevation of $[\text{Ca}^{2+}]_i$ is an essential step for platelet activation and is also vital for cytoskeleton reorganization, aggregation, firm adhesion and granule secretion.³⁵ Similar to other cell types, the increase of $[\text{Ca}^{2+}]_i$ in platelets originates from two major sources: Ca^{2+} release from intracellular stores and Ca^{2+} influx via Ca^{2+} channels in the PM.

Based on the expression pattern of two different *sarcoplasmic/endoplasmic reticulum Ca^{2+} ATPase* (SERCA) isoforms on the surface of cellular organelles and their affinity to SERCA inhibitors, two distinct Ca^{2+} stores exist in platelets. SERCA2b isoform is expressed on the Ca^{2+} store membrane which is IP_3 and *thapsigargin* (TG) sensitive. These features indicate that this store is located in the DTS. Another SERCA isoform called SERCA3, which is strongly expressed in the store membrane, shows lower sensitivity to TG but high sensitivity to *2,5-di-(*t*-butyl)-1,4-hydroquinone* (TBHQ). Although the subcellular localization of this Ca^{2+} store is unknown in platelets, this Ca^{2+} store seems to be located in acidic organelles, like lysosomes.³⁶⁻³⁹

Up to now, several intracellular messengers that control Ca^{2+} store release have been found: IP_3 , *cyclic adenosine 5'-diphosphoribose* (cADPR), *nicotinic acid-adenine dinucleotide*

phosphate (NAADP), and sphingolipid-derived messengers.⁴⁰ In platelets, the major route of store release is IP₃-induced store depletion via the *IP₃ receptor* (IP₃R), which forms a Ca²⁺-permeable channel. The N-terminus of the IP₃R binds IP₃, which is required for the channel activity. Interestingly, the N-terminus also contains an inhibitory region which suppresses the binding affinity to IP₃. The cytosolic C-terminus forms the pore unit of the Ca²⁺ channel and contains an activating domain.⁴¹ Three isoforms of IP₃R have been identified: IP₃R1, IP₃R2 and IP₃R3. In platelets, all three isoforms have been found, however the predominant ones are IP₃R1 and IP₃R2.⁴²

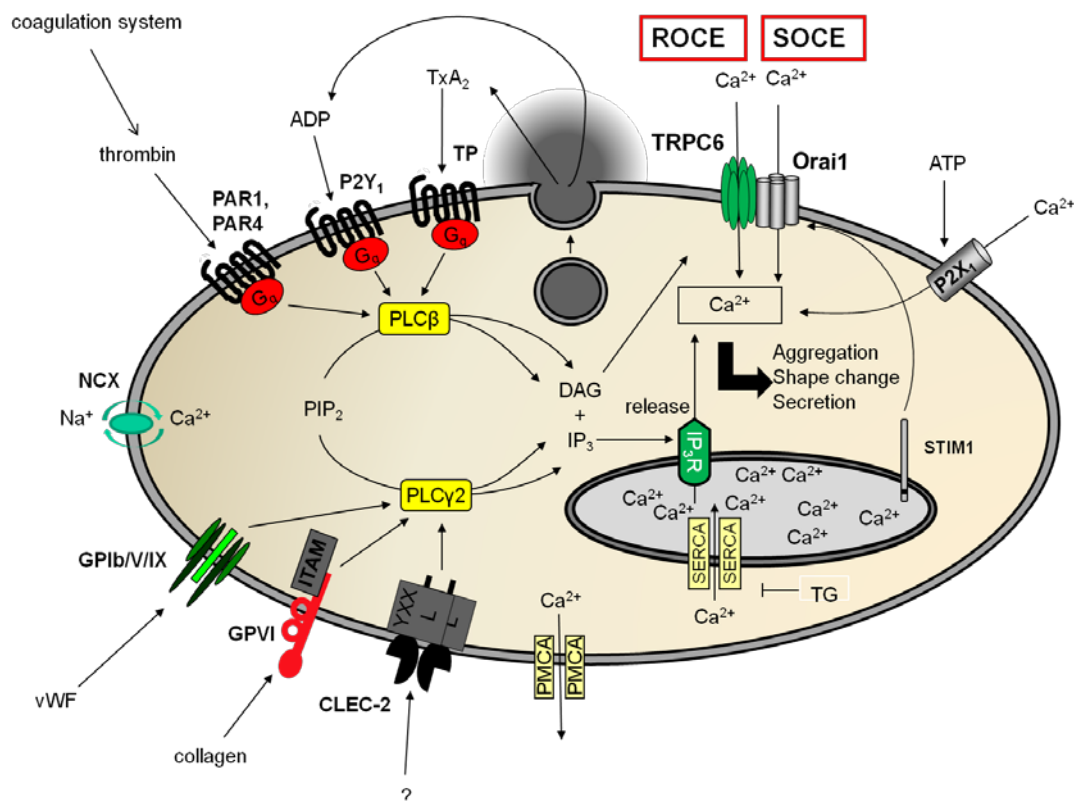


Figure 1-3: Calcium signaling in platelets. Through GPCR signaling pathways or (hem)ITAM signaling pathways, PLC isoforms can be activated to hydrolyze PIP₂ to IP₃ and DAG. IP₃ leads to store depletion and triggers STIM1 to interact with Orai1 and to open Orai1 channel in the plasma membrane, allowing SOCE. DAG mediates ROCE through TRPC6. Additionally, P2X₁ can be activated by ATP and contribute to the increase of [Ca²⁺]_i. In contrast, SERCA, PMCA and NCX can pump Ca²⁺ back into the stores or out of the cell. (Picture is modified from: Braun A, Vögtle T, Varga-Szabo D, Nieswandt B. *Front Biosci.* 2012).⁴³

Under resting conditions, the basal [Ca²⁺]_i remains constantly low due to the combined effects of Ca²⁺ pumps and exchangers located in the PM and the Ca²⁺ store membrane: upon Ca²⁺ release via the IP₃R or Ca²⁺ influx via Ca²⁺ channels, SERCA isoforms become activated and rapidly pump extra cytoplasmic Ca²⁺ into the stores. In addition, *plasma membrane Ca²⁺-ATPase* (PMCA) isoforms and *Na⁺/Ca²⁺ exchanger* (NCX) can also reduce the [Ca²⁺]_i. However, in stimulated cells this equilibrium is changed because of the activation of PLC enzymes. The PLCβ isoform is solely activated by G_q proteins, which can be stimulated by

soluble agonists such as thrombin, ADP and TxA₂, while PLC γ 2 is activated by downstream regulatory pathways of the (hem)ITAM receptors and integrin α IIb β 3. The activated PLC isoforms subsequently hydrolyze PIP₂ into IP₃ and DAG. IP₃ production leads to the depletion of the Ca²⁺ stores, which triggers the activation of the SOC channel, Orai1, via *stromal interaction molecule* (STIM) 1, inducing store-operated Ca²⁺ entry,²⁶ whereas DAG can activate the ROC channel *canonical transient receptor potential channel* (TRPC) 6 in the PM and induce receptor-operated Ca²⁺ entry (Figure 1-3).²⁷ In platelets, SOCE and ROCE are the two predominant Ca²⁺ entry routes.

1.4.1 Store-operated calcium entry

It is well established that in platelets the major Ca²⁺ entry route is SOCE.²⁶ The concept of SOCE, which was first proposed in 1986, was derived from research in investigating the relationship between Ca²⁺ release from the stores, Ca²⁺ influx and store refilling in parotid acinar cells.⁴⁴ It was found that in nonexcitable cells, the Ca²⁺ store content controls the Ca²⁺ influx, which is originally termed *capacitive calcium entry* (CCE). When the stores are full, no Ca²⁺ influx occurs, whereas when the stores are emptied, Ca²⁺ influx develops. These findings indicate that SOCE can be induced by store depletion. Under physiological conditions, store depletion is evoked by the increase of IP₃ or other Ca²⁺-releasing signals. Moreover, several experimental methods have been developed to empty the stores: (1) the elevation of IP₃ after activating PLC isoforms with agonists; (2) the application of the SERCA pump specific inhibitor, thapsigargin, to prevent store refilling; (3) the application of Ca²⁺ ionophores, like ionomycin or A23187, which permeabilize the store membrane.⁴⁵⁻⁴⁸

1.4.1.1 STIM1

Although it was long known that SOCE is triggered by store depletion, the molecular mechanism was revealed just several years ago. The breakthrough in understanding this mechanism is the discovery of STIM1. In 2005, by using RNAi-based screening, STIM1 was identified as the Ca²⁺ sensor in the *endoplasmic reticulum* (ER) in *Drosophila* S2 cells and Jurkat T cells. It was shown that the EF hand domain of STIM1, located in the ER lumen, is the key domain for binding Ca²⁺. In a wild type cell line, only when stores are depleted, the EF hand domain of STIM1 loses its bound Ca²⁺, which triggers STIM1 to redistribute to “puncta” and activate SOC channels in the PM. However in EF hand mutant cell line, EF hand domain fails to bind Ca²⁺ even under resting conditions, resulting in “false store depletion” and permanent opening of the SOC channels.^{49,50}

In platelets, the same phenomenon was found in a mouse line with a single amino acid (AA) mutation (D84G) in the canonical EF hand of STIM1, termed Sax (*Stim1*^{Sax/+}; named after the

Bulgarian king Saxe-Coburg-Gotha who suffered from a bleeding disorder). *Stim1^{Sax/+}* platelets display constitutively opened SOC channels, resulting in macrothrombocytopenia and an associated bleeding disorder.⁵¹ In contrast, the elimination of STIM1 in *Stim1^{-/-}* platelets leads to the complete lack of SOCE and a severely impaired Ca²⁺ response to all major platelet agonists.⁵² These findings together demonstrate that STIM1 is essential for SOCE in platelets. Moreover, in *Stim1^{-/-}* platelets, reduced Ca²⁺ store release upon agonist stimulation was demonstrated.⁵² A similar observation was also reported in *Stim1^{-/-}* mast cells,⁵³ indicating that STIM1 could be involved in the refilling process of the Ca²⁺ store.

1.4.1.2 Orai1

In 2006, three independent groups identified the second essential component of SOCE, Orai1, a plasma membrane protein with four predicted transmembrane domains.⁵⁴⁻⁵⁹ Feske *et al.* discovered that SOCE is defective in patients with a hereditary *severe combined immune deficiency* (SCID). By using single-nucleotide polymorphism arrays and a *Drosophila* RNAi screen, they found that these SCID patients were homozygous for a mutation in Orai1, and the expression of normal Orai1 in SCID T cells restored SOCE.⁵⁴ Vig *et al.* and Zhang *et al.* showed that Orai1 plays an essential role for SOCE, since Orai1 knockdown by RNAi severely disrupted SOCE.^{55,59} Furthermore, Prakriya *et al.* showed that the mutation of two conserved acid residues in the transmembrane domain of Orai1 resulted in diminished Ca²⁺ influx, but increased influx of monovalent cations like Cs⁺, indicating that Orai1 is a pore subunit of the SOC channel.⁵⁶ Similarly, Yeromin *et al.* and Vig *et al.* observed an altered ion selectivity after site-directed mutagenesis of Orai1, demonstrating that Orai1 itself forms the Ca²⁺ selectivity pore of the SOC channel.^{57,58}

1.4.1.3 Coupling machinery of STIM1 and Orai1

The identification of STIM1 and Orai1 led to tremendous progress towards the understanding of the molecular mechanism of SOCE. However, a critical question, how STIM1 regulates the opening of the SOC channel Orai1, still remains to be answered. Over the last decade, a large number of studies have been performed to understand this mechanism. In the current model, SOCE can be divided into four phases (from left to right, Figure 1-4). In the first phase, the Ca²⁺ store is full and the EF hand domain of STIM1 binds Ca²⁺, therefore STIM1 stays in a resting state. In the second phase, when the store is depleted, Ca²⁺ disassociates from the EF hand, resulting in the oligomerization of STIM1.⁶⁰ Subsequently, STIM1 oligomers translocate to ER-PM junctions and accumulate at the cell periphery, forming “puncta” there.⁶¹⁻⁶³ In the last phase, STIM1 oligomers bind to the SOC channel, which is formed by four Orai1 subunits, and this interaction leads to the opening of the SOC channel.^{64,65}

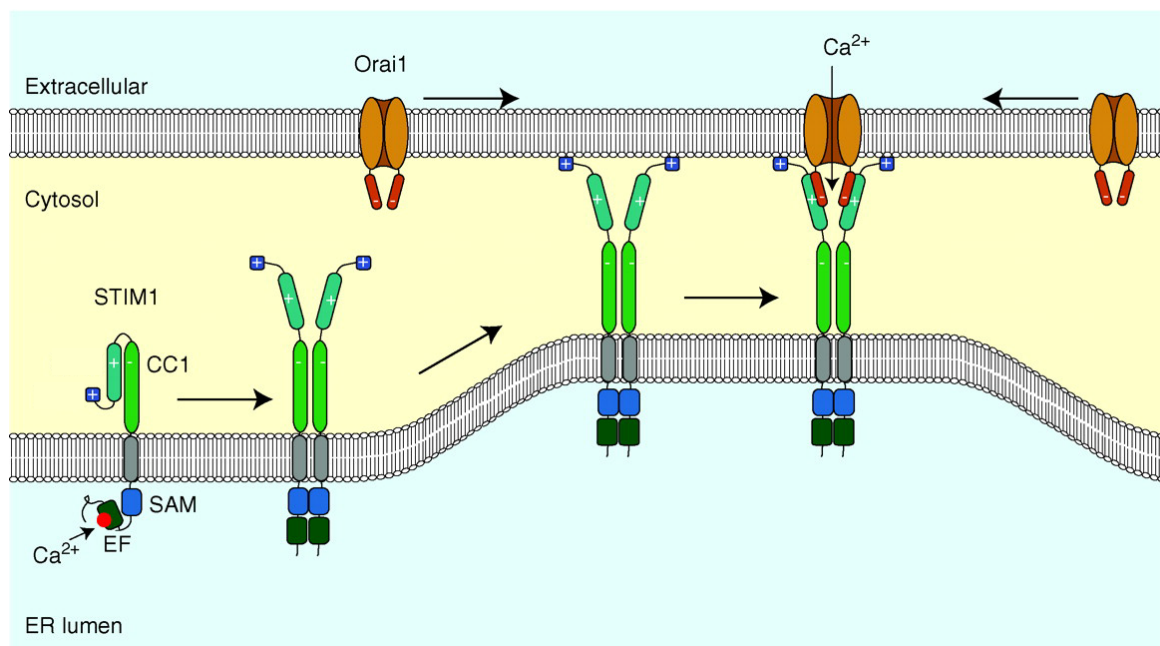


Figure 1-4: Simplified model of SOCE. The process of SOCE can be divided into four phases. The details are described in the text. (Figure is modified from Richard S. Lewis. *Cold Spring Harb Perspect Biol.* 2011).⁶⁶

1.4.1.4 Orai1 is the major SOC channel in mouse platelets

The Orai channel family comprises three isoforms, Orai1, Orai2 and Orai3. In human and mouse platelets all three isoforms have been shown to be expressed by using quantitative RT-PCR, however Orai1 is the predominant one.⁶⁷ Recently, Braun *et al.* confirmed that Orai1 is strongly expressed in mouse platelets. They generated *Orai1*^{-/-} mice and discovered that approximately 60% of the *Orai1*^{-/-} mice died shortly after birth. Moreover, the surviving *Orai1*^{-/-} mice exhibited severe developmental defects and all *Orai1*^{-/-} mice died at the latest 4 weeks after birth. In *Orai1*^{-/-} platelets, they found that TG-induced SOCE was almost completely abolished, establishing that Orai1 is the main SOC channel in mouse platelets. In addition, *Orai1*^{-/-} platelets displayed impaired platelet activation, aggregation and thrombus formation under flow. Furthermore, Orai1 deficiency resulted in the resistance to pulmonary thromboembolism, arterial thrombosis and ischemic brain infarction.²⁶ Taken together, these results established that Orai1 is the major SOC channel in mouse platelets, and it plays a critical role in platelet activation during arterial thrombosis and ischemic brain infarction.

Besides Orai1, members of the superfamily of *transient receptor potential* (TRP) channels, particularly those from TRPC subfamily, have also been suggested as SOC channels. In human platelets, TRPC1 has been proposed to mediate SOCE. Rosado *et al.* reported that in human platelets the application of an anti-human TRPC1 blocking antibody led to reduced SOCE.⁶⁸ In addition, they proposed a model where STIM1 interacts with TRPC1 and activates TRPC1.⁶⁹ However in mouse platelets, TRPC1 deficiency did not result in either

impaired Ca^{2+} store release or reduced SOCE.⁷⁰ Moreover, *Trpc1*^{-/-} mice were intercrossed with *Stim1*^{Sax/+} mice, in which SOC channels are constitutively opened,⁵¹ to generate *Trpc1*^{-/-Sax/+} mice. In these mice, TRPC1 deficiency could not rescue the phenotypes that *Stim1*^{Sax/+} mice present, such as macrothrombocytopenia and elevated $[\text{Ca}^{2+}]_i$.⁷⁰ Furthermore, the expression level of TRPC1 in megakaryocytes and platelets is extremely low.⁷⁰ Taken together, these findings reveal that TRPC1 plays a minor role in Ca^{2+} homeostasis in mouse platelets and Orai1 is the major SOC channel in mouse platelets.

1.4.2 Receptor-operated calcium entry

Besides SOCE, other Ca^{2+} influx mechanisms also exist in platelets. Among them, ROCE, operated by DAG or purinergic, is the predominant one.

1.4.2.1 Phospholipase-mediated DAG production

There are two major routes of DAG production in platelets. One is through PLC isoforms. As described above, receptor-mediated activation of PLC isoforms leads to the hydrolysis of PIP_2 into IP_3 and DAG. The other route is mediated by PLD isoforms. PLD hydrolyses phosphatidylcholine (PC) to phosphatidic acid (PA) and choline in the lipid raft. The life time of PA is very short, since PA-phosphatases convert PA to DAG and inorganic phosphate during platelet activation.^{71,72} The intracellular DAG concentration $[\text{DAG}]_i$ is tightly regulated by DAG kinase, which converts DAG back to PA.⁷³ Sustained elevations of DAG are essential to regulate Ca^{2+} channels and other DAG-dependent signaling pathways. For instance, CalDAG-GEF, Rap1b and PKC-mediated integrin activation are dependent on $[\text{Ca}^{2+}]_i$ and $[\text{DAG}]_i$ in platelets.^{27,74}

1.4.2.2 TRPC6

TRPC6, which is robustly expressed in both human and mouse megakaryocytes and platelets,^{75,76} has been suggested as a ROC channel instead of a SOC channel.^{75,77} Recently, Ramanathan *et al.* showed that in *Trpc6*^{-/-} platelets TG-induced SOCE was unaltered, confirming that TRPC6 is not a SOC channel in mouse platelets. Furthermore, they discovered that the application of *1-oleoyl-2-acetyl-sn-glycerol* (OAG), an analogue of DAG, induced Ca^{2+} influx in *Wt* platelets, however, in *Trpc6*^{-/-} platelets this Ca^{2+} influx was virtually completely abolished, establishing TRPC6 as the predominant DAG-mediated Ca^{2+} channel in mouse platelets.²⁷ However, Harper *et al.* pointed out that TRPC6 is not the only DAG-mediated ROC channel expressed in mouse platelets, but TRPC3 is also expressed in mouse platelets and operated by DAG.⁷⁸

TRPC6 seems not essential for platelet function. *Trpc6*^{-/-} platelets displayed unaltered life

span, integrin $\alpha\text{IIb}\beta\text{3}$ activation, degranulation, aggregation, adhesion, cytoskeletal reorganization and spreading compared to *Wt* platelets.²⁷ *In vivo* studies also showed that in *Trpc6*^{-/-} mice intravascular thrombus formation after mechanical injury of the abdominal aorta and after FeCl_3 -induced chemical injury of the mesenteric arterioles and the carotid artery was unaltered.²⁷ Taken together, these findings suggest that lack of TRPC6 functions is redundant and can be compensated by other Ca^{2+} channels.

1.4.2.3 P2X₁

Another ROC channel in the PM of platelets is the P2X₁ channel. P2X receptors have seven isoforms (P2X₁-P2X₇), which are identified in mammalian cells. Among these receptors, P2X₁ is the only one expressed in megakaryocytes and platelets at a significant level.^{79,80} P2X₁ is operated directly by ATP, whereas ADP has been suggested to play an inhibitory effect on this channel.⁸¹ The activation of the P2X₁ channel evokes a rapid Ca^{2+} influx, dense granule centralization, shape change and a low level of aggregation.⁸²⁻⁸⁴ In addition, P2X₁ activation promotes platelet responses to thrombin and collagen, subsequently triggering an amplifying signal.^{83,85,86} However, the activation of the P2X₁ channel is transient, because of its fast desensitization by the released ADP. Therefore, to investigate the P2X₁ channel *in vitro*, a high concentration of apyrase is required to scavenge the released ADP.^{83,84,87}

1.4.3 Crosstalk between Orai1 and TRPC6

In human platelets, the heteromeric interaction between Orai and TRPC isoforms has been suggested. It was shown that *human* (h) Orai1 interacted directly with the N- and C-termini of hTRPC3 and hTRPC6 in a GST pull-down assay. Furthermore, via this interaction Orai proteins regulated TRPC channels and enabled them to respond to the store depletion.⁸⁸ In addition, hTRPC6 was reported to interact with either both hOrai1 and hSTIM1 or hTRPC3 to participate in SOCE or ROCE, respectively. When the Ca^{2+} store was depleted, the interaction between hTRPC6 and the Orai1-STIM1 complex was enhanced and hTRPC6 contributed to SOCE. In contrast, when platelets were stimulated by OAG, the interaction between hTRPC6 and the Orai1-STIM1 complex disassociated and the interaction between hTRPC6 and hTRPC3 was enhanced, therefore hTRPC6 participated in ROCE in this situation.⁸⁹ Another dynamic coupling model between Orai proteins and TRPC isoforms was proposed in 2012. Depletion of the intracellular Ca^{2+} stores led to the formation of a signaling complex involving hSTIM1, hSTIM2, hOrai1, hOrai2, hTRPC1 and hTRPC6. Whereas, OAG stimulation resulted in the association of hOrai3 with hTRPC3.⁶⁹

However, DeHaven *et al.* reported that TRPC channels function independently of STIM1 and Orai1.⁹⁰ By using the human kidney cell line HEK293, transiently expressing TRPC1, TRPC3,

TRPC5 or TRPC6, they observed that the overexpression of STIM1 did not enhance their activities. Furthermore, RNAi knockdown of STIM1 did not affect the Ca^{2+} influx through TRPC5, TRPC6 or TRPC7. Thus, TRPC channels seem not to be regulated by STIM1. In mice, *Orai1*^{-/-} platelets displayed normal OAG-induced Ca^{2+} entry via TRPC6, and in addition, TRPC6 deficiency did not affect TG-induced SOCE via Orai1, suggesting that Orai1 and TRPC6 function independently of each other.^{26,27}

Therefore, the functional crosstalk between Orai and TRPC isoforms remains controversial.

1.5 The role of magnesium in platelets

Besides Ca^{2+} , Mg^{2+} is also a very important cation found in all tissues. In mammalian cells, Mg^{2+} can be stored in the ER and mitochondria.^{91,92} Mg^{2+} is a cofactor for many enzymes and plays a vital role in binding nucleotides and stabilizing nucleic acids. Mg^{2+} influences many cellular processes, such as neuromuscular excitability and hormone secretion. Aberrant Mg^{2+} homeostasis is associated with several disorders, including cardiovascular diseases.⁹³ Low Mg^{2+} levels in blood serum, termed hypomagnesaemia, have been shown to associate with the development of metabolic syndrome, diabetes mellitus, hypertension, acute myocardial infarction, inflammation and pre-eclampsia.⁹⁴⁻⁹⁹ In contrast, high serum Mg^{2+} concentrations, termed hypermagnesaemia, can result in neuromuscular, cardiac and nervous disorders.¹⁰⁰ Unlike the extracellular Mg^{2+} deficiency, an intracellular Mg^{2+} deficiency cannot be easily recognized during development of human diseases. Since about 99% of total body Mg^{2+} is stored in bones, muscles and liver,¹⁰¹ and these Mg^{2+} stores can maintain normal Mg^{2+} levels in the blood for a long period of time without indication of intracellular Mg^{2+} deficits.

In megakaryocytes and platelets, no intracellular Mg^{2+} stores have been described so far, however, extracellular Mg^{2+} levels have been reported to influence platelet activity. A high extracellular Mg^{2+} concentration has been shown to inhibit platelet aggregation induced by ADP, thrombin, collagen and the stable TxA_2 analogue U46619.¹⁰²⁻¹⁰⁵ In addition, Mg^{2+} can affect TxA_2 synthesis, ATP secretion and β -thromboglobulin release.¹⁰⁶ Mg^{2+} can also influence vascular PGI_2 synthesis and blood coagulation.¹⁰⁵ Furthermore, Mg^{2+} has been considered as a natural “calcium antagonist”.¹⁰⁷ Mg^{2+} and Ca^{2+} compete with each other for the same binding sites of receptors on the PM.^{98,108} It was shown that Mg^{2+} can reduce thrombin-stimulated Ca^{2+} influx in platelets.¹⁰⁶ In summary, all these studies lead to a conclusion that Mg^{2+} seems to play a role in Ca^{2+} homeostasis and platelet activity, thereby influencing thrombosis and hemostasis.

1.5.1 Mechanisms of Mg^{2+} influx

Although Mg^{2+} plays such a vital role in numerous cellular functions and it is linked to a

variety of diseases, the regulating mechanisms of intracellular Mg^{2+} mobilization and Mg^{2+} influx remain unclear. For a long time, the negative membrane potential on the inside of the cells was considered to serve as a force to drive Mg^{2+} influx either through ion channels or carriers. However, whether such Mg^{2+} transporters exist remained unclear until the 1990s. In the 1990s, metabolic or hormonal stimuli were found to result in the rapid increase of the $[Mg^{2+}]_i$ in lymphocytes, erythrocytes, cardiac myocytes and liver cells. Importantly, this Mg^{2+} influx can be influenced by ion channel blockers. These findings indicate that Mg^{2+} channels or transporters are expressed in these cells. Furthermore, genetic studies in eukaryotic cells have identified several Mg^{2+} channels and transporters to be involved in the regulation of the Mg^{2+} homeostasis.¹⁰⁹⁻¹¹⁶ So far, a variety of Mg^{2+} transporters have been identified (Table 1).

	Location	Associated Disease
<i>Mrs2</i>		
Mrs2p	Mitochondria	
<i>TRPM</i>		
TRPM7	Plasma membrane	Guamanian ALS/Parkinsonism dementia
TRPM6	Plasma membrane	HSH
<i>MagT</i>		
MagT1	Plasma membrane	
TUSC3 or N33	Plasma membrane	Tumor suppressor gene
<i>SLC41</i>		
SLC41 A1		
SLC41 A2	Plasma membrane	
SLC41 A3		
<i>ACDP</i>		
ACDP1	Plasma membrane	UFS
ACDP2 or Cnm2		
ACDP3		
ACDP4		
<i>MMgT</i>		
MMgT1	Golgi, post-Golgi vesicles	
MMgT2	Golgi, post-Golgi vesicles	
<i>NIPA</i>		
NIPA1	Plasma membrane	HSP
NIPA2	Plasma membrane	
NIPA3		
NIPA4		
<i>HIP14</i>		
HIP14	Golgi, subplasma membrane vesicles	Huntington disease
HIP14L	Golgi, subplasma membrane vesicles	Huntington disease
<i>MagC</i>		
MagC1		

Table 1: Mammalian Mg^{2+} transporters. Abbreviations: ALS, amyotrophic lateral sclerosis; HSH, hypomagnesaemia with secondary hypocalcemia; UFS, urofacial syndrome; HSP, hereditary spastic paraplegia. (Table is modified from Quamme GA. Am J Physiol Cell Physiol. 2010).¹¹⁷

As depicted in Table 1, the Mg^{2+} transporters are mainly located in the PM, and some of them are located in mitochondria and the Golgi apparatus. Among these transporters, two *transient receptor potential melastatin-like* (TRPM) ion channels, TRPM6 and TRPM7 have been reported to be essential for Mg^{2+} influx and homeostasis.^{118,119}

1.5.2 The role of TRPM6 and TRPM7 channels in Mg^{2+} homeostasis

TRPM6 and TRPM7 are constitutively opened Mg^{2+} -permeable channels. TRPM6 is uniquely found along the full length of the intestine, in the kidney nephron, and in lung and testis tissues.¹²⁰⁻¹²² This specific localization enables TRPM6 to control the whole-body Mg^{2+} homeostasis by regulating intestinal Mg^{2+} absorption and renal Mg^{2+} reabsorption.^{109,115,116} It has been shown that TRPM6 mutation results in the syndrome of HSH, which is characterized by low serum Mg^{2+} levels.^{119,123} More recently, *Trpm6*^{-/-} mice have been developed. Most *Trpm6*^{-/-} mice died by embryonic day 12.5, and only very few *Trpm6*^{-/-} mice could survive with severe neural tube defects such as exencephaly and spina bifida occulta.¹²⁴ Another group reported similar findings that homozygous TRPM6 deletion leads to embryonic lethality whereas heterozygous TRPM6 deletion results in a mild hypomagnesaemia.¹²⁵

Unlike TRPM6, TRPM7 is ubiquitously expressed in virtually all cell types and plays a role in controlling Mg^{2+} homeostasis in individual cells.^{118,126,127} It has been shown that the deletion of TRPM7 in an avian cell line results in intracellular Mg^{2+} depletion and growth arrest.^{118,128} However in murine T cell, TRPM7 deletion does not affect acute uptake of Mg^{2+} or the maintenance of intracellular Mg^{2+} concentrations.¹²⁹ These findings indicate that TRPM7 is important for regulating intracellular Mg^{2+} homeostasis, however it may be not the only Mg^{2+} transporter to fulfill this function.

Interestingly, TRPM6 and TRPM7 have been reported to form heterooligomeric complexes. TRPM7 was demonstrated to be necessary for TRPM6 trafficking to the PM, whereas TRPM6 was not essential for TRPM7 trafficking.^{119,121,130} Furthermore, it has been shown that TRPM7-deficient cells cannot be complemented by TRPM6 expression, however TRPM6 can modulate TRPM7 function by phosphorylation.¹²⁸ In addition, Chubanov *et al.* reported that in HEK293 cells or *X. Laevis* oocytes which only express TRPM6, no electrical conductance through TRPM6 can be recorded. They suggested that the co-expression of TRPM7 is needed for TRPM6 to be incorporated into channel complexes in the PM.¹²⁰ All these studies suggest that TRPM6 cannot function without TRPM7. However, another group reported that TRPM6 can fully function in heterologously expressed cell lines.^{131,132} Moreover, Yue *et al.* reported that pure TRPM6, pure TRPM7 and the TRPM6/TRPM7 complexes constitute three distinct ion channels with different divalent cation permeability.^{133,134}

1.5.3 TRPM7

TRPM7 is one of the first identified Mg^{2+} channels in mammalian cells. It is also permeable to Ca^{2+} and other divalent cations, such as Zn^{2+} , Mn^{2+} and Co^{2+} . The influx of these divalent cations into the cell is mediated by the transmembrane electrochemical gradient.^{121,132,135,136}

TRPM7 is constitutively opened, and it can be suppressed by the increase of $[Mg^{2+}]_i$ or intracellular Mg^{2+} -ATP complex levels.¹³⁶ Furthermore, TRPM7 channel activity can also be regulated by the activity of PLC isoforms. It was suggested that the activation of PLC β via GPCR signalings could further enhance the channel activity of TRPM7.¹³⁷ However, contradictory findings exist, reporting that the channel function of TRPM7 will be down-regulated if PIP₂ in the PM is hydrolyzed by PLC isoforms.^{138,139}

TRPM7 has six transmembrane domains. In addition, it bears a cytoplasmic α -kinase domain, *serine/threonine* (Ser/Thr) kinase, at its C-terminus,¹²¹ so that it can also function as Ser/Thr kinase (Figure 1-5). Since it function as both channel and kinase, it is termed “chanzyme”.

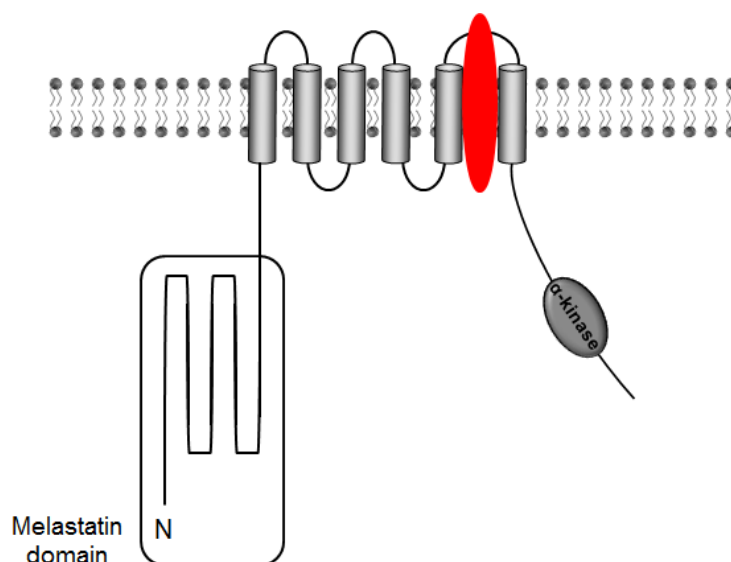


Figure 1-5: Structural features of TRPM7. TRPM7 contains six transmembrane domains. The cytoplasmic N-terminus contains a domain highly homologous to other members of the melastatin TRP channel subfamily (Melastatin domain). The channel domain (red) locates between transmembrane helices 5 and 6. At the cytoplasmic C-terminus, there is an α kinase domain, which is a serine–threonine-rich region with multiple autophosphorylation sites. (Picture is taken from Tamara M. Paravicini, Vladimir Chubanov and Thomas Gudermann. *The International Journal of Biochemistry & Cell Biology*. 2012).¹⁴⁰

1.5.3.1 The physiological role of TRPM7 protein

TRPM7 is ubiquitously expressed in virtually all cell types and has been suggested to regulate several cellular processes including cell growth, cell cycle and cell death.^{118 141-143} Recently, it has been shown that the global deletion of TRPM7 results in embryonic lethality while the tissue-specific deletion of TRPM7 leads to disrupted thymopoiesis, suggesting an

important role of TRPM7 in embryonic development and organogenesis.^{129,144} Abolished TRPM7 function *in vitro* results in the depletion of $[Mg^{2+}]_i$ and growth arrest in the presence of normal extracellular Mg^{2+} concentrations.^{118,128} It has been reported that TRPM7 plays an important role in the pathogenesis of ischemic stroke.¹⁴⁵ In the *transient middle cerebral artery occlusion* (tMCAO) model of ischemic stroke, the expression levels of TRPM7 protein were found to be up-regulated,¹⁴⁶ and the inhibition of TRPM7 function under hypoxia enhanced cell viability.^{147,148} Hence, it is assumed that the up-regulation of TRPM7 and/or the enhanced channel activity may induce Ca^{2+} entry, thereby accelerating cell death during stroke development.¹⁴⁹ TRPM7 seems to exhibit an ambivalent role in Ca^{2+} and Mg^{2+} homeostasis, since extracellular Ca^{2+} influx through TRPM7 could be increased by reactive oxygen/nitrogen species and prolonged *oxygen and glucose deprivation* (OGD).¹⁴⁷ Although TRPM7-mediated Mg^{2+} entry can support cell survival under normoxic conditions, TRPM7-induced Ca^{2+} entry seems to enhance cell death under hypoxic conditions.

1.5.3.2 The kinase domain of TRPM7

As described above, TRPM7 bears a Ser/Thr kinase domain containing multiple autophosphorylation sites at the C-terminus. The activating signal of the TRPM7 kinase and its downstream effect on cellular functions are still unknown, although the kinase domain is proposed to play a role in diverse phosphorylation events. Autophosphorylation of the kinase domain of TRPM7 enhances kinase-substrate interactions, leading to the Ser/Thr phosphorylation of different substrates.¹⁵⁰ However, up to now only a limited number of endogenous substrates for the TRPM7 kinase has been identified. Earlier, it was suggested that annexin I¹⁵¹ and the heavy chain of myosin IIA¹⁵² are phosphorylated by the TRPM7 kinase. Recently, Schmitz *et al.* reported the phosphorylation of *eukaryotic elongation factor 2* (eEF2) to be regulated by the TRPM7 kinase via the activation of eEF2-kinase.¹⁵³

The TRPM7 kinase has also been reported to directly associate with the C2 domain of PLC isoforms including PLC β , PLC γ and PLC δ .¹³⁸ In 2012, Schmitz *et al.* identified some phosphorylation sites for the TRPM7 kinase within PLC γ 2 in cell culture experiments with the DT40 B cell line. They found that the TRPM7 kinase phosphorylates PLC γ 2 at position Ser1164 in its C2 domain and at position Thr1045 in the linker region preceding the C2 domain. Furthermore they observed that under hypomagnesian conditions, the mutation of Thr1045 in PLC γ 2 leads to impaired Ca^{2+} homeostasis.¹⁵⁴ Taken together, these results demonstrate that the TRPM7 kinase may influence the enzymatic activity of PLC γ 2, thereby affecting Ca^{2+} homeostasis.

The complete deletion of the kinase domain of TRPM7 leads to the early embryonic lethality.¹⁴⁴ It was also reported that mice heterozygous for the loss of the TRPM7 kinase

reveal reduced Mg^{2+} concentrations in blood, urine and bones.¹⁵⁵ However, the interplay of kinase and channel domain remains unclear: some researchers believe that the kinase domain is essential for the channel activity,¹²⁷ while some hold the opinion that the channel domain and the kinase domain function independently of each other.¹⁵⁶

So far, the role of TRPM7, especially the kinase domain of TRPM7, in megakaryocyte or platelet function has not been determined.

1.6 AIM OF THE STUDY

During platelet activation, elevation of $[Ca^{2+}]_i$ is an important signaling step. It is well established that Orai1-mediated SOCE and TRPC6-mediated ROCE are the two major Ca^{2+} entry routes in mouse platelets. The heterodimerization of Orai and TRPC isoforms has been suggested to regulate SOCE and ROCE in human platelets. However, the functional significance of the biochemical interaction between Orai and TRPC isoforms still remains controversial. One aim of this thesis was to study the functional crosstalk between Orai1 and TRPC6 in mouse platelets.

TRPM7 contains a cytoplasmic Ser/Thr kinase domain at its C terminus. It has been shown that the TRPM7 kinase directly interacts with the C2 domain of PLC isoforms in mammalian cells. Moreover, in a DT40 cell line several Ser/Thr phosphorylation sites in PLC γ 2 were identified by the TRPM7 kinase recently, demonstrating that the TRPM7 kinase may regulate PLC γ 2. Therefore, the other aim of this thesis was to elucidate the role of the TRPM7 kinase in platelet phospholipase activity, Ca^{2+} homeostasis and the development of thrombosis and stroke.

2 MATERIALS AND METHODS

2.1 Materials

2.1.1 Chemicals and reagents

Reagent	Company
3,3',5,5'-tetramethylbenzidine (TMB)	BD Biosciences (Heidelberg, Germany)
β -mercaptoethanol	Roth (Karlsruhe, Germany)
Adenosine diphosphate (ADP)	Sigma-Aldrich (Schnelldorf, Germany)
Agarose	Roth (Karlsruhe, Germany)
Alexa Fluor 488	Invitrogen (Karlsruhe, Germany)
Amersham Hyperfilm ECL	GE Healthcare (Little Chalfont, UK)
Ammonium peroxodisulfate (APS)	Roth (Karlsruhe, Germany)
Apyrase (grade III)	Sigma (Schnelldorf, Germany)
Aspirin i.v. 500 mg	Bayer (Wuppertal, Germany)
Atipamezole	Pfizer (Karlsruhe, Germany)
Bovine serum albumin (BSA)	AppliChem (Darmstadt, Germany)
Calcium chloride	Roth (Karlsruhe, Germany)
Chrono-Lume [®] (d-luciferase/luciferin reagent +ATP standard)	Probe & go (Osburg, Germany)
Complete mini protease inhibitors (+EDTA)	Roche Diagnostics (Mannheim, Germany)
Convulxin (CVX)	Enzo Lifesciences (Lörrach, Germany)
Disodiumhydrogenphosphate	Roth (Karlsruhe, Germany)
DMEM medium	Gibco (Karlsruhe, Germany)
dNTP mix	Fermentas (St. Leon-Rot, Germany)
Dry milk, fat-free	AppliChem (Darmstadt, Germany)
Dylight-488	Pierce (Rockford, IL, USA)
EDTA	AppliChem (Darmstadt, Germany)
Ethanol	Roth (Karlsruhe, Germany)

Ethidium bromide	Roth (Karlsruhe, Germany)
Fentanyl	Janssen-Cilag (Neuss, Germany)
Fetal calf serum (FCS)	Gibco (Karlsruhe, Germany)
Fibrillar type I collagen (Horm)	Nycomed (Munich, Germany)
Flumazenil	Delta Select (Dreieich, Germany)
Fluo-3 acetoxymethyl ester (AM)	Invitrogen (Karlsruhe, Germany)
Fluorescein-isothiocyanate (FITC)	Molecular Probes (Oregon, USA)
Forene® (isoflurane)	cp-pharma (Burgdorf, Germany)
Fura2 acetoxymethyl ester (AM)	Invitrogen (Karlsruhe, Germany)
GeneRuler 1kb DNA Ladder	Fermentas (St. Leon-Rot, Germany)
Glucose	Roth (Karlsruhe, Germany)
HEPES	Roth (Karlsruhe, Germany)
Heparin sodium	Ratiopharm (Ulm, Germany)
Human fibrinogen	Sigma-Aldrich (Schnelldorf, Germany)
IGEPAL CA-630	Sigma-Aldrich (Schnelldorf, Germany)
Immobilon-P transfer membrane	Millipore (Schwalbach, Germany)
Indomethacin	Alfa Aesar (Karlsruhe, Germany)
IP ₁ ELISA kit	Cisbio (Paris, France)
Iron-III-chloride hexahydrate (FeCl ₃ 6H ₂ O)	Roth (Karlsruhe, Germany)
Isopropanol	Roth (Karlsruhe, Germany)
Lipofectamine® 2000	Invitrogen (Karlsruhe, Germany)
Loading Dye solution, 6x	Fermentas (St. Leon-Rot, Germany)
Magnesium chloride	Roth (Karlsruhe, Germany)
Magnesium sulfate	Roth (Karlsruhe, Germany)
Medetomidine (Dormitor)	Pfizer (Karlsruhe, Germany)
Midazolam (Dormicum)	Roche (Grenzach-Wyhlen, Germany)
Midori Green Advanced DNA stain	Nippon Genetics Europe (Düren, Germany)

Naloxon	Delta Select (Dreieich, Germany)
1-oleoyl-2-acetyl-sn-glycerol (OAG)	Sigma (Schnelldorf, Germany)
PageRuler prestained protein ladder	Fermentas (St. Leon-Rot, Germany)
Paraformaldehyde (PFA)	Roth (Karlsruhe, Germany)
Penicillin-Streptomycin	Gibco (Karlsruhe, Germany)
Phalloidin-rhodamine	Invitrogen (Karlsruhe, Germany)
Phalloidin-Atto647N	AttoTec GmbH (Siegen, Germany)
Phenol/chloroform/isoamylalcohol	AppliChem (Darmstadt, Germany)
Pluronic F-127	Invitrogen (Karlsruhe, Germany)
Potassium acetate	Roth (Karlsruhe, Germany)
Potassium chloride	Roth (Karlsruhe, Germany)
Prostacyclin (PGI ₂)	Sigma (Schnelldorf, Germany)
Protease inhibitor cocktail (100x)	Sigma-Aldrich (Schnelldorf, Germany)
Proteinase K	Fermentas (St. Leon-Rot, Germany)
RNeasy Mini Kit	Qiagen (Hilden, Germany)
R-phycoerythrin (PE)	EUROPA (Cambridge, UK)
Rotiphorese gel 30 acrylamide	Roth (Karlsruhe, Germany)
Serotonin ELISA kit	LDN (Nordhorn, Germany)
Sodium chloride	AppliChem (Darmstadt, Germany)
Sodium citrate	AppliChem (Darmstadt, Germany)
Sodiumdihydrogenphosphate	Roth (Karlsruhe, Germany)
Sodium hydroxide	AppliChem (Darmstadt, Germany)
Sodium orthovanadate	Sigma (Schnelldorf, Germany)
Taq polymerase	Fermentas (St. Leon-Rot, Germany)
Taq polymerase buffer (10x)	Fermentas (St. Leon-Rot, Germany)
Tetramethylethylenediamine (TEMED)	Roth (Karlsruhe, Germany)
Thapsigargin (TG)	Invitrogen (Karlsruhe, Germany)
Thrombin	Roche Diagnostics (Mannheim)

TxB ₂ ELISA kit	DRG (Marburg, Germany)
Triton X-100	AppliChem (Darmstadt, Germany)
Tween 20	Roth (Karlsruhe, Germany)
U46619	Enzo Lifesciences (Lörrach, Germany)
Western lightning chemiluminescence (ECL)	PerkinElmer LAS (Boston, USA)

Collagen-related peptide (CRP) was a gift from Prof. Dr. S.P. Watson (University of Birmingham, UK). Rhodocytin was provided by Prof. Dr. J. Eble (University Hospital Frankfurt, Germany). Annexin V-Dylight-488 was provided by Jonathan F. Tait, Medical Center, University of Washington. All Primers were purchased from Metabion (Planegg-Martinsried, Germany). All non-listed chemicals were obtained from AppliChem (Darmstadt, Germany), Sigma (Schnelldorf, Germany) or Roth (Karlsruhe, Germany).

2.1.2 Antibodies

2.1.2.1 Purchased primary and secondary antibodies

Reagent	Company
Anti-phosphotyrosine 4G10	Millipore (CA, USA)
Goat anti-rabbit IgG-Alexa-488	Invitrogen (Karlsruhe, Germany)
Rabbit anti-actin (no. A2066)	Sigma-Aldrich (Schnelldorf, Germany)
Rat anti-mouse IgG-HRP	DAKO (Hamburg, Germany)
Rat anti-tubulin IgG	Millipore (CA, USA)
Rabbit anti-LAT (no. 9166)	Cell Signaling (Danvers, MA, USA)
Rabbit anti-phospho-LAT (Y191) (no. 3584)	Cell Signaling (Danvers, MA, USA)
Rabbit anti-PLC γ 2 (product Q20)	Santa Cruz Biotechnology (Heidelberg, Germany)
Rabbit anti-phospho-PLC γ 2 (Y759) (no.3874)	Cell Signaling (Danvers, MA, USA)
Rabbit anti-Syk (clone D115Q)	Cell Signaling (Danvers, MA, USA)
Rabbit anti-phospho-Syk (Y525/526) (clone C87C1)	Cell Signaling (Danvers, MA, USA)
Mouse anti- α -tubulin (clone B-5-1-2)	Sigma-Aldrich (Schnelldorf, Germany)

Anti-TRPM7 and anti-phospho-TRPM7 antibodies were kindly provided by Prof. Dr. Thomas Gudermann (Walther-Straub Institute for Pharmacology and Toxicology, LMU München).

2.1.2.2 Monoclonal antibodies (mAbs) used for flow cytometry

mAbs generated and modified in our laboratory

Antibody	Isotype	Antigen	Described in
DOM2	IgG1	GPV	125
INU1	IgG1 κ	CLEC-2	7
JAQ1	IgG2a	GPVI	157
JON/A	IgG2b	GPIIb/IIIa	158
JON1	IgG2a	GPIIb/IIIa	159
p0p4	IgG2b	GPIb α	159
p0p6	IgG2b	GPIX	159
ULF1	IgG2a	CD9	159
WUG1.9	IgG1	P-selectin	unpublished
12C6	IgG2b	α 2 integrin	unpublished

2.1.3 Mice

Trpc6^{-/-} mice were kindly provided by Prof. Dr. Alexander Dietrich (Walther-Straub Institute for Pharmacology and Toxicology, LMU München). In *Trpc6*^{-/-} mice, the exon 7 of the *Trpc6* gene was replaced by a positive selective marker (PGK-NGO).¹⁶⁰

Orai1^{-/-} mice were generated with gene-trap technology. A “ β -Geo” cassette, encoding a fusion of β -galactosidase and neomycin phosphotransferase, was inserted in the first intron of the *Orai1* gene.¹⁶¹ Dr. Attila Braun obtained *embryonic stem* (ES) cell clone (XL922) containing the disrupted *Orai1* gene from BayGenomics (University of California San Francisco, San Francisco, CA), and the ES cells were then microinjected into C57Bl/6 blastocysts to generate *Orai1*^{-/-} mice.²⁶ However, *Orai1*^{-/-} mice displayed high mortality. 60% of *Orai1*^{-/-} mice died shortly after birth for unknown reasons. Furthermore, surviving *Orai1*^{-/-} animals had significantly development defects and all animals died at latest 4 weeks after birth. Therefore, *bone marrow* (BM) chimeric mice, transplanted with fetal liver cells or BM cells, were generated.

To obtain fetal liver cells of *Wt*, *Orai1^{-/-}* and *Orai1^{-/-}/Trpc6^{-/-}* mice, *Trpc6^{-/-}* mice were crossed with *Orai1^{+/-}* mice to generate *Trpc6^{+/-}/Orai1^{+/-}* mice. *Trpc6^{+/-}/Orai1^{+/-}* male mice crossed with *Trpc6^{+/-}/Orai1^{+/-}* female mice to generate *Trpc6^{+/+}/Orai1^{+/+}* (wild-type), *Trpc6^{+/+}/Orai1^{-/-}* (Orai1 knock-out) and *Trpc6^{-/-}/Orai1^{-/-}* (Orai1 and TRPC6 double knock-out) embryos, which were isolated at embryonic day 13.5. Thereafter, fetal liver cells were isolated for transplantation.

TRPM7 “kinase-dead” mice (*Trpm7^{Kl}*) were kindly provided by Prof. Dr. Thomas Gudermann and Dr. Vladimir Chubanov (Walther-Straub Institute for Pharmacology and Toxicology, LMU München). In *Trpm7^{Kl}* mice, an amino acid residue in the kinase domain was mutated from lysine to arginine, leading to disruption of the kinase catalytic activity.

2.1.4 Buffers and media

All buffers were prepared in deionized water obtained from a MilliQ Water Purification System (Millipore, Schwalbach, Germany). pH was adjusted with HCl or NaOH.

Acid-citrate-dextrose (ACD) buffer, pH 4.5

Trisodium citrate dehydrate	85 mM
Anhydrous citric acid	65 mM
Anhydrous glucose	110 mM

Blocking solution for immunoblotting

Washing buffer (TBS-T, see below)	
BSA or fat-free dry milk	5%

Bone marrow or fetal liver cell freezing medium

DMEM	40%
FCS	50%
DMSO	10%

FACS buffer

PBS (1x)	
FCS	1%
NaN ₃	0.02%

Immunoprecipitation (IP) buffer, pH 8.0

TRIS/HCl, pH 8.0	15 mM
NaCl	155 mM
EDTA	1 mM
NaN ₃	0.005%

Laemmli buffer for SDS-PAGE

TRIS	40 mM
Glycine	0.95 mM
SDS	0.5%

Lysis buffer (for DNA isolation), pH 7.2

TRIS base	100 mM
EDTA	5 mM
NaCl	200 mM
SDS	0.2%
Proteinase K (to be added directly before use)	100 µg/mL

Lysis buffer 2x (for tyrosine phosphorylation assay), pH 7.5

TRIS base	20 mM
NaCl	300 mM
EDTA	2 mM
EGTA	2 mM
IGEPAL CA-630	2%
NaF	10 mM
to be added directly before use:	
Na ₃ VO ₄	2 mM
Complete mini protease inhibitor <i>or</i> protease inhibitor cocktail (100x)	1 tablet/10 mL 2%

PHEM, pH 7.2

PIPES	60 mM
HEPES	25 mM
EGTA	10 mM
MgSO ₄	2 mM

PHEM complete pH 7.2

PHEM buffer	
PFA	1%
NP-40	0.005%

Phosphate buffered saline (PBS), pH 7.14

NaCl	137 mM
KCl	2.7 mM
KH ₂ PO ₄	1.5 mM
Na ₂ HPO ₄	8 mM

Sample buffer for agarose gels, 6x

Tris buffer (150 mM)	33%
Glycerine	60%
Bromophenol blue (3',3'',5',5''-tetrabromophenol-sulfonphthalein)	0.04%

SDS sample buffer, 4x

β-mercaptoethanol (for reducing conditions)	20%
TRIS buffer (1 M), pH 6.8	20%
Glycerine	40%
SDS	4%
Bromophenol blue	0.04%

Separating gel buffer (Western Blot), pH 8.8

TRIS/HCl	1.5 M
----------	-------

Stacking gel buffer (Western Blot), pH 6.8

TRIS/HCl	0.5 M
----------	-------

TAE buffer, 50x, pH 8.0

TRIS	0.2 M
Acetic acid	5.7%
EDTA	50 mM

TE buffer, pH 8.0

TRIS base	10 mM
EDTA	1 mM

Transfer buffer

Tris Ultra	50 mM
Glycine	40 mM
Methanol	20%

Tris-buffered saline (TBS), pH 7.3

NaCl	137 mM
TRIS/HCl	20 mM

Tyrode's buffer, pH 7.3

NaCl	137 mM
KCl	2.7 mM
NaHCO ₃	12 mM
NaH ₂ PO ₄	0.43 mM
CaCl ₂	0 or 2 mM
MgCl ₂	1 mM
HEPES (4-(2-hydroxyethyl)-1-piperazineethanesulfonic acid)	5 mM
to be added directly before use:	
BSA	0.35%
Glucose	0.1%

Washing buffer for immunoblotting (TBS-T)

TBS (1x)	
Tween 20	0.1%

Washing buffer for ELISA

PBS (1x)	
Tween 20	0.1%

Washing buffer for IP₁ ELISA

H ₂ O	
Tween 20	0.1%

2.2 Methods**2.2.1 RNA isolation and reverse transcription PCR (RT-PCR)**

To isolate platelet RNA, 2×10^6 platelets/ μ L were washed twice in PBS/EDTA and finally suspended in 200 μ L IP buffer with 1% NP-40. 800 μ L of Trizol reagent was added to the samples and incubated for 60 min at 4°C. After incubation, 200 μ L of chloroform were added and then incubated for 15 min at 4°C. Samples were then centrifuged at 10,000 rpm for 10 min. The upper phase of samples was collected and incubated with three volumes of 70% ethanol with 10% sodium acetate (pH 5.2) for 1 hour at -20°C. After that, samples were

centrifuged at 14,000 rpm for 15 min. The pellet was washed with 70% ethanol, then centrifuged again and dried at 37°C. 30-40 µL of RNase free water was added to solve the pellet and the concentration was determined by absorbance readings at 260 nm, whereas the ratio of absorbance at 260/280 and 260/230 was used to assess the purity. Samples with 260/280 readings of >1.8 and 260/230 readings of >1.9 were used to prepare cDNA.

1-2 µg RNA were incubated with 1 µL Oligo dNTP (0.5 µg/µL) in a total volume of 11.9 µL at 70°C for 5 min and afterwards were transferred on ice. 2 µL DTT (0.1 M), 1 µL dNTPs (10 mM), 0.5 U RNase inhibitor, 4 µL 5x first strand buffer and 200 U Super Script Reverse Transcriptase were added. The total volume was adjusted to 40 µL by using RNase-free water and the samples were incubated at 42°C for 1 hour. A gradient *polymerase chain reaction* (PCR) was used to determine the suitable annealing temperature. Afterwards, a PCR with the appropriate annealing temperature was performed.

The following RT-PCR primers were used to study the expression of Mg²⁺ channel proteins in mouse platelets:

Gene	RT-PCR primers	Size of cDNA fragment (bp)
MagT1	Fwd.: 5'-tcggaccgtgctggaagaaa-3' Rev.: 5'-gagctttaacaagacgacgg-3'	255
Tusc3	Fwd.: 5'-tactggtagctttccctcc-3' Rev.: 5'-attcttcgtagcctgcctg-3'	263
Acdp1	Fwd.: 5'-tgttcgtcaaagactggcc-3' Rev.: 5'-ggatctccgactgatgatc-3'	261
Acdp2	Fwd.: 5'-aagactggccttcgtggat-3' Rev.: 5'-acaggtctgtctcatccaag-3'	270
Acdp3	Fwd.: 5'-atacctaaactggacgctgtc-3' Rev.: 5'-cagacacctgaataaggag-3'	267
Acdp4	Fwd.: 5'-ctacactcgcattcctgtgt-3' Rev.: 5'-gatgacgtcctccagagtga-3'	289
Nipa1	Fwd.: 5'-tagtgaacgggtccacgttc-3' Rev.: 5'-ttagcagacagcccaactg -3'	267
Nipa2	Fwd.: 5'-gaactactctgccgtggta-3' Rev.: 5'-tcatagccaatcccagacca-3'	262
Nipa3	Fwd.: 5'-caatctgtatgtgggcttg-3' Rev.: 5'-ttatgagaacgctcagagcc-3'	233

Nipa4	Fwd.: 5'-accttgatcacctggcaaga-3' Rev.: 5'-tcgcaggtgcaaagcatag-3'	259
Slc41A1	Fwd.: 5'-ctcctttccattggactgc-3' Rev.: 5'-atcatccgccagagctcctt-3'	246
Slc41A2	Fwd.: 5'-catggctctgcagatattgg-3' Rev.: 5'-gtatgatggctgccacagct-3'	311
Slc41A3	Fwd.: 5'-gagacgtccctgatcattgg-3' Rev.: 5'-catcgattgccccagtggtg-3'	226
Trpm6	Fwd.: 5'-tgtgggcggtgctcatgaag-3' Rev.: 5'-caagccattcgtgcacgctg-3'	450
Trpm7	Fwd.: 5'-gagcccaacagatgcttatgg-3' Rev.: 5'-ggcccgcttcaaatacaag-3'	550
Actin	Fwd.: 5'-gtgggcccgtctaggcaccaa-3' Rev.: 5'-ctctttgatgtcacgcagatttc-3'	500

2.2.2 Mouse Genotyping

2.2.2.1 Mouse DNA isolation

Approximately half of the mouse ear was dissolved in 500 μ L lysis buffer at 55°C overnight under shaking conditions (900 rpm) in a Thermomixer comfort (Eppendorf, Hamburg, Germany). Samples were mixed with phenol/chloroform/isoamyl alcohol (1:1). After that, samples were centrifuged at 11,000 rpm for 10 min at *room temperature* (RT). The upper phase was carefully transferred to a new tube containing 500 μ L isopropanol. After vigorous shaking, the samples were centrifuged at 14,000 rpm for 10 min at 4°C. Subsequently, the supernatant was discarded and the DNA pellet was washed with 500 μ L of 70% ethanol and centrifuged again at 14,000 rpm for 10 min at 4°C. Next, ethanol was removed and the pellet was dried for approximately 30 min at 37 °C. Finally, the pellet was dissolved by adding 80-100 μ L TE buffer and shaking (300 rpm) for 30 min at 37°C. Usually, 1-2 μ L DNA solution were used for a PCR reaction.

2.2.2.2 Detection of the *Trpc6*^{-/-} by PCR

Primers:

Trpc6 Wt Fwd: 5'-cagatcatctctgaaggctttatgc-3'

Trpc6 Wt Rev: 5'-tgtgaatgcttcattctgttttgcgcc-3'

Trpc6 KO Fwd: 5'-gggtttaatgtctgtatcactaaagcctcc-3'

Trpc6 KO Rev: 5'-acgagactagtggagacgtgctactcc-3'

Pipetting scheme:

2 µL	genomic DNA
5 µL	Taq-buffer (10x)
5 µL	MgCl ₂ (25 mM)
1 µL	dNTPs (10 mM)
1 µL	<i>Trpc6</i> Wt Fwd primer (1:10 in H ₂ O, stock 100 µM)
1 µL	<i>Trpc6</i> Wt Rev primer (1:10 in H ₂ O, stock 100 µM)
1 µL	<i>Trpc6</i> KO Fwd primer (1:10 in H ₂ O, stock 100 µM)
1 µL	<i>Trpc6</i> KO Rev primer (1:10 in H ₂ O, stock 100 µM)
0.2 µL	Taq-Polymerase (0.5 U/µL)
32.8 µL	H ₂ O

PCR-Program:

96°C	3 min	
94°C	30 s	35x
56°C	30 s	
72°C	30 s	
72°C	5 min	
4°C	stop	

Results (expected band sizes):

Wt: 234 bp

Trpc6^{-/-}: 339 bp

2.2.2.3 Detection of the *Orai1*^{-/-} by PCR

Primers:

Orai1 Wt Fwd: 5'-ctcttgagaggaagaactt-3'

Orai1 Wt Rev: 5'-gatccctaggacccatgtgg-3'

Orai1 KO Fwd: 5'-ttatcgatgagcgtgggttatcc-3'

Orai1 KO Rev: 5'-gcgcgtagatcgggcaaataatc-3'

Pipetting scheme for *Wt* allele:

1 μ L	genomic DNA
5 μ L	Taq-buffer (10x)
5 μ L	MgCl ₂ (25 mM)
1 μ L	dNTPs (10 mM)
1 μ L	<i>Orai1 Wt</i> Fwd primer (1:10 in H ₂ O, stock 100 μ M)
1 μ L	<i>Orai1 Wt</i> Rev primer (1:10 in H ₂ O, stock 100 μ M)
0.5 μ L	Taq-Polymerase (0.5 U/ μ L)
35.5 μ L	H ₂ O

Pipetting scheme for *KO* allele:

1 μ L	genomic DNA
2.5 μ L	Taq-buffer (10x)
2.5 μ L	MgCl ₂ (25 mM)
0.5 μ L	dNTPs (10 mM)
0.5 μ L	<i>Orai1 KO</i> Fwd primer (1:10 in H ₂ O, stock 100 μ M)
0.5 μ L	<i>Orai1 KO</i> Rev primer (1:10 in H ₂ O, stock 100 μ M)
0.25 μ L	Taq-Polymerase (0.5 U/ μ L)
19.25 μ L	H ₂ O

PCR-Program for *Wt*:

96°C	3 min	
94°C	30 s	35x
56°C	30 s	
72°C	30 s	
72°C	5 min	
4°C	stop	

PCR-Program for *Orai1*^{-/-}:

96°C	3 min	
94°C	30 s	40x
51.4°C	30 s	
72°C	60 s	
72°C	5 min	
4°C	stop	

Results (expected band sizes):

Wt: 900 bp
Orai1^{-/-}: 650 bp

2.2.2.4 Detection of the *Trpm7^{KI}* by PCR**Primers:**

Trpm7 KIN Fwd: 5'-aatgggaggtggttacg-3'
Trpm7 KIN Rev: 5'-ctcagatcacagcttacagtca-3'

Pipetting scheme:

1 µL	genomic DNA
5 µL	Taq-buffer (10x)
5 µL	MgCl ₂ (25 mM)
1 µL	dNTPs (10 mM)
1 µL	<i>Trpm7 KIN Fwd</i> primer (1:10 in H ₂ O, stock 100 µM)
1 µL	<i>Trpm7 KIN Rev</i> primer (1:10 in H ₂ O, stock 100 µM)
0.2 µL	Taq-Polymerase (0.5 U/µL)
35.8 µL	H ₂ O

PCR-Program:

96°C	3 min	
94°C	30 s	40x
62°C	30 s	
72°C	30 s	
72°C	5 min	
4°C	stop	

Results (expected band sizes):

Wt: 120 bp + 85 bp
Trpm7^{KI}: 205 bp

2.2.3 Fetal liver cell or bone marrow transplantation

For the generation of bone marrow chimeras, 5-6 week-old C57Bl/6 mice were irradiated with a single dose of electron beam radiotherapy (10 Gy). Fetal liver cells from *Wt*, *Orai1^{-/-}* and *Orai1^{-/-}/Trpc6^{-/-}* embryos or bone marrow cells from 6-8 week-old *Wt*, *Orai1^{-/-}* and *Orai1^{-/-}/Trpc6^{-/-}* BM chimeric mice were injected intravenously into the irradiated C57Bl/6 mice

(4×10^6 cells/mouse) for transplantation. Acidified water containing 2 g/L neomycin was provided to the mice for 2 weeks.

2.2.4 Tyrosine phosphorylation assay

For tyrosine phosphorylation assay, washed platelets at a concentration of 7×10^5 platelets/ μL were activated with 1 $\mu\text{g}/\text{mL}$ CRP under constant stirring conditions. Stimulation was stopped by adding an equal volume of ice-cold lysis buffer at the indicated time points. After incubation on ice for 30 min, lysed samples were centrifuged at 14,000 rpm for 5 min at 4°C and the supernatant was mixed with 4 \times SDS sample buffer. Samples were incubated at 70°C for 10 min. After that, 15-25 μL per sample were loaded onto a gel with 4% stacking part and 12% separating part. After separation, proteins were transferred onto a *polyvinylidene difluoride* (PVDF) membrane. PVDF Membrane was blocked for 1 hour at RT in blocking buffer and then incubated with the primary antibody at 4°C overnight. The membrane was then washed 3 \times 10 min in washing buffer before incubation with the appropriate secondary HRP-labeled antibody for 1 hour at RT. Finally, the membrane was washed three times and proteins were visualized by ECL.

2.2.5 Cell cultures, transient expression

For transient expression of TRPM7 constructs, human embryonic kidney (HEK) 293 cells were maintained at 37°C and 5% CO_2 in Earle's minimal essential medium supplemented with 10% *fetal calf serum* (FCS), 100 $\mu\text{g}/\text{mL}$ streptomycin and 100 U/mL penicillin. Cells were transiently transfected using the Lipofectamine 2000 reagent.

2.2.6 Electrophysiology

Mouse embryonic fibroblast (MEF) cells were isolated from *Wt* or *Trpm7^{Kl}* embryos. On these MEF cells, patch clamp experiments were performed at a whole-cell configuration. Currents were elicited by a ramp protocol from -100 mV to +100 mV over 50 ms acquired at 0.5 Hz and a holding potential of 0 mV. Inward current amplitudes were extracted at -80 mV, outward currents at +80 mV and plotted versus time. Data were normalized to cell size as pA/pF. Capacitance was measured using the automated capacitance cancellation function of the EPC10 (HEKA, Lambrecht, Germany). Values over time were normalized to the cell size measured immediately after whole-cell break-in. Nominally Mg^{2+} -free extracellular solution contained (in mM): 140 NaCl, 3 CaCl_2 , 2.8 KCl, 0 MgCl_2 , 10 HEPES-NaOH, 11 Gluc (pH 7.2, 300 mOsm). Intracellular solution contained (in mM): 120 Cs-glutamate, 8 NaCl, 1 MgCl_2 , 10 HEPES, 10 BAPTA, 5 EDTA (pH 7.2, 300 mOsm).

2.2.7 Determination of Mg²⁺ levels in the serum and bones

8 week-old male mice were killed and the blood samples were obtained from the heart. The corresponding serum samples were isolated by centrifugation (1.2 g, 15 min at RT). Right tibias were dissected and cleaned from the muscle tissues. Next, the bones were dried for 48 hours at 65 °C. Mg²⁺ levels in the obtained serum and bone samples were determined using inductively coupled plasma-sector field mass spectrometry (ALS laboratories, Sweden).

2.2.8 *In vitro* analysis of platelet function

2.2.8.1 Platelet preparation and washing

Mice, under isoflurane anesthesia, were bled from the retroorbital plexus. 700 µL blood were collected into a 1.5 mL tube containing either 300 µL heparin in TBS (20 U/mL, pH 7.3) or 300 µL ACD. 200 µL heparin or ACD were added and blood was centrifuged at 1800 rpm (Eppendorf Centrifuge 5415C) for 5 min at RT. Supernatant and buffy coat were transferred to a tube containing 200 µL heparin or ACD, and were centrifuged at 800 rpm for 5 min at RT to obtain *platelet rich plasma* (PRP). For washed platelets, PRP was centrifuged at 2800 rpm for 5 min at RT in the presence of apyrase (0.02 U/mL) and *prostacyclin* (PGI₂) (0.1 µg/mL), and the pellet was suspended in 1 mL Ca²⁺-free Tyrode's buffer with PGI₂ and apyrase. After 10 min incubation at 37°C, the sample was centrifuged at 2,800 rpm for 5 min. After centrifugation, platelets were resuspended once more in 1 mL Ca²⁺-free Tyrode's buffer with PGI₂ and apyrase, the platelet numbers were determined by taking a 1:1 dilution of the platelet solution and the platelet count was measured in a Sysmex KX-21N automated hematology analyzer (Sysmex Corp., Kobe, Japan). Finally, the platelets was resuspended in the appropriate volume of Tyrode's buffer containing apyrase (0.02 U/mL) to reach the required platelet concentration.

2.2.8.2 Platelet counting

To determine platelet count and size, 50 µL blood were taken from the retroorbital plexus of anesthetized mice by using heparinized microcapillaries and collected into a tube containing 300 µL heparin in TBS (20 U/mL, pH 7.3). Platelet count and size were determined by using a Sysmex KX-21N automated hematology analyzer.

2.2.8.3 Flow cytometry

50 µL of blood were taken and collected into a tube containing 300 µL heparin in TBS (20 U/mL, pH 7.3). 1 mL Ca²⁺-free Tyrode's buffer was added into the tube. To determine basal glycoprotein expression levels, 50 µL of diluted blood were stained with saturating

amounts of fluorophore-conjugated antibodies for 15 min at RT, and were analyzed directly after addition of 500 μ L PBS on a FACSCalibur flow cytometer using Cell Quest™ software (Becton Dickinson, Heidelberg, Germany). For platelet activation studies, blood samples were washed twice (2,800 rpm, 5 min, RT) in Tyrode's buffer without Ca^{2+} and finally resuspended in Tyrode's buffer with 2 mM Ca^{2+} . Platelets were activated with appropriately diluted agonists for 7 min at 37°C followed by 7 min at RT in the presence of saturating amounts of PE-coupled JON/A (4H5) and FITC-coupled anti-P-selectin (5C8) antibodies. The reaction was stopped by addition of 500 μ L PBS and samples were analyzed with a FACSCalibur. For a two-color staining, the following settings were used:

Detectors/Amps:

Parameter	Detector	Voltage
P1	FSC	E01
P2	SSC	380
P3	FI1	650
P4	FI2	580
P5	FI3	150

Threshold:

Value	Parameter
253	FSC-H
52	SSC-H
52	FI1-H
52	FI2-H
52	FI3-H

Compensation:

Detector	Setting
FI1	2.4% of FI2
FI2	7.0% of FI1
FI2	0% of FI3
FI3	0% of FI2

2.2.8.4 Determination of phosphatidylserine exposure by flow cytometry

Washed platelets were resuspended in Tyrode's buffer with 2 mM Ca^{2+} at the concentration of 5×10^4 platelets/ μL . 50 μL of this suspension were stimulated with agonists for 15 min at 37°C in the presence of DyLight-488 coupled annexin V, which stains exposed PS. After that, 500 μL Tyrode's buffer with 2 mM Ca^{2+} were added to stop the reaction and the samples were immediately analyzed with a FACSCalibur flow cytometer.

2.2.8.5 Aggregometry

For determination of platelet aggregation, washed platelets in Ca^{2+} -free Tyrode's buffer were adjusted to a concentration of 5×10^5 platelets/ μL . Alternatively, heparinized PRP (for measurements with ADP) was used at a concentration of 5×10^5 platelets/ μL . 50 μL of washed platelets suspension or PRP were transferred into a cuvette containing 110 μL Tyrode's buffer with 2 mM Ca^{2+} . For all measurements with washed platelets, except those with thrombin as agonist, 100 $\mu\text{g}/\text{mL}$ human fibrinogen were added into Tyrode's buffer. Platelet agonists or reagents (100-fold concentrated) were added to the cuvette and light transmission was recorded over 10 min on a Fibrinometer 4 channel aggregometer (Apact 4-channel optical aggregation system, APACT, Hamburg, Germany). For calibration, Tyrode's buffer (for washed platelets) or plasma (for PRP) was set as 100% aggregation and washed platelet suspension or PRP without stimulation was set as 0% aggregation.

2.2.8.6 Adhesion under flow conditions

Rectangular coverslips (24 x 60 mm) were coated with 200 $\mu\text{g}/\text{mL}$ fibrillar type-I collagen (Horm) at 37°C overnight and then were blocked with 1% BSA at RT for 1 hour. Blood (700 μL) was collected into 300 μL heparin (20 U/ mL in TBS, pH 7.3). Whole blood was diluted 2:1 in Tyrode's buffer with Ca^{2+} and labeled with a DyLight-488 conjugated α -GPIX Ig derivative (0.2 $\mu\text{g}/\text{mL}$) for 6 min at 37°C. The diluted blood then was filled into a 1 mL syringe, which was connected to a transparent flow chamber with a slit depth of 50 μm , equipped with the coated coverslips. Perfusion was performed using a pulse-free pump under high shear stress equivalent to a wall shear rate of 1,000 s^{-1} for 4 min. Thereafter, coverslips were washed for 2 min by perfusion with Tyrode's buffer at the same shear rate and phase-contrast and fluorescent images were recorded from at least five different microscopic fields (40 \times objective) using a Zeiss Axiovert 200 microscope equipped with a CoolSNAP-EZ camera (Visitron, Munich, Germany). Image analysis was performed off-line using MetaVue software (Visitron, Munich, Germany). Thrombus formation was expressed as the mean percentage of total area covered by thrombi and as the mean integrated fluorescence intensity per mm^2 .

2.2.8.7 Determination of PS exposing platelets after perfusion

Rectangular coverslips were coated with 200 µg/mL type I collagen overnight at 37°C, and blocked with 1% BSA. Chamber and tubing were prewashed with HEPES buffer with 5 U/mL heparin to prevent coagulation. The heparinized whole blood was perfused through the flow chamber for 4 min at a shear rate of 1000 s⁻¹. HEPES buffer containing 5 U/mL heparin, 2 mM CaCl₂ and 250 ng/mL of Annexin V-Dylight-488 was then perfused through the flow chamber for 4 min, and then HEPES buffer was perfused for 2 min to remove unbound Annexin V-Dylight-488. Phase-contrast and fluorescent images were obtained from at least 10 different collagen-containing microscopic fields, which were randomly chosen. Image analysis was performed off-line using Metavue software.

2.2.8.8 Intracellular Ca²⁺ measurements

Platelets were washed once and adjusted to a concentration of 2×10⁵ platelets/µL in Tyrode's buffer without Ca²⁺. Platelets were loaded with Fura2/AM (5 µM) by incubating with Fura2/AM in the presence of Pluronic F-127 (0.2 µg/mL) for 30 min at 37°C. After incubation, labeled platelets were washed and resuspended in Tyrode's buffer with or without 1 mM Ca²⁺. Magnetically stirred platelets were activated with different agonists and fluorescence was determined with a PerkinElmer LS 55 fluorimeter (Waltham, MA) with excitation at 340 and 380 nm and emission at 509 nm. Each measurement was calibrated using Triton X-100 and EGTA. To determine the relative Ca²⁺ concentrations in the cytoplasm ([Ca²⁺]_{cyt}), anticoagulated blood samples from *Wt* and mutant mice were loaded with 5 µM Fluo-3/AM in the presence of Pluronic F-127 for 30 min and diluted in Tyrode's buffer with 1 mM Ca²⁺. Platelets were stained and gated with *phycoerythrin* (PE)-conjugated anti-αIIbβ3 complex monoclonal antibody (14A3-PE, Emfret Analytics, Würzburg, Germany). *Mean fluorescence intensity* (MFI) of Fluo-3 in resting platelets was measured using flow cytometry.

2.2.8.9 Measurement of ATP release

Platelets were washed twice and adjusted to a concentration of 5×10⁵ platelets/µL. ATP secretion was measured using CHRONO-LUME reagent according to the manufacturer's protocol on a Chronolog aggregometer (Chrono-Log Corp. Philadelphia, PA, USA). 5µL of luciferase reagent was added directly to the platelets under constant stirring, and then indicated concentrations of various agonists were added to study ATP release. The luminescence intensity was measured at a setting of ×0.005.

2.2.8.10 Measurement of *inositol 1 phosphate* (IP₁)

Platelets were washed twice with phosphate- and Ca²⁺-free Tyrode's buffer, and were

adjusted to the final concentration of 8×10^5 platelets/ μL in phosphate-free Tyrode's buffer containing 2 mM Ca^{2+} , 50 mM Li^+ , 10 μM Indomethacin and 2 U/mL apyrase. Platelets were activated with the indicated agonists for 5 min at 37°C with constant shaking at 450 rpm. After stimulation, platelets were lysed in the buffer supplied with the kit. 50 μL of lysed platelets were used for the IP_1 ELISA assay according to the manufacturer's protocol (Cisbio, Codolet, France).

2.2.8.11 Measurement of *thromboxane B₂* (TxB₂) release

Washed platelets were adjusted to a concentration of 5×10^5 platelets/ μL and stimulated with the indicated agonists for 5 min. Then, 5 mM EDTA and 1 mM aspirin were added. Platelets were removed by centrifugation and the supernatant was collected. TxB_2 concentrations in the supernatant were measured with the TxB_2 ELISA kit according to the manufacturer's instructions of TxB_2 ELISA kit (DRG, Marburg, Germany).

2.2.8.12 Measurement of serotonin release

Washed platelets (5×10^5 platelets/ μL) were prepared as for standard aggregometry and were stimulated with indicated concentrations of various agonists for 5 min. Activated platelets were removed by centrifugation, and the supernatant was kept for ELISA, which was performed according to the manufacturer's protocol (LDN, Nordhorn, Germany) to measure serotonin concentrations.

2.2.8.13 Measurement of PLD activity

Washed platelets (3×10^5 platelets/ μL) were labeled with [^3H]myristic acid for 1.5 hours at 37°C . After labeling, platelets were pre-incubated with 0.5% ethanol then activated with agonists or TG in the presence or absence of 1 mM Ca^{2+} . Reactions were stopped by addition of 500 μL ice-cold chloroform/methanol followed by incubation on ice. 500 μL of ice-cold chloroform and 350 μL of water were added to extract the lipids via thin layer chromatography. [^3H]Ptd-EtOH bands were identified and quantified via scintillation counting. PLD activity is depicted as percentage of phosphatidylethanol of total [^3H]-labeled phospholipids.

2.2.8.14 Spreading assay

Rectangular coverslips (24 x 60 mm) were coated with 100 $\mu\text{g}/\text{mL}$ human fibrinogen overnight at 4°C under humid conditions and blocked for at least 1 hour with 1% BSA at RT. The coverslips were rinsed with Tyrode's buffer. Platelets were isolated from blood, washed twice with Ca^{2+} -free Tyrode's buffer, and then adjusted to a concentration of 1×10^5

platelets/ μL . 100 μL of the platelet suspension were activated with 0.01 U/mL thrombin and immediately placed on fibrinogen-coated coverslips. Platelets were allowed to spread for the indicated time, and then the process was stopped by addition of 300 μL 4% PFA/PBS. Excessive liquid was removed and platelets were visualized by *differential interference contrast* (DIC) microscopy with a Zeiss Axiovert 200 inverted microscope (100 \times /1.4 oil objective) equipped with a CoolSNAP-EZ camera. Representative images were taken and evaluated according to different platelet spreading stages with ImageJ (National Institutes of Health, Bethesda, MD, USA). Spreading stages were defined as follows: 1: round, no filopodia, no lamellipodia. 2: only filopodia. 3: filopodia and lamellipodia. 4: full spreading.

2.2.8.15 Fluorescence microscopy of platelets

After thrombin (0.01 U/mL) stimulation, washed platelets were allowed to fully spread on fibrinogen-coated surface and were fixed in PHEM complete buffer for 20 min at 4°C, then blocked with 5% BSA and 1% goat serum for 2 hours at 37°C. Fully-spreaded platelets were stained with rabbit anti-TRPM7 antibody for 2 hours followed by 4x washing with PBS and incubation of 1 hour with secondary Alexa 488-labeled anti-rabbit IgG antibody (Invitrogen) and phalloidin-Atto647N (Sigma-Aldrich, Schnellendorf, Germany). Then, samples were washed again with PBS, mounted with Vectashield mounting medium and finally left to dry overnight at 4°C. Samples were visualised on a Leica SP5 confocal microscope with a 100 \times oil objective (Leica Microsystems GmbH, Wetzlar, Germany). Images were further processed using Image J software.

2.2.9 *In vivo* analysis of platelet function

2.2.9.1 Platelet life span

5 μg Dylight-488-anti-GPIX Ig derivative were injected i.v. in the retro-orbital plexus to label circulating platelets. 30 min later (and every 24 hours for 5 days), 50 μL blood was taken from the retro-orbital plexus of the treated mice and the percentage of the positive labeled platelets was determined by flow cytometry.

2.2.9.2 Tail bleeding time assay

Mice were anesthetized by intraperitoneal injection of the triple anesthesia (dormitor, dormicum and fentanyl), and a 1 mm segment of the tail tip was cut off with a scalpel. Tail bleeding was monitored by gently absorbing the drop of blood with a filter paper in 20 s intervals without interfering with the wound site. When no blood was observed on the paper, bleeding was determined to have ceased. The experiment was manually stopped after 20 min by cauterization.

2.2.9.3 Intravital microscopy of thrombus formation in FeCl₃-injured mesenteric arterioles

Mice (15-18 g body weight) were anesthetized i.p. with ketamine/xylazine (100/5 mg/kg; Parke-Davis, Berlin, Germany and Bayer, Leverkusen, Germany) and the mesentery was exteriorized through a midline abdominal incision. Arterioles with a diameter of 35 - 60 µm were visualized using a Zeiss Axiovert 200 inverted microscope equipped with a 100-W HBO fluorescent lamp source and a CoolSNAP-EZ camera. Endothelial damage was induced by application of a 3 mm² filter paper saturated with 20% FeCl₃. Adhesion and aggregation of fluorescently labeled platelets (Dylight-488 conjugated anti-GPIX antibody derivative) in arterioles was monitored for 40 min or until complete occlusion occurred (blood flow stopped for >1 min). Digital images were recorded and analyzed using the Metavue software.

2.2.9.4 Mechanical injury of the abdominal aorta

Mice (20-26 g body weight) were anesthetized and the abdominal cavity was opened by a longitudinal midline incision. The abdominal aorta was carefully exposed, and a Doppler ultrasonic flow probe (Transonic Systems, New York, USA) was placed around the vessel. Mechanical injury was induced by a single firm compression with a forceps. Blood flow was monitored until complete occlusion of vessel or experiments were stopped manually after an observation period of 30 min.

2.2.9.5 Transient middle cerebral artery occlusion (tMCAO) model

Experiments were conducted on 8-12 week old male mice according to published recommendations for research in mechanism-driven basic stroke studies.¹⁶² tMCAO was induced under inhalation anesthesia using the intraluminal filament (6021PK10; Doccol Company) technique.¹⁶³ A midline neck incision was made and a standardized silicon rubber-coated 6.0 nylon monofilament (6021PK10, Doccol, Redlands, CA, USA) was inserted into the right common carotid artery and advanced via the internal carotid artery to occlude the origin of the middle cerebral artery. After 60 min, the filament was withdrawn to allow reperfusion. 24 hours after tMCAO the global neurological status was assessed by the Bederson score.¹⁶⁴ Motor function and coordination were graded with the grip test.¹⁶⁵ For measurements of ischemic brain (infarct) volume, animals were sacrificed 24 hours after induction of tMCAO and brain sections were stained with 2% *2,3,5-triphenyltetrazolium chloride* (TTC; Sigma-Aldrich, Germany). Brain infarct volumes were calculated and corrected for oedema as described.¹⁶³ This work was performed in collaboration with Dr. Peter Kraft and colleagues in the group of Prof. Guido Stoll, Department of Neurology, University Hospital, Würzburg.

2.2.9.6 *Magnetic resonance imaging (MRI)*

For the assessment of infarct dynamics and intracranial bleeding complications, MRI was performed serially at 24 hours and again on day 7 after tMCAO on a 1.5 Tesla unit (Vision, Siemens).¹⁶⁶ A custom-made dual channel surface coil was used for examining mice (A063HACG; Rapid Biomedical). The imaging protocol comprised a coronal T2-weighted sequence (slice thickness 2 mm) and a blood-sensitive coronal three dimensional T2-weighted gradient echo constructed interference in steady state (CISS; slice thickness 1 mm) sequence. Infarct volumes were calculated by planimetry from the hyper-intense areas on T2-weighted images by an investigator blinded to the different mouse groups.

2.2.9.7 *Platelet transfusion*

Purity of platelet suspensions from *Wt* and *Trpm7^{Kl}* donor mice were confirmed by flow cytometry and microscopical inspection. Platelet count and contamination by other blood cell types were further determined by hematology analyzer Sysmex. Thrombocytopenia was induced in *Wt* recipients by intravenous injection of an anti-GPIb antibody (0.185 µg/g of body weight). After 12 hours of platelet depletion, platelet counts of *Wt* recipients was determined by flow cytometry as previously described.¹⁶⁷ *Wt* recipients were injected intravenously with 1×10^9 washed platelets from either *Wt* or *Trpm7^{Kl}* donor mice. Peripheral platelet count was determined after 60 min of platelet transfer and mice were subsequently subjected to tMCAO.

2.3 *Data analysis*

The results presented in this thesis are mean \pm SD from at least three independent experiments per group, if not otherwise stated. When applicable, differences between the groups were statistically analyzed using the Student's t-test. For analyzing variance in occurrence of occlusion, the Fischer's exact test was used. For the Bederson score and the grip test analysis, the Mann-Whitney-U-test was applied. *P*-values < 0.05 were considered as statistically significant (*), $p < 0.01$ (**), and $p < 0.001$ was taken as the level of highest significance (***).

3 RESULTS

3.1 Functional crosstalk between Orai1 and TRPC6

Elevation of $[Ca^{2+}]_i$ is an essential step for platelet activation. It is well established that the major Ca^{2+} entry route in platelets is mediated by the SOC channel Orai1.²⁶ Recently, it was found that DAG-induced ROCE is almost completely abolished in *Trpc6*^{-/-} platelets, indicating that TRPC6 is the major DAG-regulated Ca^{2+} channel in mouse platelets.²⁷ A dynamic coupling model suggests that the heterodimerization of Orai and TRPC isoforms regulates ROCE and SOCE.^{69,89} However, the functional significance of the biochemical interaction between Orai and TRPC isoforms remains controversial, since *Trpc6*^{-/-} platelets displayed unaltered TG-induced SOCE, while *Orai1*^{-/-} platelets showed normal DAG-induced ROCE.^{26,27} Thus, it seems that the physical association of Orai1 with TRPC6 does not influence their channel functions. One aim of this thesis was to investigate the functional crosstalk between Orai1 and TRPC6.

To study the functional crosstalk between Orai1 and TRPC6, *Wt*, *Orai1*^{-/-} and *Orai1*^{-/-}/*Trpc6*^{-/-} BM chimeric mice were generated by transferring either *Wt*, *Orai1*^{-/-}, or *Orai1*^{-/-}/*Trpc6*^{-/-} fetal liver cells into lethally irradiated C57Bl6J recipient mice. *Trpc6*^{-/-} and *Orai1*^{-/-} mice have been generated and described previously.^{26,27}

3.1.1 TRPC6 contributes to TG-induced SOCE and regulates Ca^{2+} store content together with Orai1

TRPC6 has been proposed to be involved in TG-induced SOCE in human platelets.¹⁶⁸ Recently, it was shown that *Trpc6*^{-/-} platelets have normal SOCE and Ca^{2+} influx in response to treatment with TG and stimulation by platelet agonists, respectively, indicating that the loss of TRPC6 may be fully compensated for by Orai1.²⁷ To study the role of TRPC6 in SOCE, TG-induced SOCE in *Wt*, *Orai1*^{-/-}, or *Orai1*^{-/-}/*Trpc6*^{-/-} platelets was measured. Platelets were loaded with 5 μ M Fura2, which allows to measure $[Ca^{2+}]_i$ fluorometrically. In the absence of extracellular Ca^{2+} , TG was applied to trigger store release. Afterwards, 1 mM extracellular Ca^{2+} was added to induce SOCE.

Orai1^{-/-}/*Trpc6*^{-/-} platelets displayed reduced basal $[Ca^{2+}]_i$. The basal $[Ca^{2+}]_i$ in *Wt* and *Orai1*^{-/-} platelets were 21.6 ± 5.8 nM and 21.0 ± 5 nM, respectively. In contrast, *Orai1*^{-/-}/*Trpc6*^{-/-} platelets exhibited 12.4 ± 3.2 nM basal $[Ca^{2+}]_i$ (Figure 3-1 B). Store release, triggered by the application of TG in the absence of extracellular Ca^{2+} , in *Orai1*^{-/-}/*Trpc6*^{-/-} platelets was also defective. After TG stimulation, *Orai1*^{-/-}/*Trpc6*^{-/-} platelets displayed 48 ± 10.4 nM store release, which was significantly lower than *Wt* (79 ± 11.3 nM) and *Orai1*^{-/-} (84 ± 12.6 nM) platelets (Figure 3-1 C). These data indicated that Orai1 together with TRPC6 may regulate basal

$[Ca^{2+}]_i$ and store release. Furthermore, TG-induced SOCE was further reduced in *Orai1^{-/-}/Trpc6^{-/-}* platelets compared to *Orai1^{-/-}* platelets (1521 ± 276 nM for *Wt*, 155 ± 38 nM for *Orai1^{-/-}* and 92 ± 11 nM for *Orai1^{-/-}/Trpc6^{-/-}*, Figure 3-1 D), indicating a role for TRPC6 in regulating SOCE.

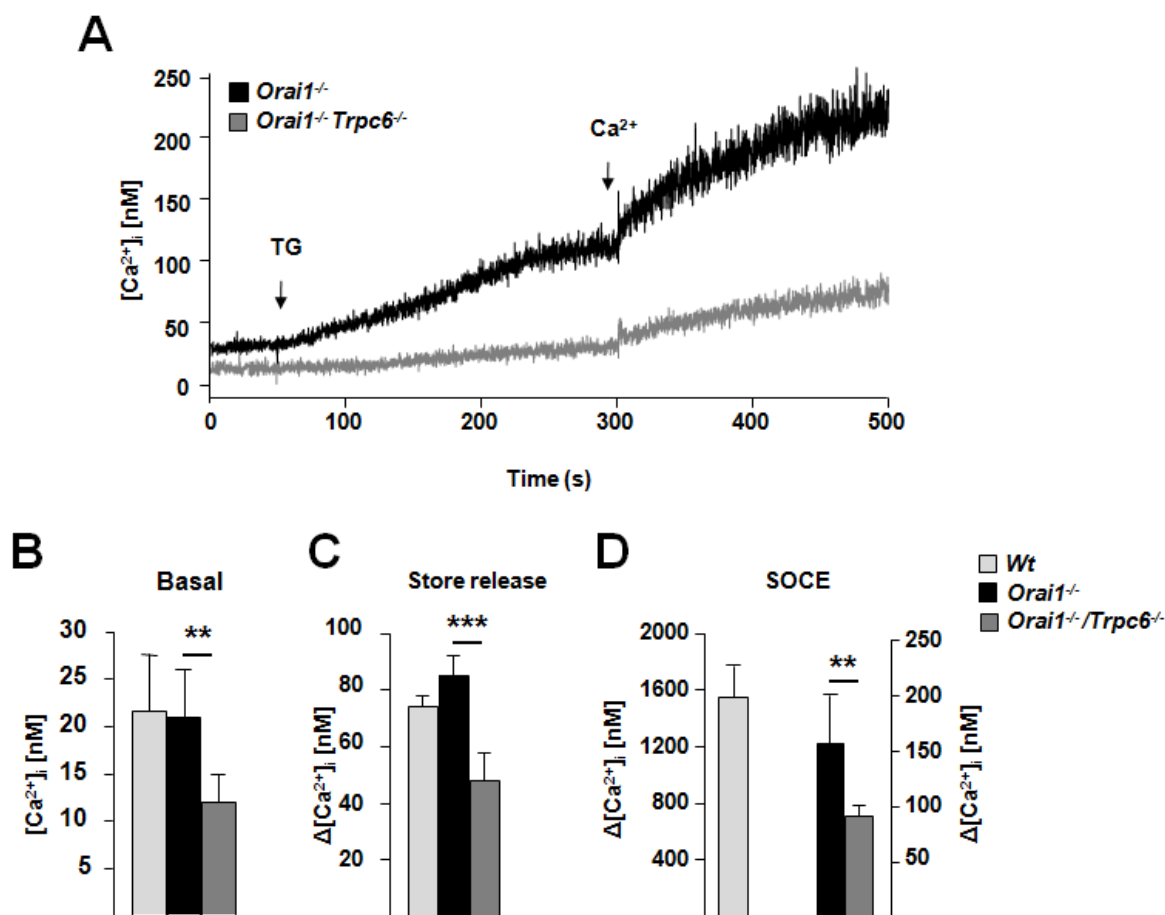


Figure 3-1: TRPC6 contributes to TG-induced SOCE. (A) SOCE was measured in Fura2-loaded platelets. Platelets were treated with 5 μ M TG for 5 min followed by the addition of 1 mM extracellular Ca^{2+} . (B-D) Quantification of $[Ca^{2+}]_i$ before (basal) and after (store release) TG application, and SOCE upon addition of extracellular Ca^{2+} . Data are mean \pm standard deviation (SD). ** $p < 0.01$, *** $p < 0.001$. (Chen et al., *J Thromb Haemost* 2014)¹⁶⁹

To confirm the findings that Orai1 together with TRPC6 regulates basal $[Ca^{2+}]_i$, a flow cytometric assay was used to determine the basal $[Ca^{2+}]_i$ of *Wt*, *Orai1^{-/-}*, *Trpc6^{-/-}* and *Orai1^{-/-}/Trpc6^{-/-}* platelets, which were preloaded with Fluo-3. Consistent with previous results, the relative fluorescence intensity was comparable between *Wt*, *Trpc6^{-/-}* and *Orai1^{-/-}* platelets, while a 40% reduction of $[Ca^{2+}]_i$ in *Orai1^{-/-}/Trpc6^{-/-}* platelets was found (Figure 3-2 A). Furthermore, the store content was also measured by using ionomycin. It was found that ionomycin-induced Ca^{2+} store release was reduced in *Orai1^{-/-}/Trpc6^{-/-}* platelets compared to *Wt*, *Orai1^{-/-}* and *Trpc6^{-/-}* platelets (Figure 3-2 B). These data lead to the conclusion that Orai1 together with TRPC6 regulates the store content and basal $[Ca^{2+}]_i$, however, either Orai1 or TRPC6 alone is not sufficient to fulfill this function.

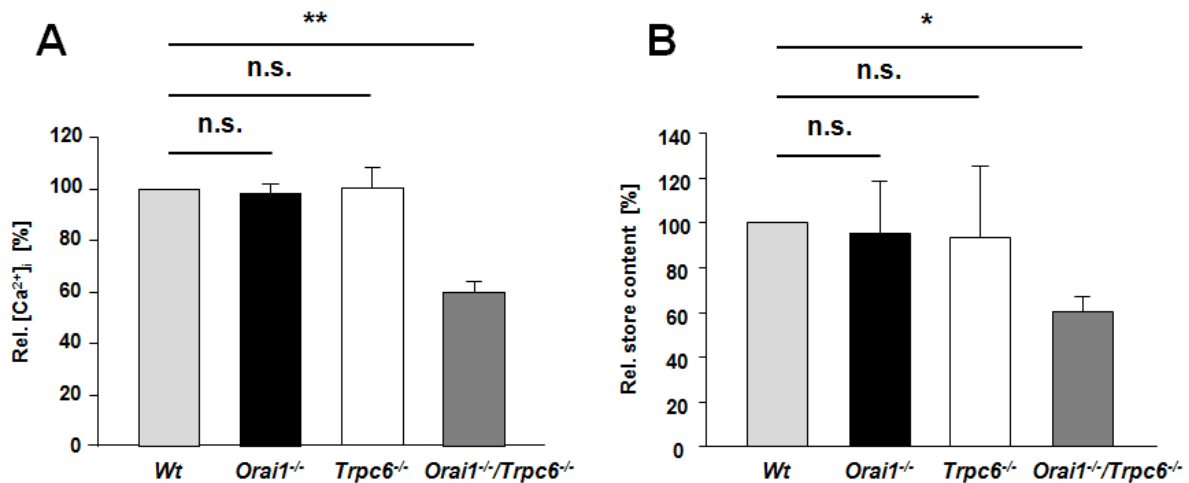


Figure 3-2: Orai1 together with TRPC6 regulates basal [Ca²⁺]_i and store content. (A) Relative [Ca²⁺]_i levels in *Wt* and mutant platelets was measured using Fluo-3/AM labeled anti-coagulated whole blood. Resting platelets in diluted blood were gated by 14A3-PE antibody. Mean fluorescence intensity (MFI) was determined by flow cytometry. The MFI in *Wt* platelets was set as 100%. **(B)** Store content was determined upon treatment of platelets with 20 μM ionomycin in the presence of 0.5 mM EGTA. The average Ca²⁺ release from the stores of *Wt* platelets was 160 nM after ionomycin treatment and it was set as 100%. Data are presented as mean percentage ± SD. **p* < 0.05, ***p* < 0.01. (Chen *et al.*, *J Thromb Haemost* 2014)¹⁶⁹

3.1.2 Orai1 regulates TG-induced phospholipase activity

It is well established that the channel activity of TRPC6 is triggered by DAG,⁷⁷ and in platelets DAG production is regulated by PLC and PLD isoforms. In addition, the previous results indicate that TRPC6 contributes to TG-induced SOCE (Figure 3-1 A). These findings suggest that TG stimulation may induce *phospholipase* (PL) activation and DAG production, which subsequently enable TRPC6 to contribute to SOCE. To address a potential role of PL-mediated pathways in the regulation of SOCE, TG-induced SOCE was analyzed in the presence of the PLC antagonists 1-[6-[[[(17β)-3-Methoxyestra-1,3,5[10]-trien-17-yl)amino]hexyl]-1H-pyrrole-2,5-dione (U73122)¹⁷⁰ and the PLD blocker 5-fluoro-2-indolyl des-chlorohalopemide (FIPI).¹⁷¹ In the presence of U73122, FIPI or both, a significant reduction of SOCE was observed in *Wt* and *Orai1*^{-/-} platelets (Figure 3-3 A), indicating that PL-mediated pathways are involved in SOCE.

To assess the direct contribution of SOCE on PLD activity, a radioactive PLD assay was performed detecting the time-dependent accumulation of phosphatidylethanol, a non-degradable product of PLD. This experiment was performed in collaboration with Ina Thielmann in our group. During TG-induced store release, PLD activity was enhanced in *Wt* platelets, but only residual PLD activity was detected in *Orai1*^{-/-} platelets (Figure 3-3 B). During SOCE, PLD activity was further enhanced in *Wt* platelets, while only a slight elevation of PLD activity was found in *Orai1*^{-/-} platelets indicating that PLD activity is tightly regulated by Orai1 (Figure 3-3 B). Furthermore, to assess the effect of SOCE on the enzymatic activity of

PLC, an IP₁-ELISA was performed to investigate the time-dependent accumulation of IP₁, a non-degradable stable product of IP₃. Interestingly, store release upon addition of TG in the absence of extracellular Ca²⁺ produced comparable amounts of IP₁ in *Wt* and *Orai1*^{-/-} platelets (Figure 3-3 C). In sharp contrast, in the presence of extracellular Ca²⁺, the production of IP₁ in *Wt* platelets was strongly enhanced, while only a moderate increase was observed in *Orai1*^{-/-} platelets (Figure 3-3 C). Altogether, these results suggest that Orai1-induced Ca²⁺ influx enhances PLC and PLD activity, thereby accelerating PLC- and PLD-mediated DAG production in platelets. Since TRPC6 is regulated by DAG, it can be concluded that PLC and PLD activity mediates a functional crosstalk between Orai1 and TRPC6.

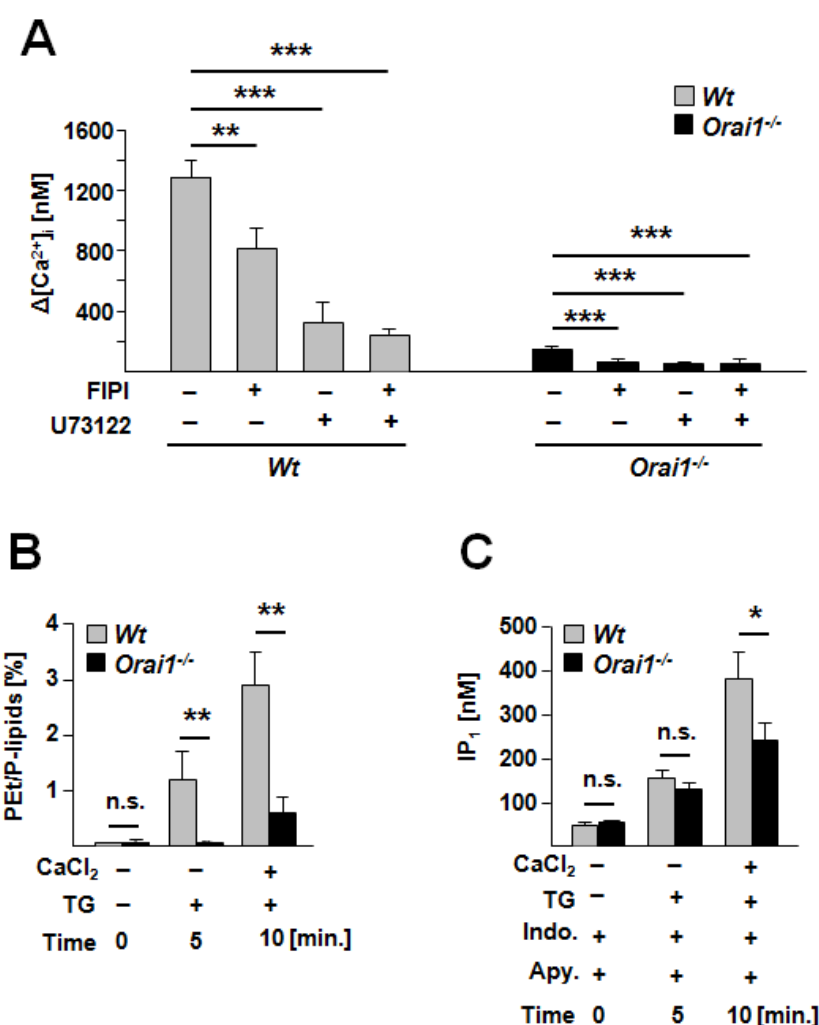


Figure 3-3: Orai1 regulates TG-induced phospholipase activity. (A) In the presence of 100 nM FIPI (PLD inhibitor), 5 μ M U73122 (PLC inhibitor) or both, SOCE was induced by using 5 μ M TG in *Wt* and *Orai1*^{-/-} platelets. Data are mean \pm SD. (B) PLD activity was measured in [³H] myristic acid pre-labeled platelets, which were stimulated in the same way as in the SOCE measurements. PLD activity is shown as percentage of phosphatidylethanol (PEt) of total ³H-labeled phospholipids (PEt/P-lipids). Data are mean \pm SD. (C) The amount of accumulated IP₁, a specific metabolite of IP₃, was quantified by an ELISA assay. Results are mean of IP₁ concentrations (nM) \pm SD. 0 min: unstimulated platelets in the absence of extracellular Ca²⁺; 5 min: activated platelets by 5 μ M TG for 5 min in the absence of extracellular Ca²⁺; 10 min: addition of 1 mM extracellular Ca²⁺ after 5 min of TG-induced store depletion. **p* < 0.05, ***p* < 0.01, ****p* < 0.001. (Chen *et al.*, *J Thromb Haemost* 2014)¹⁶⁹

3.1.3 Platelet agonists can activate PLC and PLD independently of Orai1

Agonist-induced platelet activation and aggregation requires elevations of $[Ca^{2+}]_i$ and intracellular DAG. This is maintained through the release of Ca^{2+} from intracellular stores followed by SOCE, which further enhances PL activity during platelet activation. Since the store content and the basal $[Ca^{2+}]_i$ are reduced in *Orai1^{-/-}/Trpc6^{-/-}* platelets, and PL activity is reduced in *Orai1^{-/-}* platelets, it can be assumed that Ca^{2+} responses to platelet agonists may be strongly affected in *Orai1^{-/-}/Trpc6^{-/-}* platelets. To test this, store release and Ca^{2+} influx of *Wt*, *Orai1^{-/-}* and *Orai1^{-/-}/Trpc6^{-/-}* platelets were measured upon stimulation with platelet agonists (thrombin, CRP, ADP, U46619). Indeed, store release and Ca^{2+} influx were significantly reduced in *Orai1^{-/-}/Trpc6^{-/-}* platelets in response to almost all agonists compared to *Orai1^{-/-}* or *Wt* platelets (Figure 3-4 A and B). These data confirmed that the Ca^{2+} store content in *Orai1^{-/-}/Trpc6^{-/-}* platelets was significantly reduced, while platelets lacking solely Orai1 or TRPC6 harbored normal Ca^{2+} levels in the stores.

TG can be used as a shortcut to activate only store-dependent Ca^{2+} entry mechanisms. Platelet agonists, on the other hand, induce Orai1, TRPC6 and ATP-operated P2X₁ channels activation simultaneously,^{35,43} which could substantially enhance PL-mediated DAG production. The previous results (Figure 3-3) have shown that TG stimulation can enhance DAG production, and that this process is tightly Orai1-dependent. To study whether platelet agonist-induced DAG production is also Orai1-dependent, PLD and PLC activity were measured by the PLD assay and the IP₁ ELISA, respectively. The platelet agonists thrombin, CRP and TxA₂-analogue U46619 were used to stimulate *Wt* and *Orai1^{-/-}* platelets for 2 or 15 min. Thereafter, PLD activity and IP₁ production were quantified. Under all conditions, *Orai1^{-/-}* platelets displayed normal PLD activity (Figure 3-4 C) and IP₁ production (Figure 3-4 D), indicating that platelet agonist-induced PLD and PLC activation (or platelet agonist-induced DAG production) is not Orai1-dependent. These results suggest that in the presence of high concentrations of physiological agonists, ITAM-PLC γ 2 signaling, GPCR-PLC β signaling and PKC-PLD signaling can enhance DAG production independently of Orai1. Therefore, it can be concluded that Orai1-mediated SOCE is not essential for platelet receptor-induced PLD and PLC activation under *in vitro* conditions. However, under *in vivo* conditions where concentrations of platelet agonists are much lower than under *in vitro* conditions presented in this study, Orai1-induced PL activity may exhibit its physiological significance.

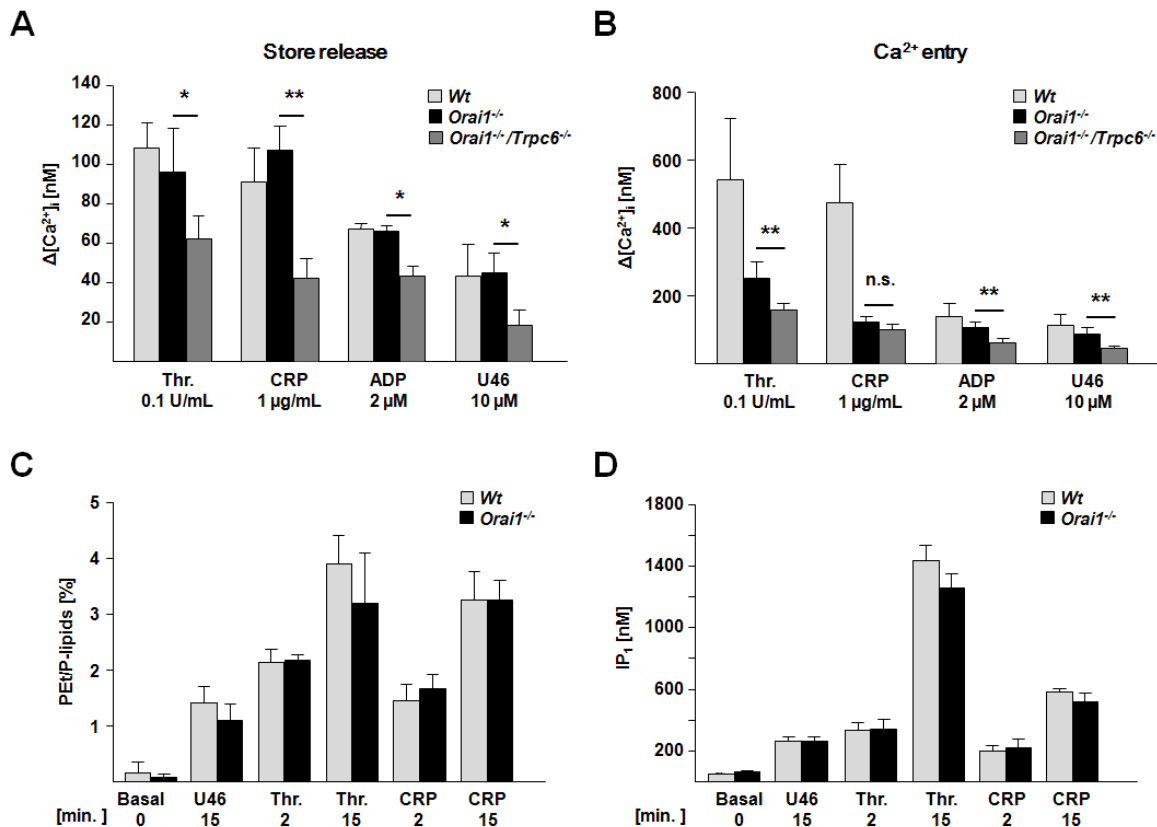


Figure 3-4: Platelet agonists activate PLC and PLD independently of Orai1. (A) Reduced Ca²⁺ store release and (B) Ca²⁺ influx in *Orai1*^{-/-}/*Trpc6*^{-/-} platelets. Fura2-loaded *Wt*, *Orai1*^{-/-} and *Orai1*^{-/-}/*Trpc6*^{-/-} platelets were stimulated with indicated agonists in the presence of 0.5 mM EGTA or in the presence of 1 mM Ca²⁺ and changes in [Ca²⁺]_i were measured with a fluorimeter. Representative measurements and maximal increase in [Ca²⁺]_i compared to baseline levels before stimulus are depicted as ($\Delta[Ca^{2+}]_i$) \pm SD. (C) *Wt* and *Orai1*^{-/-} platelets were labeled with [³H] myristic acid and stimulated with the indicated agonists for different time intervals (thrombin: 0.1 U/mL, CRP: 10 μ g/mL, U46619: 3 μ M) and PLD activity was quantified. (D) IP₁ production in *Wt* and *Orai1*^{-/-} platelets was quantified upon activation with indicated agonists (thrombin 0.1 U/mL, CRP: 10 μ g/mL, U46619: 3 μ M). IP₁ concentrations, as a specific metabolite of IP₃, were quantified with an ELISA assay. Data are mean \pm SD. **p* < 0.05, ***p* < 0.01, ****p* < 0.001. (Chen *et al.*, *J Thromb Haemost* 2014)¹⁶⁹

3.1.4 TxA₂-induced second phase of Ca²⁺ signaling is controlled by Orai1

The initial phase of receptor activation-induced Ca²⁺ and DAG signaling is followed by a second signaling phase which further increases the levels of both [Ca²⁺]_i and intracellular DAG in platelets. The second wave mediator TxA₂ strongly amplifies TP-PLC β -mediated IP₃ and DAG production which further accelerates Ca²⁺ store release and DAG-mediated ROCE in this process. Earlier, it has been shown that in human platelets TG-mediated SOCE strongly enhance TxA₂ formation.¹⁷² To study whether platelet agonists or TG-induced TxA₂ secretion is Orai1 dependent, *Wt*, *Orai1*^{-/-} and *Orai1*^{-/-}/*Trpc6*^{-/-} platelets were stimulated with TG, thrombin and CRP, and TxA₂ formation was measured by a TxB₂ ELISA. In line with published results,¹⁷² TG stimulation of *Wt* platelets resulted in large amount of TxA₂ formation, however, in *Orai1*^{-/-} and *Orai1*^{-/-}/*Trpc6*^{-/-} platelets TxA₂ formation was nearly abolished (Figure

3-5), indicating that TG-induced TxA₂ formation is tightly Orai1-dependent. Compared to *Orai1*^{-/-} platelets, *Orai1*^{-/-}/*Trpc6*^{-/-} platelets exhibited a decreased TxA₂ formation, suggesting that TRPC6 plays a role in TG-induced TxA₂ formation. In response to CRP a significant reduction of TxA₂ formation was observed in *Orai1*^{-/-} and *Orai1*^{-/-}/*Trpc6*^{-/-} platelets compared to *Wt* platelets. In sharp contrast, thrombin-induced TxA₂ formation was unaltered in both mutant platelets (Figure 3-5), indicating that GPVI- but not GPCR-mediated TxA₂ formation is Orai1 and TRPC6 independent.

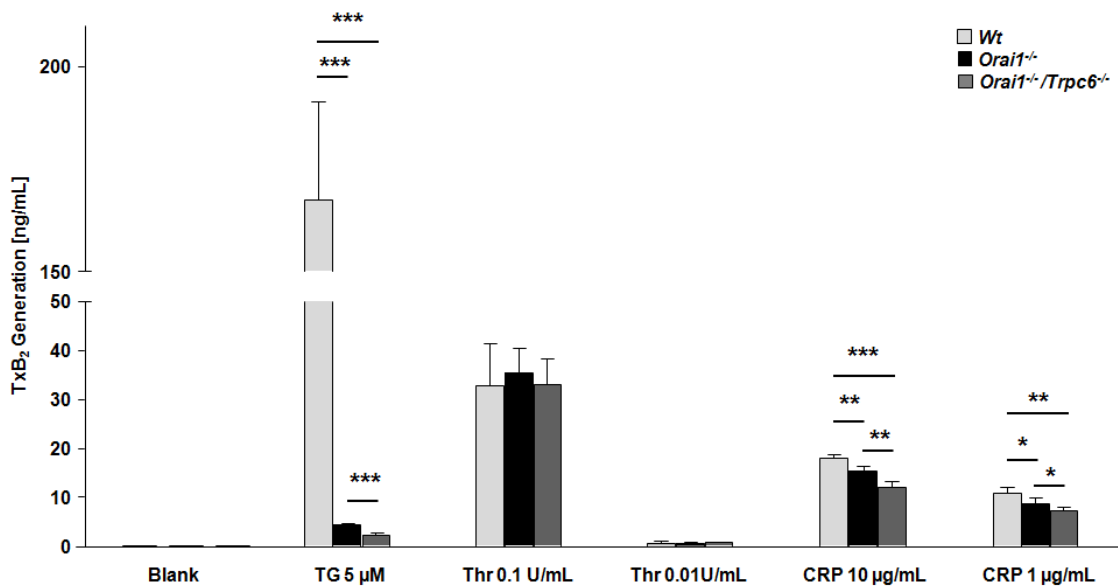


Figure 3-5: TxA₂-induced second phase of Ca²⁺ signaling is controlled by Orai1. TxA₂ production was measured by a TxB₂ ELISA. 5 μM TG, 0.1 U/mL thrombin and 10 μg/mL CRP were used for platelet activation. Results are presented as mean of TxB₂ production (ng) ± SD. **p* < 0.05, ***p* < 0.01, ****p* < 0.001. (Chen *et al.*, *J Thromb Haemost* 2014)¹⁶⁹

In summary, TG-induced SOCE through Orai1 can enhance PLC and PLD activity. Furthermore, TxA₂ formation can be increased during Orai1-mediated SOCE, which could further enhance PLCβ activity via the TP receptor. Subsequently, enhanced PLC and PLD activity leads to DAG production, resulting in TRPC6 activation.

3.1.5 Normal platelet count, size and glycoprotein expression in *Orai1*^{-/-}/*Trpc6*^{-/-} platelets

To investigate the effects of Orai1 and TRPC6 double deficiency on platelet physiology, peripheral platelet count and size were determined using a Sysmex KX-21N automated hematology analyzer. *Orai1*^{-/-} and *Orai1*^{-/-}/*Trpc6*^{-/-} mice displayed normal platelet count (Figure 3-6 A) and size (Figure 3-6 B) as *Wt* mice. In addition, the surface expression of major glycoproteins, including GPIb-IX-V, GPVI, CLEC-2, as well as integrin αIIbβ3 and α2β1, were measured by a flow cytometric assay. The abundance of these glycoproteins

was unaltered in *Orai1*^{-/-} and *Orai1*^{-/-}/*Trpc6*^{-/-} platelets compared to *Wt* platelets (Figure 3-6 C).

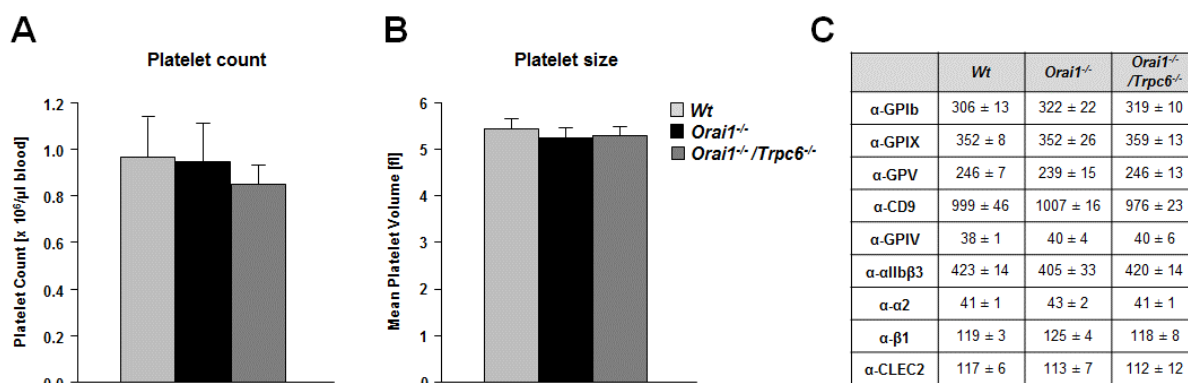


Figure 3-6: Deficiency of *Orai1* and TRPC6 does not impair platelet count, size and glycoprotein expression. Peripheral platelet count (A) and platelet size (B) of *Wt*, *Orai1*^{-/-} and *Orai1*^{-/-}/*Trpc6*^{-/-} mice measured with a blood cell counter are depicted. Results are mean \pm SD. (C) Diluted whole blood was incubated with saturating concentrations of FITC-labeled antibodies for 15 min at RT and analyzed by flow cytometry. Results are shown as MFI \pm SD (n=4) and are representative of 3 individual experiments.

3.1.6 Defective platelet activation in response to the GPVI agonists, but normal responses to the GPCR agonists in *Orai1*^{-/-}/*Trpc6*^{-/-} platelets

Orai1^{-/-} platelets display defective responses to GPVI stimulation, but unaltered platelet activation in response to the GPCR agonists.²⁶ To determine whether the double deficiency of *Orai1* and TRPC6 has additional effects on platelet activation, platelets were stimulated by the GPCR agonists and the ITAM-coupled receptor agonists, and analyzed by flow cytometry. Two markers for platelet activation were assessed: inside-out activation of $\alpha\text{IIb}\beta 3$ integrin and degranulation. The $\alpha\text{IIb}\beta 3$ integrin activation was assessed by using JON/A-PE antibody, which specifically binds the activated conformation of the integrin,¹⁵⁸ and degranulation was determined by P-selectin surface exposure, which is a marker of α -granule release.

Upon stimulation of the ITAM-coupled collagen receptor GPVI, either with CRP or the snake venom toxin *convulxin* (CVX), the $\alpha\text{IIb}\beta 3$ integrin activation and P-selectin exposure were severely reduced compared to *Wt* platelets, which is in line with previous observations.²⁶ Furthermore, compared to *Orai1*^{-/-} platelets, *Orai1*^{-/-}/*Trpc6*^{-/-} platelets had reduced platelet activation in response to low concentrations of CRP and CVX (Figure 3-7 A), indicating a significant role of TRPC6 in integrin activation and degranulation. However, when stimulated by the GPCR agonists (thrombin, ADP and U46619), *Orai1*^{-/-} and *Orai1*^{-/-}/*Trpc6*^{-/-} platelets had normal $\alpha\text{IIb}\beta 3$ integrin activation and P-selectin exposure (Figure 3-7 B), demonstrating that *Orai1* and TRPC6 are not required for GPCR-induced platelet activation.

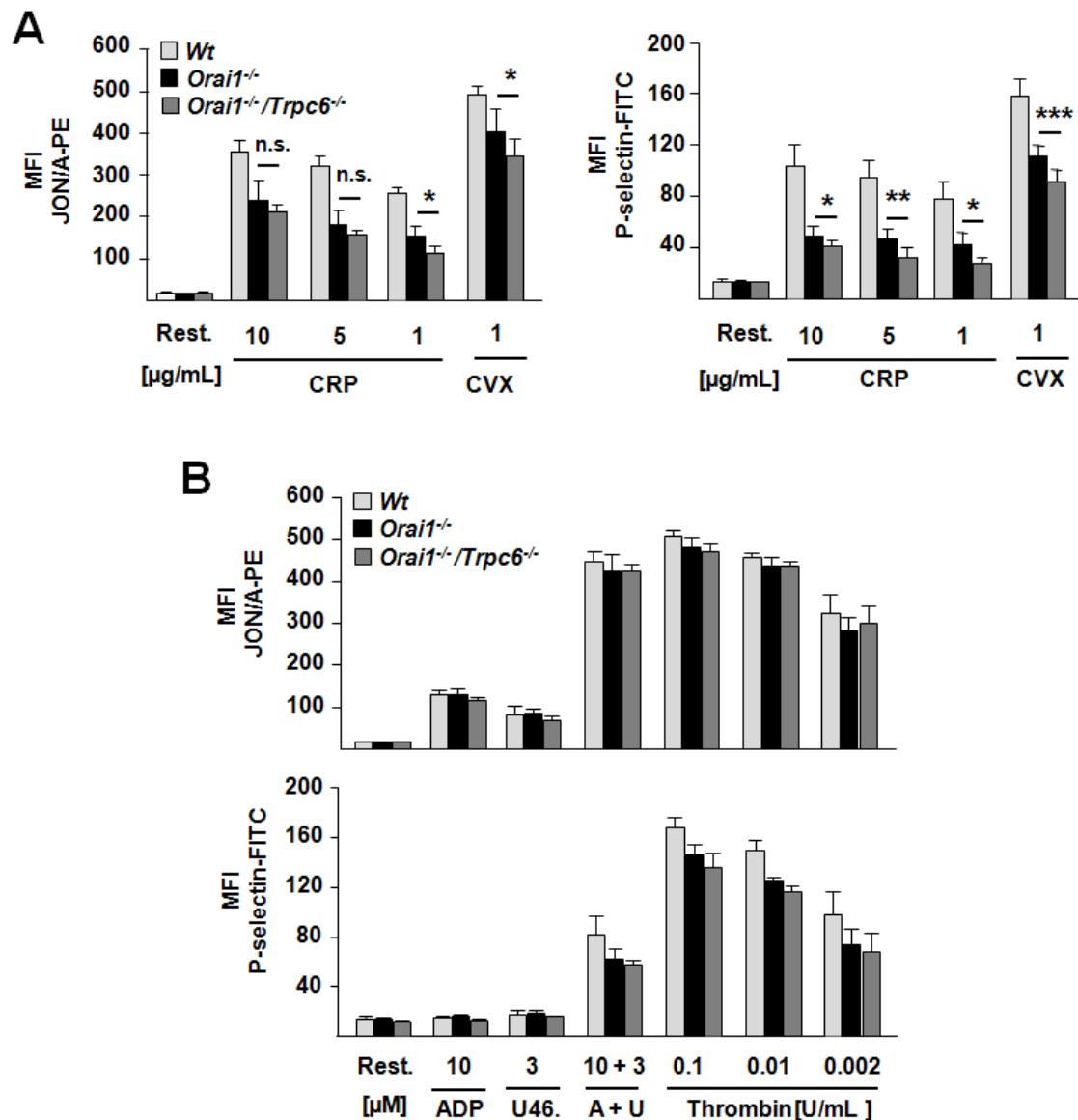


Figure 3-7: Impaired platelet activation in response to the GPVI agonists in *Orai1*^{-/-}/*Trpc6*^{-/-} platelets. Flow cytometric analysis of α IIb β 3 activation and P-selectin exposure in *Wt*, *Orai1*^{-/-} and *Orai1*^{-/-}/*Trpc6*^{-/-} platelets in response to platelet agonists as indicated (CRP: 1 – 10 μ g/mL, CVX: 1 μ g/mL ADP: 10 μ M, U46619: 3 μ M, thrombin: 0.1 – 0.002 U/mL). Results are depicted as MFI \pm SD of 4 mice per group and representative of 4 individual experiments. * p < 0.05, ** p < 0.01, *** p < 0.001. (Chen *et al.*, *J Thromb Haemost* 2014)¹⁶⁹

3.1.7 Defective aggregation in response to the GPVI agonists in *Orai1*^{-/-}/*Trpc6*^{-/-} platelets

Since *Orai1*^{-/-}/*Trpc6*^{-/-} platelets display a more defective GPVI-dependent integrin activation and degranulation compared to *Orai1*^{-/-} platelets, the ability to aggregate of *Orai1*^{-/-}/*Trpc6*^{-/-} platelets may also be further impaired. To investigate this, *in vitro* aggregation studies were performed. In line with the flow cytometry data, *Orai1*^{-/-} platelets and *Orai1*^{-/-}/*Trpc6*^{-/-} platelets aggregated normally upon stimulation with the GPCR agonists thrombin, ADP and U46619 at all tested concentrations. In contrast, the response to the GPVI agonists CRP and

collagen was partially impaired at intermediate and abrogated at low agonist concentrations in *Orai1^{-/-}/Trpc6^{-/-}* platelets (Figure 3-8). These data indicate that Orai1 and TRPC6 are required for GPVI-induced platelet aggregation, but not essential for GPCR-induced aggregation.

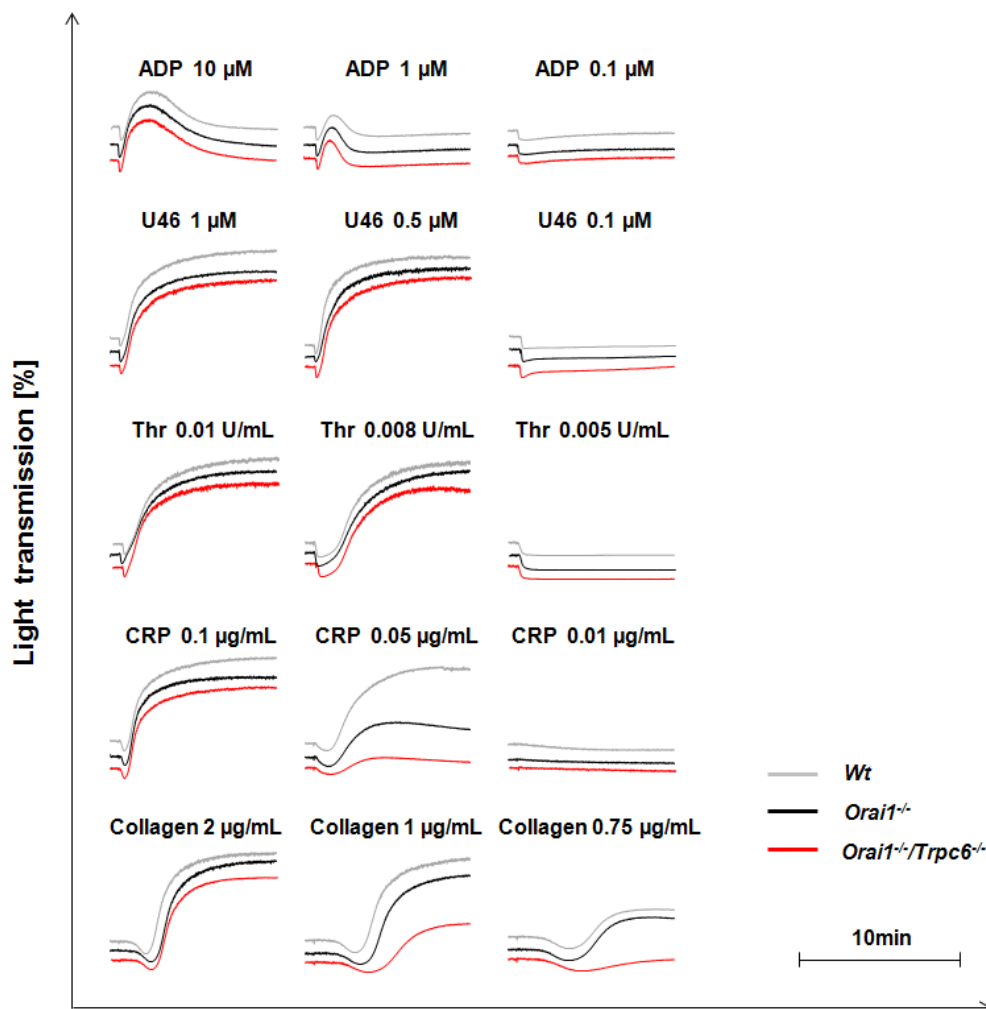


Figure 3-8: Defective aggregation of *Orai1^{-/-}/Trpc6^{-/-}* platelets in response to the GPVI agonists. Aggregation curves of *Wt* (grey line), *Orai1^{-/-}* (black line) and *Orai1^{-/-}/Trpc6^{-/-}* (red line) platelets in response to indicated agonists and concentrations. Washed platelets were incubated for 10 min in the presence of indicated agonists and changes in light transmission were recorded. (Chen *et al.*, *J Thromb Haemost* 2014)¹⁶⁹

3.1.8 *Orai1^{-/-}/Trpc6^{-/-}* platelets display normal spreading on fibrinogen

Integrin α IIb β 3 outside-in signaling is triggered by extracellular ligand binding, which leads to cytoskeletal reorganization and platelet spreading.¹¹ To investigate the role of Orai1 and TRPC6 in integrin outside-in signaling, a spreading assay was performed. After stimulation with 0.01 U/mL thrombin, *Wt*, *Orai1^{-/-}* and *Orai1^{-/-}/Trpc6^{-/-}* platelets were allowed to spread on a fibrinogen coated surface. *Orai1^{-/-}* and *Orai1^{-/-}/Trpc6^{-/-}* platelets could form filopodia and

lamellipodia and fully spread like *Wt* platelets (Figure 3-9). These data indicate that Orai1 and TRPC6 are not essential for integrin outside-in signaling and cytoskeletal reorganization.

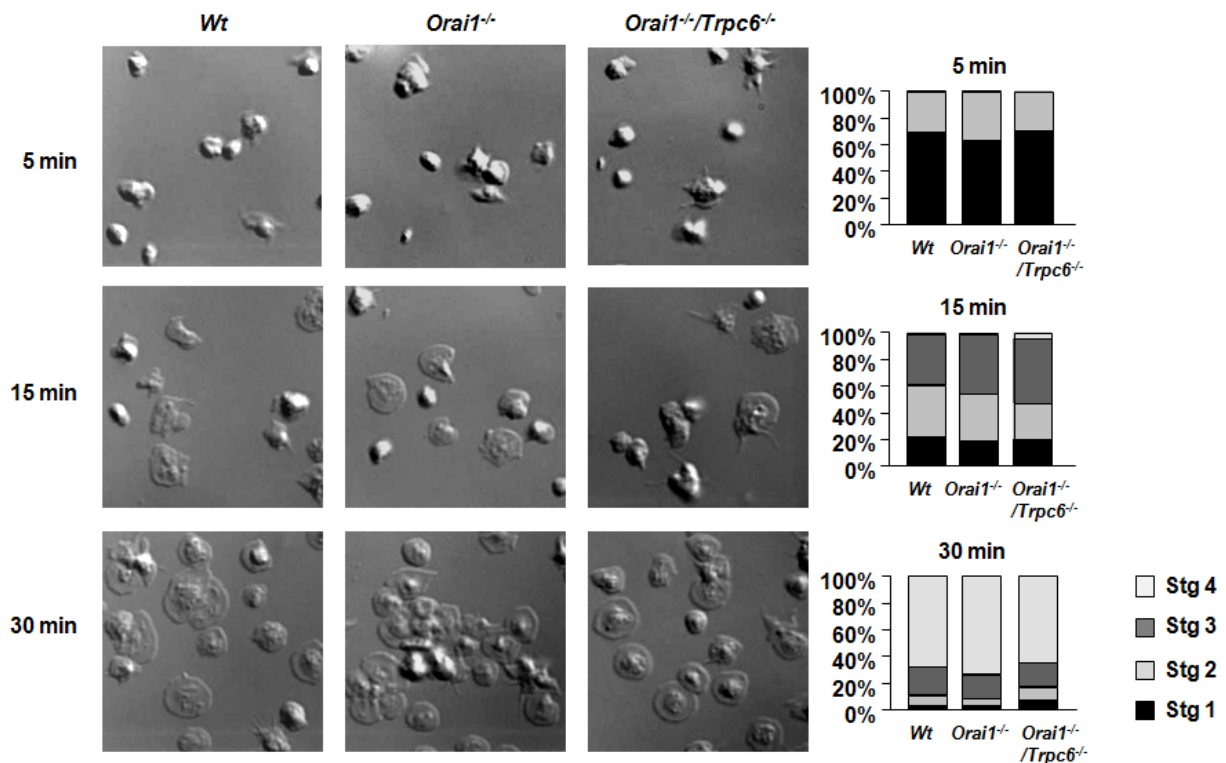


Figure 3-9: Unaltered spreading of *Orai1*^{-/-}/*Trpc6*^{-/-} platelets. Washed platelets of *Wt*, *Orai1*^{-/-} and *Orai1*^{-/-}/*Trpc6*^{-/-} BM chimeric mice were stimulated with 0.01 U/mL thrombin and allowed to spread on fibrinogen (200 µg/mL). Representative DIC images of 3 individual experiments from the indicated time points (left) and statistical evaluation of the percentage of platelets at different stages of spreading (right). Stg 1: roundish, Stg 2: only filopodia, Stg 3: filopodia and lamellipodia, Stg 4: fully spread.

3.1.9 Normal *in vivo* thrombus formation in *Orai1*^{-/-}/*Trpc6*^{-/-} mice

In the next step, the functional consequence of Orai1 and TRPC6 double deficiency was addressed *in vivo*. This experiment was performed in collaboration with Ina Thielmann in our group. Intravital microscopy was used to visualize thrombus formation in the mesenteric arterioles after chemical injury (20% FeCl₃). This arterial thrombosis model has been frequently used to study tissue factor/thrombin-driven thrombus formation *in vivo*, but has also been shown to be dependent on collagen-mediated GPVI activation.¹⁷³ *Orai1*^{-/-} mice were already protected in a model where thrombus growth is induced by mechanical injury of the aorta, whereas they showed normal thrombus formation in the FeCl₃ injury model.²⁶ In order to investigate whether Orai1 and TRPC6 have redundant functions in *in vivo* thrombus formation, *Orai1*^{-/-}/*Trpc6*^{-/-} mice were subjected to the FeCl₃ model. However, no differences were observed in thrombus growth between *Orai1*^{-/-} and *Orai1*^{-/-}/*Trpc6*^{-/-} (19.04 ± 2.75 min vs. 17.42 ± 1.33 min) mice (Figure 3-10). These data indicated that Orai1 and TRPC6 functions are not essential for thrombus formation in this experimental setting or an alternative

signaling mechanism could compensate the severe Ca^{2+} deficits in *Orai1*^{-/-}/*Trpc6*^{-/-} platelets *in vivo*.

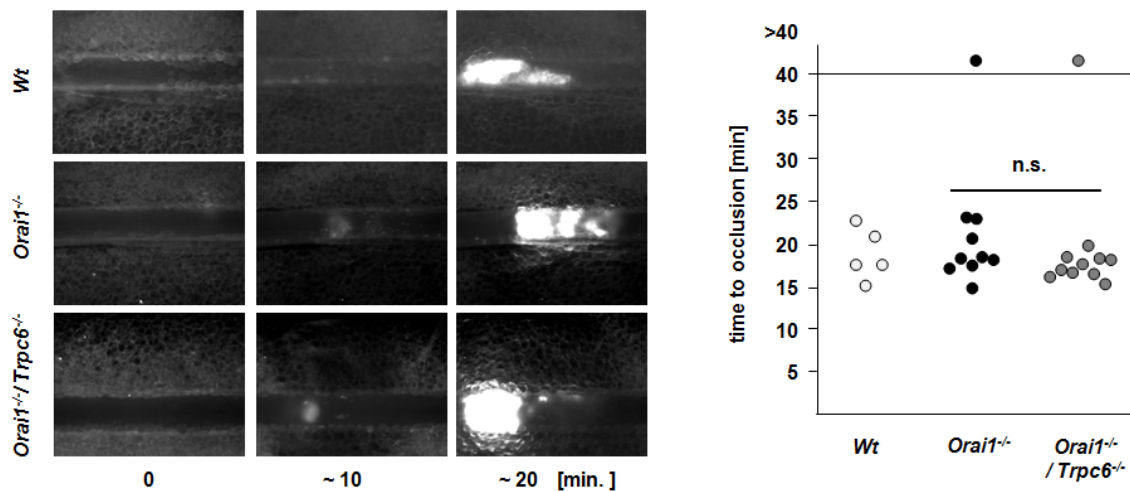


Figure 3-10: Normal arterial thrombus formation in *Orai1*^{-/-}/*Trpc6*^{-/-} mice. Thrombus formation in small mesenteric arterioles was induced by topical application of 20% FeCl_3 . In order to monitor thrombus formation by intravital microscopy platelets were labeled fluorescently. Representative pictures and time to stable occlusion of *Wt*, *Orai1*^{-/-} and *Orai1*^{-/-}/*Trpc6*^{-/-} mice are shown. (Chen *et al.*, *J Thromb Haemost* 2014)¹⁶⁹

3.1.10 Enhanced *ex vivo* thrombus formation, but reduced PS exposure in *Orai1*^{-/-}/*Trpc6*^{-/-} platelets

At sites of vessel wall injury, the GPVI-collagen interaction is critical for integrin $\alpha\text{IIb}\beta 3$ activation, which is important for firm platelet adhesion and thrombus growth. *Orai1*^{-/-} and *Orai1*^{-/-}/*Trpc6*^{-/-} platelets display impaired GPVI-induced $\alpha\text{IIb}\beta 3$ integrin activation, degranulation and aggregation, however, *in vivo* thrombus formation is normal (Figure 3-10). To study the effect of impaired GPVI signaling of *Orai1*^{-/-} and *Orai1*^{-/-}/*Trpc6*^{-/-} platelets on thrombus formation under flow, an *ex vivo* whole blood perfusion assay was used. This experiment was performed in collaboration with Prof. Johan Heemskerk, Department of Biochemistry, Maastricht University. Whole anti-coagulated blood was perfused over a collagen-coated surface at a shear rate of 1000s^{-1} , the area covered by platelets was measured. In line with flow cytometry and aggregometry results, perfusion of *Orai1*^{-/-} platelets resulted in a significantly reduced surface coverage. Surprisingly, *Orai1*^{-/-}/*Trpc6*^{-/-} platelets displayed enhanced platelet adhesion and thrombus formation compared to *Orai1*^{-/-} platelets (Figure 3-11 A and B), indicating that in *Orai1*^{-/-}/*Trpc6*^{-/-} platelets an alternative signaling mechanism exists to compensate the severe Ca^{2+} deficits.

It is well established that upon platelet activation PS can be exposed on the outer surface of the plasma membrane, which provides high affinity binding sites for key coagulation factors

to trigger coagulation.¹⁷⁴⁻¹⁷⁶ During this process, high levels of intracellular Ca^{2+} are essential. Since *Orai1*^{-/-} and *Orai1*^{-/-}/*Trpc6*^{-/-} platelets display a defective Ca^{2+} response, the coagulant activity of platelets may be impaired. To study this, Annexin V-Dylight-488, which specifically binds to platelets exposing PS at their outer surface, was used to in the flow chamber assay. When perfusing *Orai1*^{-/-} and *Orai1*^{-/-}/*Trpc6*^{-/-} blood, the percentage of PS-positive platelets was significantly lower than when perfusing *Wt* blood. Furthermore, PS exposure was also analyzed by flow cytometry upon agonist stimulation. Similarly, a strong reduction of PS exposure in *Orai1*^{-/-} and *Orai1*^{-/-}/*Trpc6*^{-/-} platelets was observed after agonist or TG treatment, whereas control experiments showed that Ca^{2+} ionophore (A23187)-dependent PS exposure was similar to *Wt* platelets (Figure 3-11 C). These data confirm that the defective Ca^{2+} response in *Orai1*^{-/-} and *Orai1*^{-/-}/*Trpc6*^{-/-} platelets lead to impaired procoagulant activities.

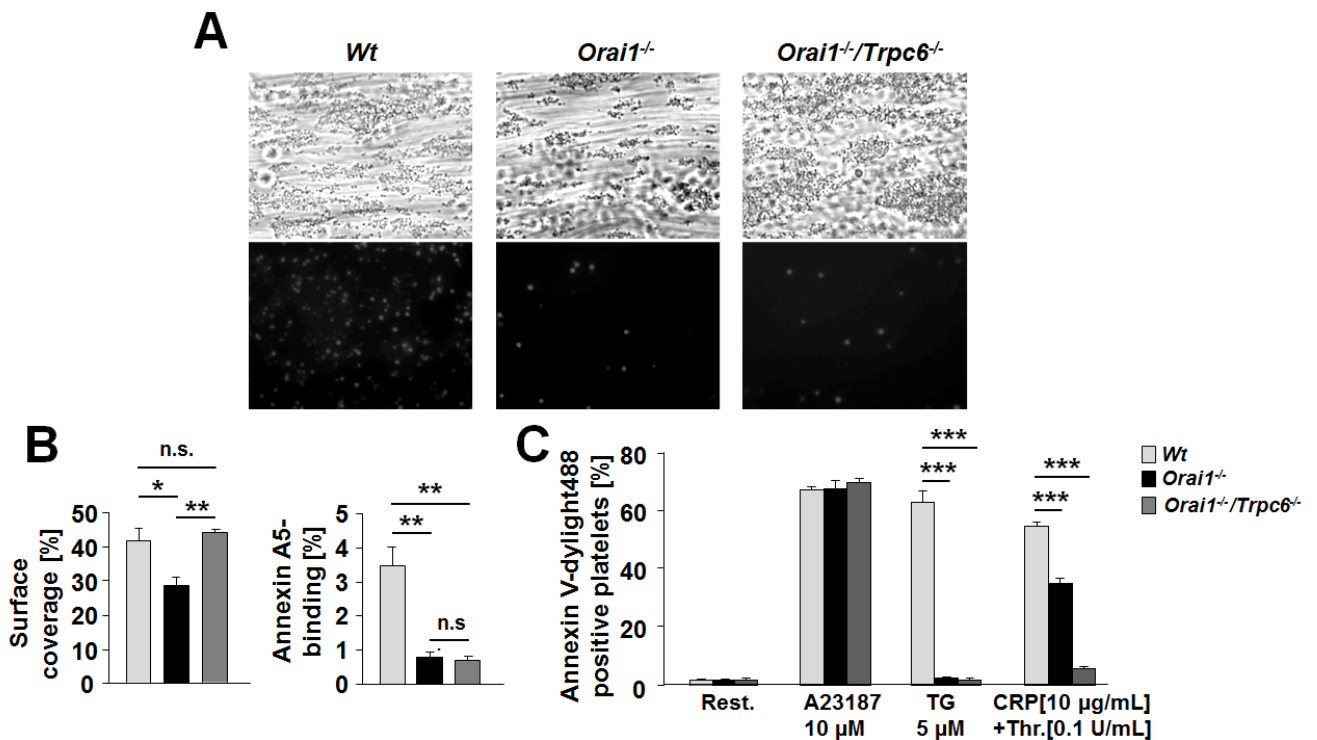


Figure 3-11: Enhanced ex vivo thrombus formation but reduced PS exposure in *Orai1*^{-/-}/*Trpc6*^{-/-} platelets. (A) Heparinized whole blood from *Wt*, *Orai1*^{-/-} and *Orai1*^{-/-}/*Trpc6*^{-/-} mice was perfused over 0.2 mg/mL of immobilized collagen at a shear rate of 1000 s⁻¹ (4 min) followed by 2 min perfusion with Tyrode HEPES buffer at the same shear rate. Adherent platelets were stained with Annexin V-Dylight-488 (0.25 $\mu\text{g}/\text{mL}$). Representative phase contrast (upper panel) and fluorescence images (lower panel) are shown. (B) Mean surface coverage \pm SD (left panel) and mean percentage of Annexin V positive platelets \pm SD (right panel) are shown. (C) PS exposure of platelets was determined using Annexin-V-DyLight-488 upon stimulation with the indicated agonists and A23187. Results are represented as percentage of Annexin V positive platelets \pm SD. * $p < 0.05$, ** $p < 0.01$, *** $p < 0.001$.

3.1.11 Enhanced ATP secretion in *Orai1*^{-/-}/*Trpc6*^{-/-} platelets in response to GPCR agonists

Since *Orai1*^{-/-}/*Trpc6*^{-/-} platelets display enhanced ex vivo thrombus formation, an Ca^{2+} entry

pathway besides Orai1 and TRPC6 may be enhanced to compensate for the severe Ca^{2+} deficits in *Orai1*^{-/-}/*Trpc6*^{-/-} platelets. It is known that the two major Ca^{2+} entry routes in platelets are SOCE and ROCE. SOCE is mediated by Orai1, and ROCE is mainly regulated by TRPC6, TRPC3 and P2X₁. In *Orai1*^{-/-}/*Trpc6*^{-/-} platelets Orai1-mediated SOCE and TRPC6-mediated ROCE are abolished, and DAG production is not increased in *Orai1*^{-/-}/*Trpc6*^{-/-} platelets indicating that TRPC3-mediated ROCE should not be enhanced. Therefore, P2X₁-induced Ca^{2+} entry in *Orai1*^{-/-}/*Trpc6*^{-/-} platelets was studied. Since P2X₁ is operated by ATP, the secretion of ATP was measured. In response to high concentrations of thrombin, ATP-secretion in platelets of the three mouse lines was comparable, indicating that the ATP content is normal. However, at threshold concentrations of thrombin or U46619, ATP-secretion was significantly increased in *Orai1*^{-/-}/*Trpc6*^{-/-} platelets compared to *Orai1*^{-/-} or *Wt* platelets. In sharp contrast, in response to CRP and TG, ATP secretion was completely abolished (Figure 3-12 A). These results indicate that GPCR-mediated stimulation can lead to enhanced ATP-secretion in *Orai1*^{-/-}/*Trpc6*^{-/-} platelets, thereby resulting in activation of P2X₁. To further study whether P2X₁ function was enhanced in *Orai1*^{-/-}/*Trpc6*^{-/-} platelets after stimulation with the GPCR agonists, an aggregation assay was performed in the presence of ACD buffer and a high concentration of apyrase (2 U/mL), which prevents P2X₁ channels from desensitization and block ADP-mediated aggregation responses. As expected, thrombin- or U46619-induced platelet aggregation was strongly enhanced in *Orai1*^{-/-}/*Trpc6*^{-/-} platelets while *Orai1*^{-/-} platelets responded similarly to *Wt* platelets (Figure 3-12 B), confirming the previous results. According to these data, P2X₁ channel is speculated to compensate for the severe Ca^{2+} deficits of *Orai1*^{-/-}/*Trpc6*^{-/-} platelets under *in vivo* conditions.

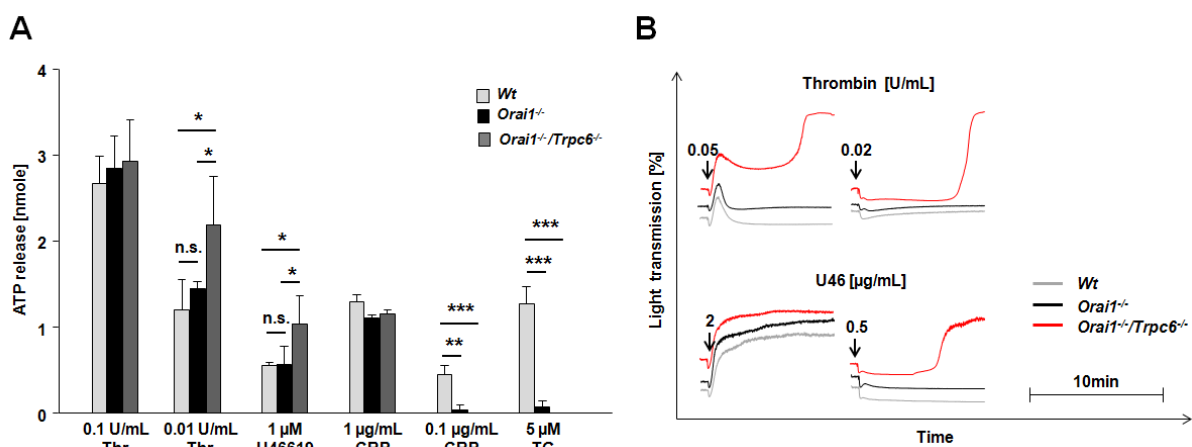


Figure 3-12: Enhanced ATP secretion in response to the GPCR agonists in *Orai1*^{-/-}/*Trpc6*^{-/-} platelets. (A) Washed platelets were incubated with Luciferase-Luciferin reagent, and ATP secretion was measured using a Chronolog aggregometer after stimulation with indicated agonists. **p* < 0.05, ***p* < 0.01, ****p* < 0.001. (B) Aggregation responses of *Wt* (grey line), *Orai1*^{-/-} (black line) and *Orai1*^{-/-}/*Trpc6*^{-/-} (red line) platelets in the presence of ACD and a high concentration of apyrase (2 U/mL). (Chen et al., *J Thromb Haemost* 2014)¹⁶⁹

3.2 The role of the TRPM7 kinase in mouse platelets

Mg²⁺ has been shown to be associated with several diseases. In many cardiovascular diseases, such as metabolic syndrome, diabetes mellitus, hypertension and stroke, altered Mg²⁺ homeostasis is described.⁹⁴⁻⁹⁷ Moreover, Mg²⁺ has been considered as a “natural antagonist” of Ca²⁺ for more than 50 years. It has been suggested that Mg²⁺ competes with Ca²⁺ for the same binding sites of receptors in the PM and influences Ca²⁺ entry.⁹⁸ In platelets high levels of extracellular Mg²⁺ were shown to reduce Ca²⁺ influx¹⁰⁶ and inhibit platelet aggregation,¹⁰³⁻¹⁰⁵ indicating that Mg²⁺ channels or transporters on platelet surface may play a role in platelet Ca²⁺ homeostasis and platelet activation.

TRPM7 is one of the most interesting Mg²⁺ channels since it is expressed in virtually all cell types and the structure and the physiological role of TRPM7 is well studied. TRPM7 contains an atypical α -kinase domain at the C-terminus, which has been proposed to play a role in diverse phospho-signaling events. The TRPM7 kinase domain contains multiple autophosphorylation sites, whose autophosphorylation enhance the kinase to interact with different substrates, leading to Ser/Thr phosphorylation of the substrates.¹⁵⁰ Up to date, only a limited number of endogenous substrates of the TRPM7 kinase has been identified in mammalian cells.^{151,177} It has been reported that the kinase domain of TRPM7 directly interacts with the C2 domain of PLC isoforms.¹³⁸ Furthermore, several Ser/Thr phosphorylation sites in the C2 domain of PLC γ 2 was identified by using the TRPM7 kinase in a DT40 cell line.¹⁵⁴ Taken together, these findings indicate that the TRPM7 kinase may regulate the activity of PLC isoforms, thereby influencing Ca²⁺ homeostasis. One aim of this thesis was to elucidate the role of the TRPM7 kinase in platelet Ca²⁺ homeostasis and platelet function.

3.2.1 Impaired Ca²⁺ homeostasis in the presence of high levels of extracellular Mg²⁺

In many cell types, Mg²⁺ has been reported to inhibit Ca²⁺ entry.¹⁰⁷ To study whether Mg²⁺ can influence Ca²⁺ influx in platelets, two major Ca²⁺ entry routes, ROCE and SOCE, were measured in the presence of physiological concentration (1 mM) and high concentration (5 mM) of extracellular Mg²⁺. To induce ROCE, platelets were stimulated with 150 μ M DAG analogue, OAG, which directly activates TRPC6. For SOCE measurement, TG was applied to activate Orai1 and the changes of [Ca²⁺]_i were determined. As expected, reduced ROCE (Figure 3-13 A) and SOCE (Figure 3-13 B) were observed in the presence of 5 mM extracellular Mg²⁺, suggesting an inhibiting effect of elevated extracellular Mg²⁺ levels on platelet Ca²⁺ homeostasis.

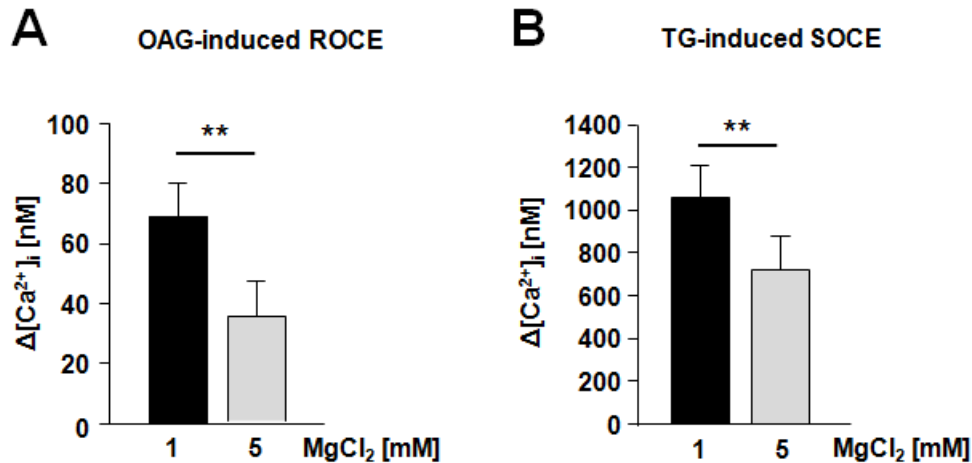


Figure 3-13: High extracellular Mg²⁺ levels inhibit Ca²⁺ influx in platelets. Fura2-loaded platelets from normal C57Bl6 mice were incubated in physiological (1 mM) or high (5 mM) concentrations of extracellular Mg²⁺. OAG-induced ROCE (**A**) and TG-induced SOCE (**B**) were determined by a fluorimeter with excitation at 340 and 380 nm and emission at 509 nm.

3.2.2 Inhibiting effects of high extracellular Mg²⁺ concentrations on platelet activation

In human platelets, high extracellular Mg²⁺ levels have been reported to inhibit platelet activation and aggregation.¹⁰²⁻¹⁰⁵ Moreover, in mouse platelets the elevation of extracellular Mg²⁺ concentrations leads to impaired Ca²⁺ homeostasis, indicating that high levels of extracellular Mg²⁺ may also play an inhibiting role in platelet activity in mouse platelets. To study this, platelets from C57Bl6 mice were used and their function was determined in the presence of high concentrations of extracellular Mg²⁺. Integrin α IIb β 3 inside-out activation and P-selectin exposure were measured by flow cytometric assay. Washed platelets were incubated in physiological concentration (1 mM) or high concentration (5 mM) of extracellular Mg²⁺ for 10 min, then were stimulated with thrombin, CRP or Rhodocytin. Consistent with results from human platelets, integrin activation and degranulation were reduced in the presence of 5 mM Mg²⁺ compared to 1 mM Mg²⁺, indicating that high extracellular Mg²⁺ can inhibit platelet activation (Figure 3-14 A). In the next step, platelet aggregation in the presence of high Mg²⁺ concentrations was investigated. Similarly, platelet aggregation in response to GPCR-PLC β and (hem)ITAM-PLC γ 2 agonists was severely impaired in platelets treated with 5 mM Mg²⁺ (Figure 3-14 B). In line with these findings, elevation of extracellular Mg²⁺ resulted in the inhibition of thrombus formation on immobilized collagen under flow conditions (Figure 3-14 C). Taken together, these results suggest that high levels of extracellular Mg²⁺ play an inhibiting effect on platelet activation, aggregation and thrombus formation.

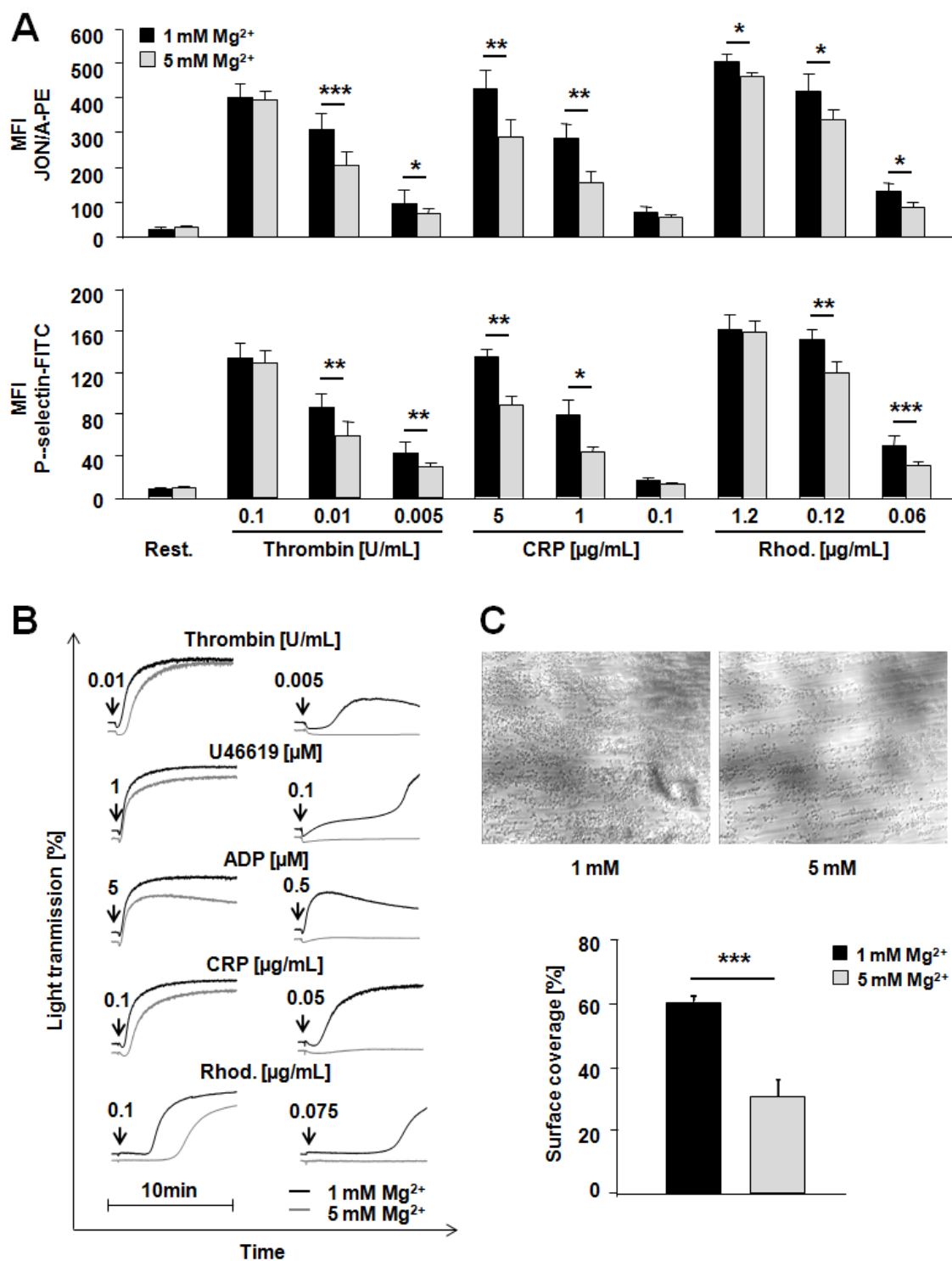


Figure 3-14: High extracellular Mg^{2+} levels inhibit platelet activation, aggregation and thrombus formation. (A) Washed platelets from C57Bl6 mice were incubated in 1 mM or 5 mM of extracellular Mg^{2+} . Thereafter, platelets were stimulated with indicated agonists (thrombin: 0.1 – 0.005 U/mL, CRP: 5 – 0.1 μ g/mL, Rhodocytin: 1.2 – 0.06 μ g/mL), and integrin α IIb β 3 activation and P-selectin exposure was analyzed by flow cytometer. Results are represented as MFI \pm SD. (B) Washed platelets, incubated in 1 mM and 5 mM extracellular Mg^{2+} , were stimulated with GPCR-PLC β (thrombin, U46619, ADP) or ITAM-PLC γ 2 (CRP, Rhod.) agonists. Light transmission was recorded on a FibrinTimer 4-channel aggregometer. ADP measurements were performed in platelet-rich plasma. (C) Different amounts of $MgCl_2$ were added into heparinized blood samples and incubated for 10 min. Afterwards, blood samples were perfused over a collagen-coated surface at a shear rate of 1000 s^{-1} . Representative phase contrast images of control (1 mM, left) and Mg^{2+} -treated (5 mM, right) are shown. Mean surface coverage of platelets was measured. * $p < 0.05$, ** $p < 0.01$, *** $p < 0.001$.

3.2.3 TRPM7 is expressed in mouse platelets

In mammalian cells, more than 20 Mg^{2+} channels or transporters have been identified on the plasma membrane, the ER membrane, the mitochondrial membrane and also the membrane of Golgi apparatus.^{117,178,179} To identify the major Mg^{2+} channels in mouse platelets, mRNA expression profiles of plasma membrane Mg^{2+} channels were studied. Total mRNAs were isolated from mouse platelets and brain tissue (as positive control) and RT-PCRs were performed using Mg^{2+} channel specific primers. In platelets, only MagT1 and TRPM7 were predominantly expressed and TUSC3 was also detectable at mRNA level, while most of the investigated Mg^{2+} channels could be detected in brain tissues (Figure 3-15 A). Furthermore, at protein level, the expression of TRPM7 was confirmed by immunofluorescent confocal microscopy. In fully spreaded *Wt* platelets, TRPM7 protein was detectable and was found to mainly locate on the cell surface (Figure 3-15 B).

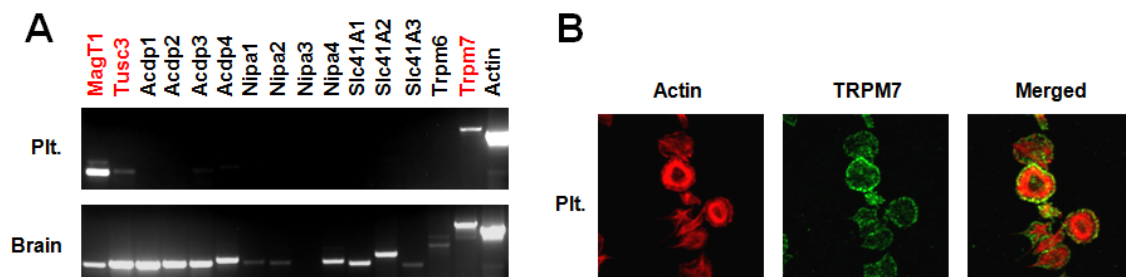


Figure 3-15: TRPM7 is expressed in mouse platelets. (A) mRNA expression profiles of plasma membrane Mg^{2+} channels and transporters in mouse platelets and brain tissues were detected by RT-PCR. Actin was used as loading control. **(B)** Protein expression and subcellular localization of TRPM7 in *Wt* platelets was confirmed. Upon stimulation with 0.01 U/mL thrombin, platelets were allowed to spread on fibrinogen-coated surface for 30 min. Thereafter platelets were fixed and permeabilized, then were stained with phalloidin Atto647N and TRPM7 antibody to detect F-actin and TRPM7. Representative confocal microscopy images are shown using TRPM7 antibody and phalloidin staining to label the actin cytoskeleton.

3.2.4 Generation of TRPM7 "kinase-dead" mice *Trpm7^{KI}*

To investigate the physiological significance of the TRPM7 kinase, a "kinase-dead" knock-in mouse line (*Trpm7^{KI}*) was generated (kindly provided by Prof. Dr. Thomas Gudermann and Dr. Vladimir Chubanov, Walther-Straub Institute for Pharmacology and Toxicology, LMU München), in which a single base pair in exon 33 of the *Trpm7* gene was mutated, resulting in the single AA substitution of arginine for lysine at position 1646 (Figure 3-16 A).

ATP and Mg^{2+} bindings to the kinase domain are required for the optimal enzymatic activity of the TRPM7 kinase, and amino acid TRPM7^{K1646} is critical for their bindings. Mutation of TRPM7^{K1646R} abolishes ATP and Mg^{2+} bindings, thereby inhibiting the autophosphorylation of TRPM7^{S1511}, one of the major autophosphorylation sites in the kinase domain. Moreover,

mutation of TRPM7^{S1511} completely abolishes the kinase activity.¹⁵⁶ Therefore, in TRPM7^{K1646R} mutant, the indirect inhibition of phosphorylation of TRPM7^{S1511} also inactivates the kinase (Figure 3-16 B, upper panel).

To test whether the targeting vector is functional, *hemagglutinin* (HA)-tag TRPM7 with mutation of TRPM7^{K1646R} or TRPM7^{S1511C} (as negative control) was overexpressed in HEK293 cells. The autophosphorylation of the TRPM7 kinase was detected with anti-phospho-serine 1511 antibody. These experiments were performed in collaboration with Prof. Dr. Thomas Gudermann, Dr. Vladimir Chubanov and their colleagues, Walther-Straub Institute for Pharmacology and Toxicology, LMU München. In wild-type (positive control), the phosphorylation of TRPM7^{S1511} was detectable. However, in TRPM7^{S1511C} mutant (negative control), phosphorylation of TRPM7^{S1511} was completely abolished. In line with negative control, TRPM7^{K1646R} mutant also exhibited abolished TRPM7^{S1511} phosphorylation (Figure 3-16 B, lower panel), establishing that the knock-in strategy is successful.

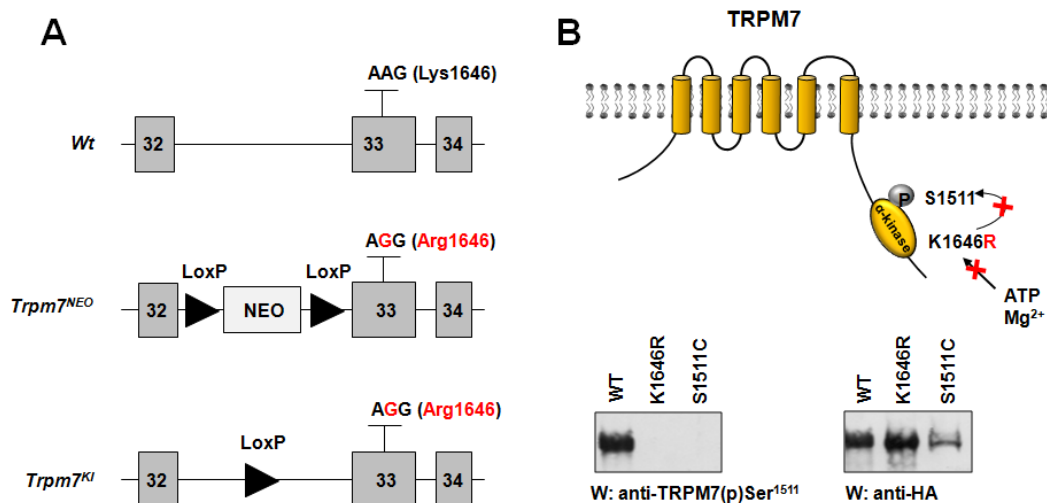


Figure 3-16: Generation of *Trpm7^{KI}* mice. (A) Targeting strategy of the "kinase-dead" knock-in mouse was based on homologous recombination of a targeting vector into the *Trpm7* locus carrying a single base pair substitution (K1646R) in exon 33. A floxed neomycin (NEO) knock-in cassette was inserted into intron 32 for selecting the targeted ES cells. By crossing the *Trpm7^{NEO}* mice with deleter-Cre mice the floxed NEO cassette was removed *in vivo* to generate *Trpm7^{KI}* mice. **(B)** Upper panel: a model about TRPM7^{K1646R} mutant inhibiting TRPM7^{S1511} phosphorylation and inactivate the kinase activity. Lower panel: HA-tagged TRPM7 carrying mutation on K1646R or S1511C was overexpressed in HEK293 cells. Anti-phospho-serine 1511 antibody was used to detect the phosphorylation of the TRPM7 kinase, and HA expression was shown as loading control. K1646R mutation in the kinase domain completely blocks autophosphorylation on amino acid residue of S1511 in HEK293 cells.

3.2.5 Normal TRPM7 channel activity in *Trpm7^{KI}* mice

The role of the TRPM7 kinase domain in regulating its channel activity remains controversial and only partially understood. Recent studies suggest that the kinase activity is not essential for channel activation, but plays a role in modulating channel activity. Similarly, channel

activity affects kinase activity, since Mg^{2+} influx via the channel can regulate the kinase activity.^{128,155} To study whether the "kinase-dead" knock-in affects TRPM7 channel activity, TRPM7 current in primary *mouse embryonic fibroblast* (MEF) cells, which were isolated from *Trpm7^{Kl}* embryos, was measured. This work was performed in collaboration with Prof. Dr. Thomas Gudermann, Dr. Vladimir Chubanov and their colleagues, Walther-Straub Institute for Pharmacology and Toxicology, LMU München. Compared to *Wt* MEF cells, *Trpm7^{Kl}* MEF cells exhibited unaltered TRPM7 current (Figure 3-17 A). Similarly, in blood serum and bone from *Trpm7^{Kl}* mice Mg^{2+} concentrations were unchanged (Figure 3-17 B), suggesting a normal long-term *in vivo* Mg^{2+} status in *Trpm7^{Kl}* mice. In line with these results, the basal $[Mg^{2+}]_i$ and $[Ca^{2+}]_i$ in *Trpm7^{Kl}* platelets were found to be normal (Figure 3-17 C). Altogether, these results indicate that the kinase activity of TRPM7 is dispensable for Mg^{2+} homeostasis, at least under our experimental conditions.

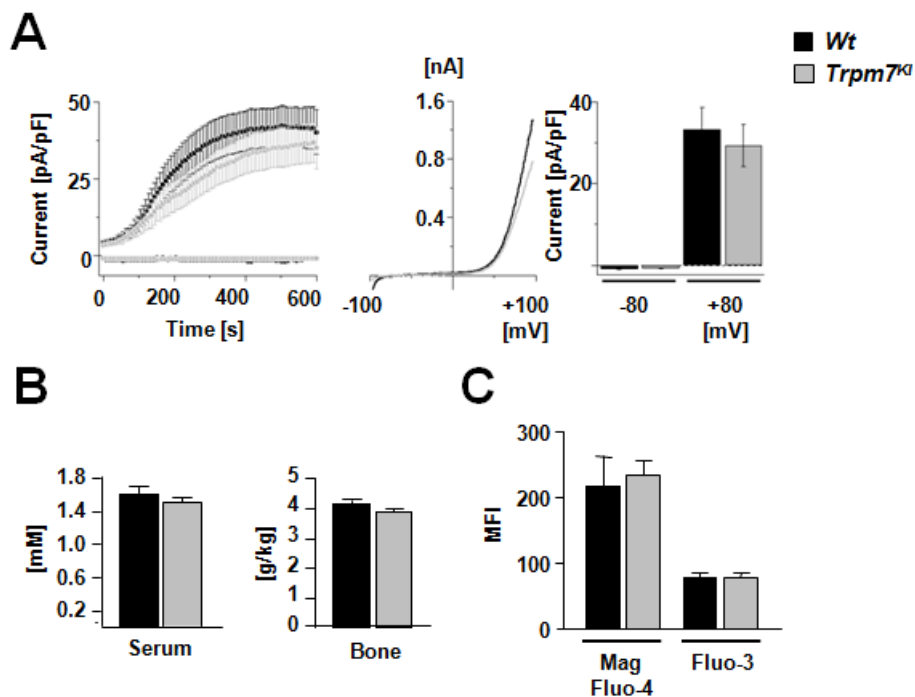


Figure 3-17: Unaltered TRPM7 channel activity in *Trpm7^{Kl}* mice. (A) TRPM7 currents in primary MEF cells derived from *Wt* and *Trpm7^{Kl}* embryos are shown. Currents were elicited by a ramp protocol from -100 to +100 mV over 50 ms acquired at 0.5 Hz. Inward current amplitudes were extracted at -80 mV, outward currents at +80 mV and plotted versus time of the experiment. Data were normalized to cell size as pA/pF. Representative current-voltage relationships extracted at 600 s. Quantification of inward and outward currents at -80 mV and +80 mV at 600 s. Measurements were conducted in the absence of extracellular Mg^{2+} to enhance current sizes. No changes in channel activation were observed under these conditions. (B) Quantification of Mg^{2+} concentrations in blood serum and bone in adult mice. (C) In Mag-Fluo-4 and Fluo-3 loaded resting platelets of washed blood cytoplasmic Mg^{2+} and Ca^{2+} concentrations were respectively detected with flow cytometer.

3.2.6 TRPM7 kinase function is dispensable for platelet generation

To analyze the role of the TRPM7 kinase activity in platelet physiology, platelet count and size were determined with an automated hematology analyzer. *Trpm7^{Kl}* mice exhibited

normal platelet count and size (Figure 3-18 A). Additionally the expression levels of major surface glycoproteins were also measured by flow cytometer, and found to be unaltered in *Trpm7^{Kl}* mice (Figure 3-18 B). These results indicate that the disruption of the TRPM7 kinase activity has no significant effect on peripheral platelet count, size and glycoprotein expression. Furthermore, platelet life span in blood stream was determined. Mouse platelets display a life span of approximate 5 days. After that they are cleared by the reticulo-endothelial system in spleen and liver. To determine platelet life span, circulating platelets were labeled by intravenous injection of a fluorescence-coupled anti-GPIX antibody derivative, which does not influence platelet function.¹⁵⁹ One hour after antibody injection, the percentage of labeled platelets was assessed by flow cytometry and more than 90% of circulating platelets were labeled in both *Wt* and *Trpm7^{Kl}* mice. Over the next 5 days, the percentage of labeled platelets was monitored (Figure 3-18 C). In *Trpm7^{Kl}* mice, platelet life span was normal compared to *Wt* mice, demonstrating that the TRPM7 kinase activity is dispensable for platelet production and turnover in normal physiology.

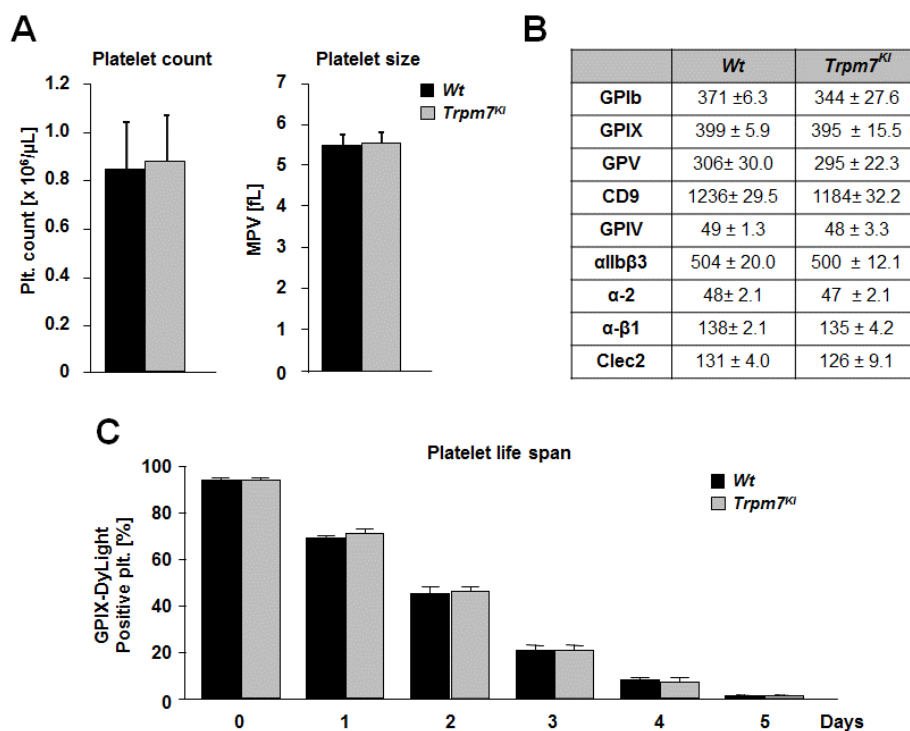


Figure 3-18: TRPM7 kinase function is dispensable for platelet generation. (A) Peripheral platelet count and platelet size of *Wt* and *Trpm7^{Kl}* mice were measured with an automated hematology analyzer. Results are mean ± SD. (B) Diluted whole blood was incubated with saturating concentrations of indicated FITC-labeled antibodies for 15 min at RT. Afterwards the expression of major surface glycoproteins were analyzed by flow cytometry. Results are shown as MFI ± SD. (C) Platelet life span determination. *Wt* and *Trpm7^{Kl}* mice were injected intravenously with DyLight-488 conjugated anti-GPIX derivative (0.5 mg/kg). The percentage of fluorescently labeled platelets was determined over 5 days using a flow cytometer.

3.2.7 Impaired PLC γ 2-ITAM-mediated and partially defective PLC β -GPCR-mediated activation in *Trpm7*^{Kl} platelets

The TRPM7 kinase has been suggested to directly interact with the C2 domain of PLC isoforms in mammalian cells,¹³⁸ and in platelets the activation of PLC isoforms (PLC β and PLC γ 2) is critical for agonist-induced activation. To study the effect of the TRPM7 kinase activity on platelet activation, agonist-induced activation of the major platelet integrin α IIb β 3 and degranulation-dependent P-selectin exposure were analyzed by flow cytometry. Upon stimulation with high concentrations of the GPCR-specific agonists (ADP, U46619 and thrombin), *Trpm7*^{Kl} platelets responded normally. Only at threshold concentrations of thrombin, integrin α IIb β 3 activation and P-selectin exposure in *Trpm7*^{Kl} platelets were reduced (Figure 3-19 A), indicating that the TRPM7 kinase partially influences PLC β -GPCR-mediated platelet activation. In contrast, in response to both high and low concentrations of the GPVI-specific agonists (CRP and CVX), integrin α IIb β 3 activation and P-selectin exposure were markedly reduced (Figure 3-19 B), suggesting that the TRPM7 kinase plays an important role in PLC γ 2-ITAM-mediated platelet activation.

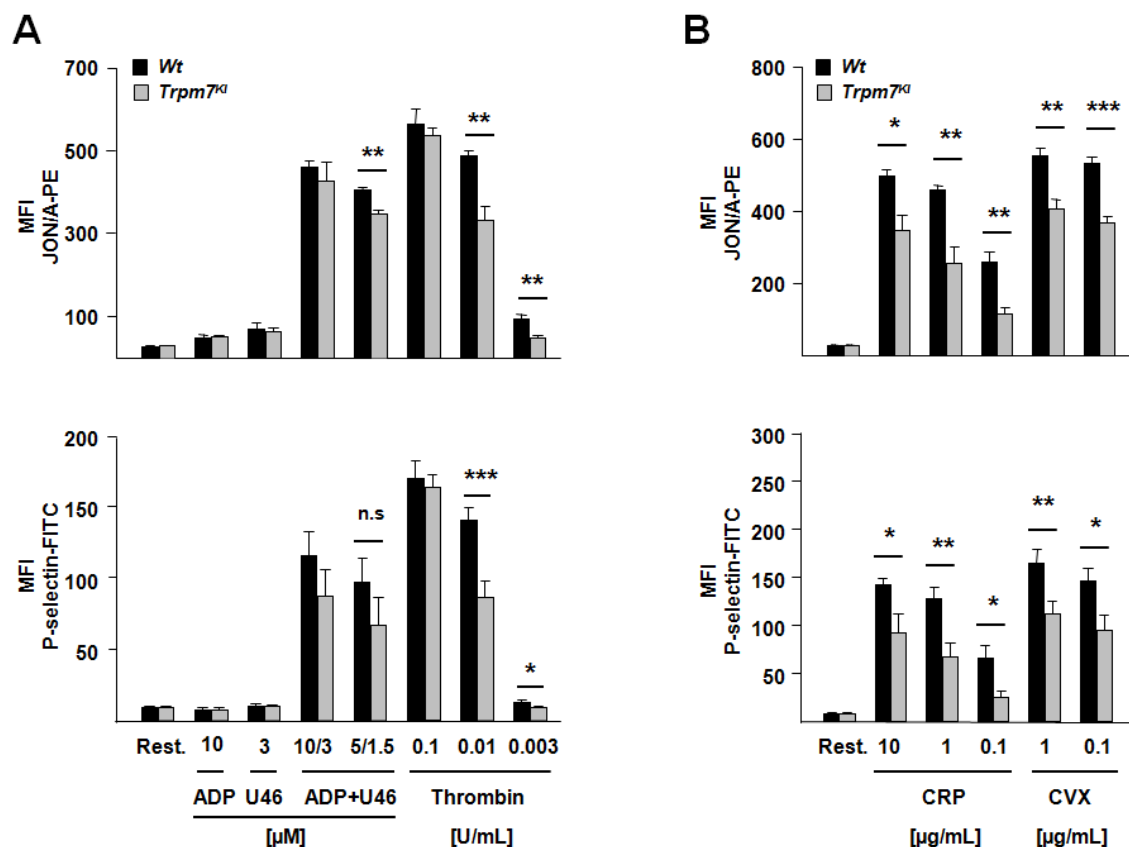


Figure 3-19: Severely impaired ITAM-PLC γ 2- and partially defective GPCR-PLC β -mediated platelet activation. Different concentrations of the GPCR-specific agonists (A) and the GPVI-specific agonists (B) were used to stimulate platelets. Integrin α IIb β 3 activation (upper panel) and P-selectin exposure (lower panel) were assessed using PE-labeled JON/A antibody and FITC-labeled anti-P-selectin antibody, respectively. Results are represented as MFI \pm SD. * p < 0.05, ** p < 0.01, *** p < 0.001.

To investigate how these defects in integrin inside-out activation and degranulation influence aggregation of *Trpm7^{Kl}* platelets, an *in vitro* aggregation experiment was performed. Consistent with the flow cytometric results, *Trpm7^{Kl}* platelets exhibited partially impaired aggregation in response to low concentrations of thrombin, but upon stimulation with ADP, U46619 and high concentrations of thrombin, *Trpm7^{Kl}* platelets aggregated normally. In contrast, in response to the GPVI-specific agonists, CRP and collagen, *Trpm7^{Kl}* platelets exhibited severely reduced aggregation (Figure 3-20). In summary, disruption of the TRPM7 kinase activity results in strong defects of PLC γ 2-ITAM-mediated platelet activation and aggregation, and partial defects of PLC β -GPCR-dependent platelet activity.

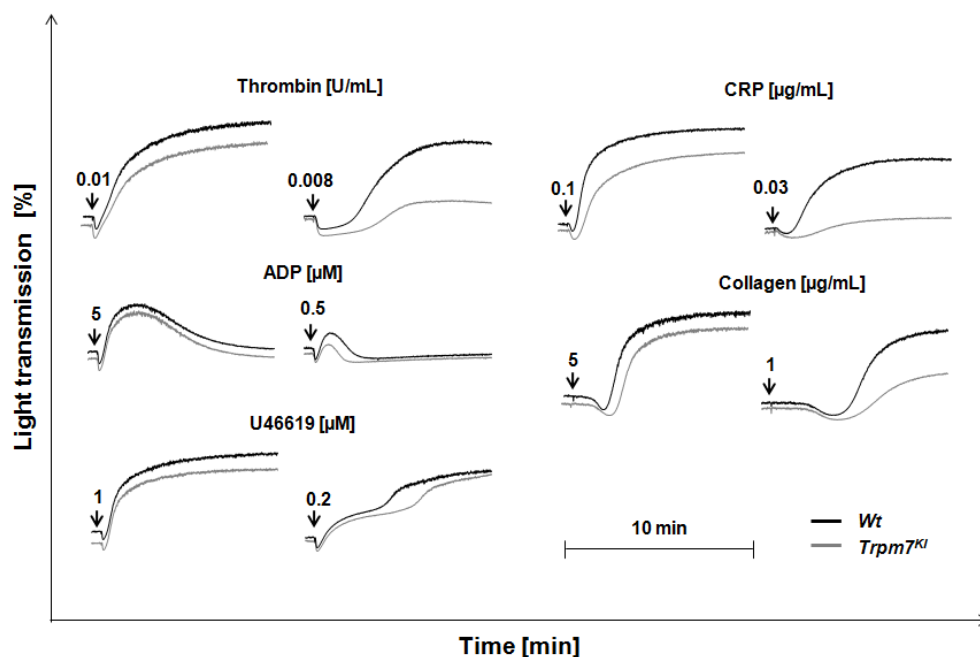


Figure 3-20: Severely impaired ITAM-PLC γ 2 and partially defective GPCR-PLC β -mediated platelet aggregation. Washed platelets from *Wt* (black line) and *Trpm7^{Kl}* (grey line) mice were stimulated with GPCR-PLC β (thrombin, ADP and U46619) or ITAM-PLC γ 2 (CRP and collagen) agonists at the indicated concentrations. Light transmission was recorded on a Fibrinometer 4-channel aggregometer. ADP measurements were performed in platelet-rich plasma, all other measurements were performed in buffer with 100 μ g/mL human fibrinogen (except for thrombin).

3.2.8 *Trpm7^{Kl}* platelets display normal spreading on fibrinogen

To investigate integrin outside-in signaling, a spreading assay was performed. Upon stimulation with 0.01 U/mL thrombin, platelets were allowed to spread on immobilized fibrinogen for 30 min and analyzed at different time points. Compared to *Wt* platelets, *Trpm7^{Kl}* platelets were able to form filopodia and lamellipodia to the same extent with similar kinetics. Moreover, *Trpm7^{Kl}* platelets could fully spread as *Wt* platelets after 30 min (Figure 3-21). These data indicate that the TRPM7 kinase activity is not required for integrin outside-in signaling and cytoskeletal reorganization in platelets.

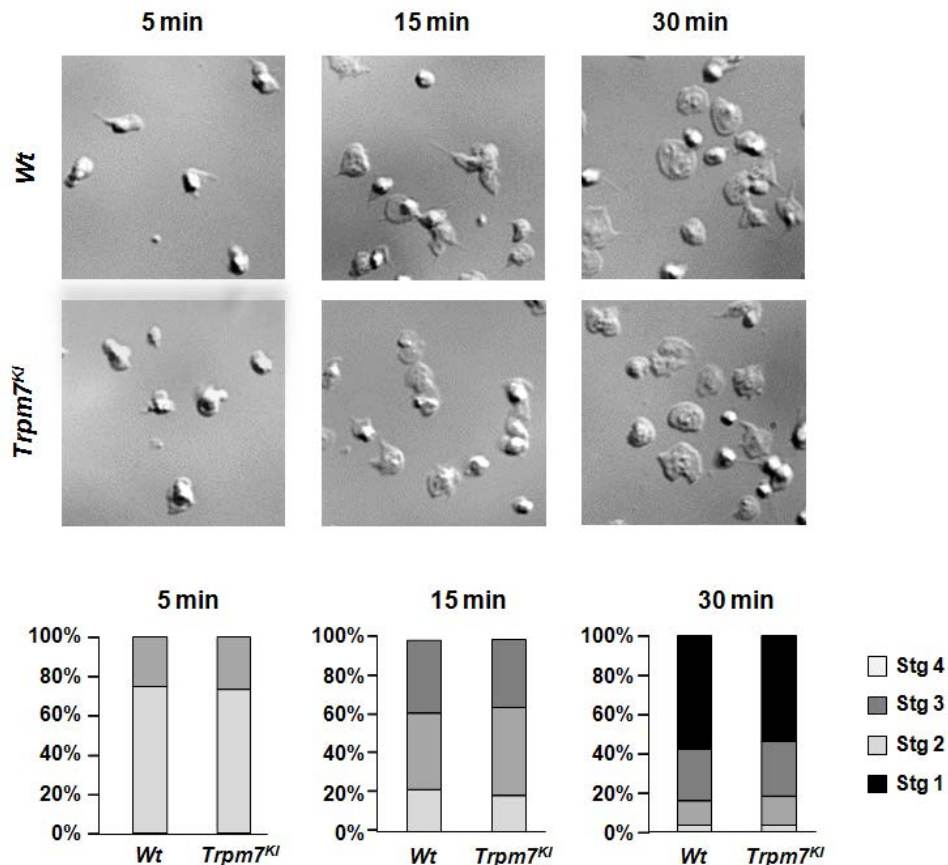


Figure 3-21: Unaltered spreading of *Trpm7^{Kl}* platelets on fibrinogen. Washed platelets from *Wt* and *Trpm7^{Kl}* mice were allowed to spread on immobilized fibrinogen (200 $\mu\text{g}/\text{mL}$) for 30 min after stimulation with 0.01 U/mL thrombin. Upper panel: representative DIC images of 3 individual experiments from the indicated time points. Lower panel: statistical evaluation of the percentage of platelets at different stages of spreading. Stg 1: roundish, Stg 2: only filopodia, Stg 3: filopodia and lamellipodia, Stg 4: fully spread.

3.2.9 Impaired dense granule secretion in *Trpm7^{Kl}* platelets

Flow cytometric results showed defective P-selectin exposure in *Trpm7^{Kl}* platelets in response to GPVI agonists, indicating that α -granule degranulation is affected. To test whether dense granule secretion is also affected in *Trpm7^{Kl}* platelets, the amount of released ATP and serotonin were measured. Washed platelets from *Wt* and *Trpm7^{Kl}* mice were stimulated with thrombin (0.1 U/mL and 0.01 U/mL) or CRP (0.1 $\mu\text{g}/\text{mL}$ and 0.05 $\mu\text{g}/\text{mL}$), and ATP secretion was determined by using CHRONO-LUME reagent, while serotonin secretion was quantified by an ELISA assay. In line with flow cytometry and aggregometry results, ATP (Figure 3-22 A) and serotonin (Figure 3-22 B) secretion in response to low concentrations of thrombin and CRP were reduced, suggesting that agonist-induced dense granule secretion is also impaired in *Trpm7^{Kl}* platelets.

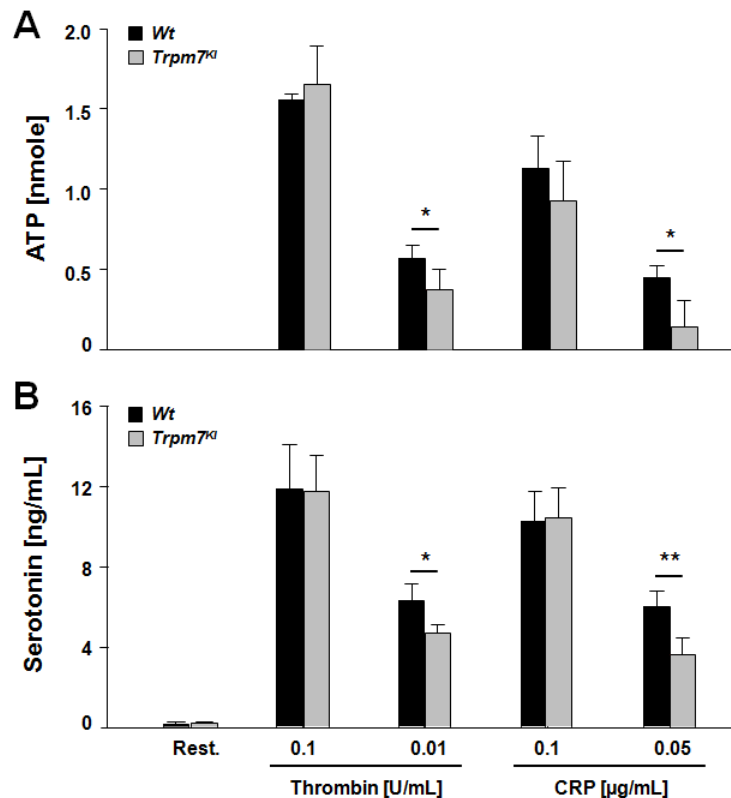


Figure 3-22: Impaired dense granule secretion in *Trpm7^{Kl}* platelets. (A) Washed platelets from *Wt* and *Trpm7^{Kl}* mice were adjusted to 500,000 platelets/ μ L and incubated with Luciferase-Luciferin reagent. Upon stimulation with different concentrations of thrombin or CRP, ATP release was measured using a Chronolog aggregometer. (B) 500,000 platelets/ μ L of washed platelets were stimulated with the indicated agonists for 5 min. Afterwards, platelets were spun down and the supernatant was taken. The amount of serotonin in the supernatant was quantified by an ELISA assay. * $p < 0.05$, ** $p < 0.01$.

3.2.10 The TRPM7 kinase regulates PL-mediated Ca^{2+} responses in platelets

The enzymatic activity of PLs has been well established to play a critical role in Ca^{2+} homeostasis in platelets, which is essential for platelet activation, aggregation and degranulation. It has been suggested that the TRPM7 kinase can directly interact with the C2 domain of PLC isoforms.¹³⁸ Furthermore, flow cytometric and aggregometric results showed that platelet activation and aggregation were impaired in *Trpm7^{Kl}* platelets. These findings lead to a proposal that the TRPM7 kinase may influence PL activity and Ca^{2+} homeostasis in platelets, thereby affecting their activation and aggregation. To study the effect of the TRPM7 kinase on PL activity, the time-dependent accumulation of IP_1 , a non-degradable stable product of IP_3 , was measured by using an IP_1 ELISA (Figure 3-23 A). Upon stimulation with a high concentration (0.1 U/mL) of thrombin, *Trpm7^{Kl}* platelets exhibited normal IP_1 production, however at low concentration (0.01 U/mL), the amount of IP_1 in *Trpm7^{Kl}* platelets was slightly lower than *Wt* platelets. In contrast, in response to both high (1 μ g/mL) and low (0.1 μ g/mL) concentrations of CRP, *Trpm7^{Kl}* platelets showed defective IP_1 production. These results indicate that the TRPM7 kinase plays an important

role in regulating the activity of PLC γ 2, but a minor role in the regulation of PLC β activity.

Further, the activation of PLC isoforms leads to DAG and IP $_3$ production. DAG directly activates ROC channels (mainly TRPC6) and induces ROCE, while IP $_3$ production results in Ca $^{2+}$ release from the intracellular stores and induces subsequent Ca $^{2+}$ influx via Orai1 channels. Since *Trpm7^{Kl}* platelets exhibit defective PL activity, it can be reasoned that their Ca $^{2+}$ response may also be impaired. Therefore, intracellular Ca $^{2+}$ store release and extracellular Ca $^{2+}$ entry were measured (Figure 3-23 B). Upon stimulation with thrombin, ADP and U46619, *Trpm7^{Kl}* platelets exhibited normal store release and Ca $^{2+}$ entry. However, in response to CRP, *Trpm7^{Kl}* platelets displayed severely reduced store release and Ca $^{2+}$ entry. These results confirm the role of the TRPM7 kinase in regulating PLC γ 2 activity.

In summary, the TRPM7 kinase can regulate phospholipase activity and influence Ca $^{2+}$ homeostasis in platelets, which results in impaired platelet activation, degranulation and aggregation.

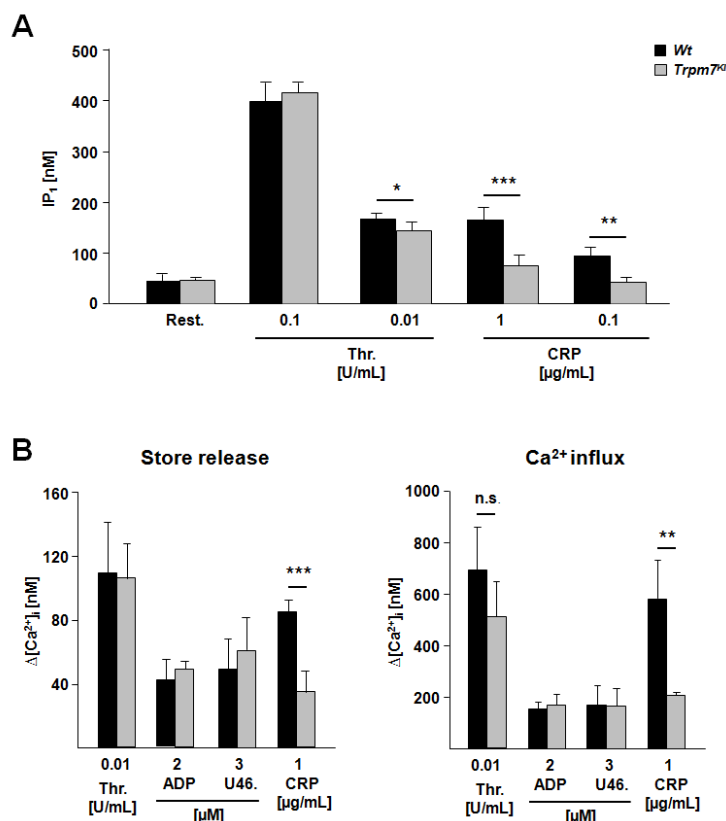


Figure 3-23: The TRPM7 kinase regulates PLC γ 2-mediated Ca $^{2+}$ mobilization. (A) IP $_1$ (a specific metabolite of IP $_3$) concentrations were quantified with an ELISA assay. *Wt* platelets (black) could produce 165 ± 25 or 92 ± 18 nM IP $_1$ in response to 1 μ g/mL or 0.1 μ g/mL CRP, respectively. In sharp contrast, *Trpm7^{Kl}* platelets (grey) could only generate 74 ± 22 and 40 ± 6 nM IP $_1$, respectively. As for thrombin, *Wt* platelets could generate 397 ± 36 and 168 ± 9 nM IP $_1$ in response to 0.1 U/mL or 0.01 U/mL thrombin respectively, however *Trpm7^{Kl}* platelets produced 414 ± 19 and 143 ± 16 nM IP $_1$ respectively. **(B)** Fura2-loaded *Wt* (black) and *Trpm7^{Kl}* platelets (grey) were stimulated with indicated agonists in the presence of 0.5 mM EGTA (store release) or in the presence of 1 mM Ca $^{2+}$ (Ca $^{2+}$ influx) and changes in [Ca $^{2+}$]_i were measured with a fluorimeter. Representative measurements and maximal increase in [Ca $^{2+}$]_i compared with baseline levels before stimulus are depicted as $(\Delta[\text{Ca}^{2+}]_i) \pm \text{SD}$. * $p < 0.05$, ** $p < 0.01$, *** $p < 0.001$.

3.2.11 Normal GPVI-induced tyrosine phosphorylation in *Trpm7^{Kl}* platelets

Changes in the tyrosine phosphorylation of the proteins in GPVI-signaling cascade have been extensively studied in the past,¹⁸⁰ however the physiological significance of Ser/Thr phosphorylation in this signaling cascade remains largely unknown. The tyrosine kinase Syk plays a central role in the GPVI signaling pathway. Syk phosphorylation at Y519/520 has been suggested to enhance the kinase's activity, which subsequently mediates LAT phosphorylation (Y191) and contributes to PLC γ 2 phosphorylation (Y759).^{181,182} Furthermore, deletion of Syk or LAT *in vivo* severely impairs PLC γ 2 function and IP₃-induced Ca²⁺ mobilization in platelets.^{183,184} To investigate whether the TRPM7 kinase regulates tyrosine kinases or phosphatases in the GPVI-signaling cascade, time-dependent tyrosine phosphorylation of GPVI-signaling was monitored in *Wt* and *Trpm7^{Kl}* platelets. This experiment was performed in collaboration with Dr. Heike Hermanns, Rudolf Virchow Center, University of Würzburg. Neither global tyrosine phosphorylation, as assessed by the 4G10 antibody (Figure 3-24 A), nor phospho-Syk^{Y525/526}, phospho-LAT^{Y191}, or phospho-PLC γ 2^{Y759} were altered in *Trpm7^{Kl}* platelets after activation of GPVI (Figure 3-24 B). These results suggest that tyrosine kinases and phosphatases involved in the GPVI-signaling cascade are not regulated by the TRPM7 kinase.

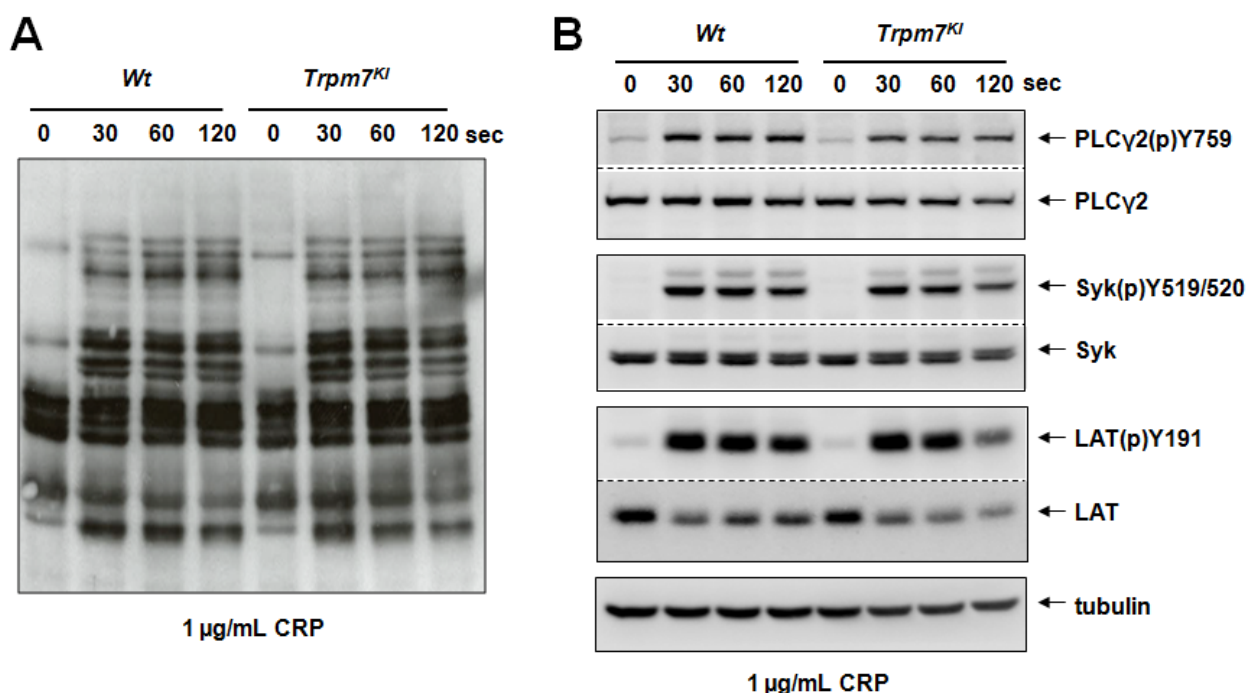


Figure 3-24: Normal GPVI-induced tyrosine phosphorylation. 1 µg/mL CRP was used to stimulate washed platelets for 0, 30, 60 and 120 seconds under stirring condition. **(A)** The whole cell tyrosine phosphorylation in *Wt* or *Trpm7^{Kl}* platelet were detected by western blot using phosphotyrosine antibody 4G10. **(B)** Tyrosine phosphorylation of the GPVI-signaling cascade was determined with the indicated antibodies by Western blotting.

3.2.12 *Trpm7^{Kl}* platelets exhibit impaired procoagulant activity

The exposure of PS to the outer surface of the plasma membrane is a key mechanism how platelets promote coagulation. It has been suggested that high $[Ca^{2+}]_i$ is essential for PS exposure. Impaired Ca^{2+} homeostasis in *Trpm7^{Kl}* platelets may influence PS exposure and then affect platelet-dependent coagulation. To study this, *Wt* and *Trpm7^{Kl}* platelets were activated with thrombin and/or CRP, and PS exposure was measured using Dylight-488-labeled annexin V, which specifically binds to PS-exposed platelets. In line with Ca^{2+} measurement results, *Trpm7^{Kl}* platelets displayed reduced PS exposure in response to CRP, but normal PS exposure to thrombin. In addition, under stimulation of a combination of low dose of thrombin and CRP, PS exposure was also impaired in *Trpm7^{Kl}* platelets (Figure 3-25). These results indicate that disruption of the TRPM7 kinase activity leads to impaired procoagulant activity.

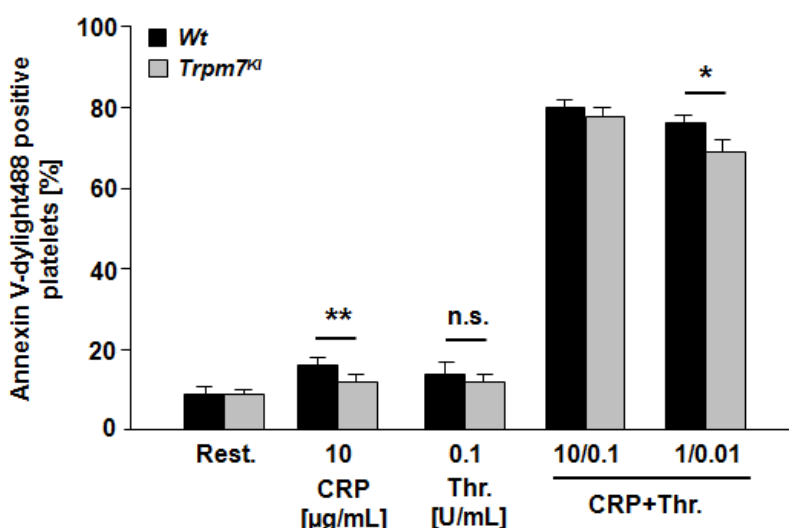


Figure 3-25: Impaired PS exposure in *Trpm7^{Kl}* platelets. PS exposure in response to the indicated agonists was measured by flow cytometric analysis. Washed blood from *Wt* and *Trpm7^{Kl}* mice were incubated with annexin V-DyLight-488, and then stimulated with the indicated agonists in the presence of 2 mM Ca^{2+} . The percentage of annexin V-DyLight-488 positive platelets was determined by flow cytometry. * $p < 0.05$, ** $p < 0.01$.

3.2.13 Impaired thrombus formation of *Trpm7^{Kl}* platelets on collagen under flow conditions

Since it is well established that GPVI-collagen interaction is a critical step for platelet adhesion and thrombus growth at sites of vessel wall injury, the TRPM7 kinase may play a role in thrombus formation under flow. To study this, anti-coagulated whole blood from *Wt* or *Trpm7^{Kl}* mice was perfused over collagen-coated surface at a shear rate of $1000s^{-1}$, mimicking the flow conditions in large arteries. *Wt* platelets could adhere to collagen fibers quickly, aggregate stably and form large three-dimensional thrombi at the end of the perfusion period. In sharp contrast, *Trpm7^{Kl}* platelets exhibited markedly reduced adhesion

to the collagen-coated surface, and the subsequent three-dimensional thrombus formation was virtually abrogated (Figure 3-26). These results demonstrate that the TRPM7 kinase plays a role in the regulation of platelet adhesion and thrombus formation on collagen fibers under physiological flow conditions.

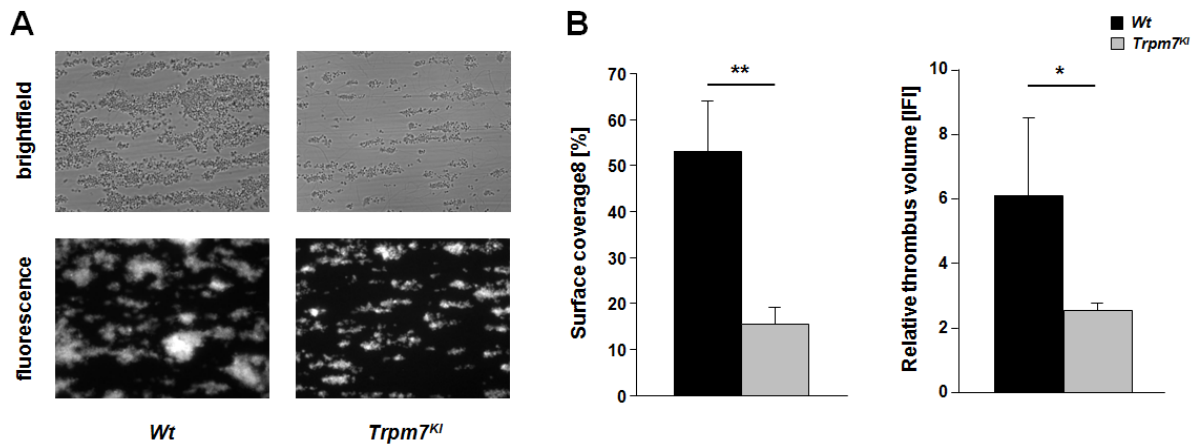


Figure 3-26: Impaired thrombus formation of *Trpm7^{Kl}* platelets on collagen under flow conditions. (A) Heparinized whole blood from *Wt* and *Trpm7^{Kl}* mice was perfused over 0.2 mg/mL immobilized collagen at a shear rate 1000 s⁻¹ for 4 min, followed by 2 min perfusion with Tyrode HEPES buffer at the same shear rate. Platelets were stained with anti-GPIX-Dylight-488 antibody. Representative phase contrast (upper panel) and fluorescence images (lower panel) are shown. (B) Mean surface coverage \pm SD (left panel) and relative thrombus volume \pm SD was shown. IFI: integrated fluorescence intensity. * $p < 0.05$, ** $p < 0.01$.

3.2.14 Impaired arterial thrombus formation and hemostasis in *Trpm7^{Kl}* mice

Trpm7^{Kl} mice displayed defective *ex vivo* thrombus formation, therefore in the next step the requirement of the TRPM7 kinase for *in vivo* thrombus formation was addressed by subjecting *Trpm7^{Kl}* mice in two different models of arterial thrombosis. These experiments were performed in collaboration with Martina Morowski in our group. In the first model, arterial thrombosis was induced by a single firm compression with a forceps and the blood flow was monitored with an ultrasonic flow probe. *Trpm7^{Kl}* mice formed instable thrombi (mean occlusion time *Wt*: 293 \pm 92 s, vs. *Trpm7^{Kl}*: 520 \pm 136 s, and 6 out of 10 vessels did not occlude in the *Trpm7^{Kl}* mice; Figure 3-27 A). In the second model, thrombus formation was induced by injuring mesenteric arterioles with 20% FeCl₃ and monitored by intravital fluorescence microscopy. The kinetics of initial adhesion and accumulation of fluorescently labeled platelets during the early time period was comparable between *Wt* and *Trpm7^{Kl}* mice. However, 7 out of 15 vessels failed to occlude in *Trpm7^{Kl}* mice during the later stage of thrombus growth (Figure 3-27 B). These findings indicate that the TRPM7 kinase contributes to platelet activation and thrombus growth *in vivo*.

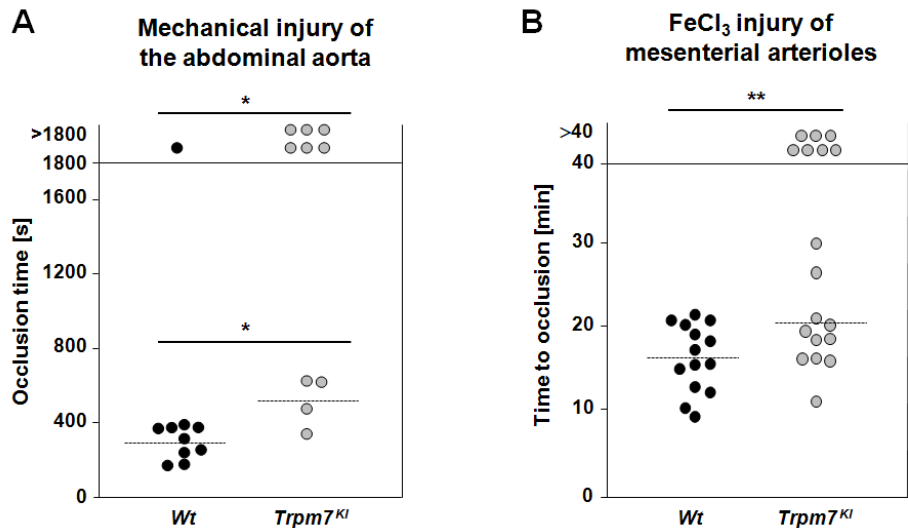


Figure 3-27: Impaired arterial thrombus formation in *Trpm7^{Kl}* mice. (A) The abdominal aorta of *Wt* and *Trpm7^{Kl}* mice was injured by tight compression with a forceps and blood flow was monitored for 30 min with an ultrasonic flow probe. The time to stable vessel occlusion is shown. Each symbol represents one individual. (B) Thrombus formation in FeCl₃-injured mesenteric arterioles was monitored by intravital microscopy of fluorescently labeled platelets. Each symbol represents one individual. **p* < 0.05, ***p* < 0.01.

To study the role of the TRPM7 kinase in hemostasis, a tail bleeding time assay was performed. 1 mm of the mouse tail tip was amputated and the drop of blood was absorbed with a filter paper in 20 s intervals. *Trpm7^{Kl}* mice exhibited prolonged tail bleeding times compared to *Wt* mice. The average tail bleeding time of *Wt* mice was 287 ± 221 s and in *Trpm7^{Kl}* mice it was 581 ± 285 s (Figure 3-28, left panel) with high variability. In *Trpm7^{Kl}* mice, 13.3% of the mice stopped bleeding at 0 – 300 s; 30% at 301 -600 s; 30% at 600 – 1200 s; and 26.7% did not stop within 1200 s. In *Wt* mice, 66.7% at 0 – 300 s; 26.7% at 301 – 600 s; and 6.6% at 601 – 1200 s (Figure 3-28, right panel). These results indicate that the TRPM7 kinase plays a role in normal hemostasis.

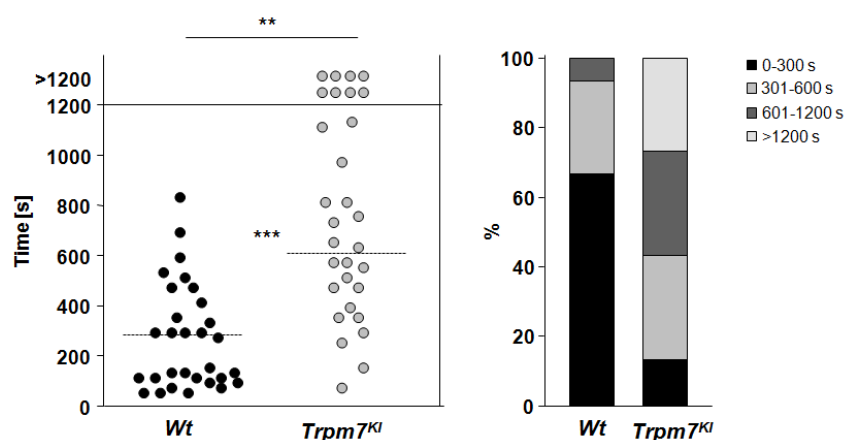


Figure 3-28: Impaired hemostasis in *Trpm7^{Kl}* mice. 1 mm segment of the mouse tail tip was cut off using a scalpel. Blood drops were absorbed every 20 s using a filter paper without touching the wound site until bleeding ceased. Each symbol represents the bleeding time of one animal (left panel). The percentages of mice which stopped bleeding at different time points was shown (right panel). ***p* < 0.01, ****p* < 0.001.

3.2.15 The TRPM7 kinase plays an important role in ischemic stroke

Ischemic stroke is the second leading cause of death and severe disability worldwide.¹⁸⁵ Ischemic stroke has been proposed to involve in the blockage of vessels via thrombosis in brain,¹⁸⁶ and during this process platelets play a critical role via GPIb-, GPVI- and integrin α IIb β 3-dependent platelet activation, adhesion and aggregation.¹⁶³ However the exact underlying mechanisms are still not understood.

To determine whether the observed thrombus instability and prolonged occlusion time in *Trpm7^{KI}* mice affect ischemic stroke, mice were challenged in the tMCAO model of focal cerebral ischemia. This work was performed in collaboration with Dr. Peter Kraft and colleagues in the group of Prof. Guido Stoll, Department of Neurology, University Hospital, Würzburg. To initiate transient cerebral ischemia, a thread was advanced via the internal carotid artery into the middle cerebral artery, and 60 min later reperfusion was allowed. 24 hours after reperfusion, the extent of infarction was quantified on TTC-stained brain slices. In *Trpm7^{KI}* mice, the infarct volumes were dramatically reduced to < 40% compared to those of *Wt* controls (*Wt*: 122 mm³ \pm 20 mm³; *Trpm7^{KI}*: 50 mm³ \pm 32 mm³) demonstrating that the disruption of the TRPM7 kinase activity protects mice from ischemic stroke (Figure 3-29 A).

Additionally, to determine whether this protective effect is due to the effect of lacking the TRPM7 kinase activity on non-hematopoietic cells (i.e. neurons)¹⁴⁷ or on blood cells, BM chimeras were generated by injecting *Wt* BM cells into lethally irradiated *Trpm7^{KI}* mice and *vice versa*. Interestingly, both *Trpm7^{KI}* animals substituted with *Wt* BM (47 mm³ \pm 11 mm³) and *Wt* animals substituted with *Trpm7^{KI}* BM (59 mm³ \pm 35 mm³) were protected when compared to *Wt* animals which received *Wt* BM (97 mm³ \pm 22 mm³) regarding infarct volumes (Figure 3-29 B). The reduction in infarct size was functionally relevant as the global neurological function (Bederson score) and motoric function (Grip test) were better in *Trpm7^{KI}* animals substituted with *Wt* BM and *Wt* animals substituted with *Trpm7^{KI}* BM, when compared to *Wt* control at day 1 after tMCAO (Figure 3-29 D and E). Notably, the disruption of the TRPM7 kinase activity either in bone marrow-derived cells or in non-hematopoietic cells is sufficient to protect the brain from acute ischemic insult (Figure 3-29 C).

Furthermore, to demonstrate that altered platelet function of *Trpm7^{KI}* mice contributes to this process, *Wt* mice were transplanted with *Wt* or *Trpm7^{KI}* platelets after 12 hours of immunothrombocytopenia induced by injection of anti-GPIb antibody. tMCAO was performed again in these chimeras 2 hours after platelet transfusion. Remarkably, *Wt* mice transfused with *Trpm7^{KI}* platelets developed significantly smaller brain infarcts compared to controls (Figure 3-29 F). The global neurological and motoric functions were slightly better in mice transfused with *Trpm7^{KI}* platelets (Figure 3-29 G). These results indicate that the TRPM7 kinase activity in platelets has a pivotal role in the development of stroke.

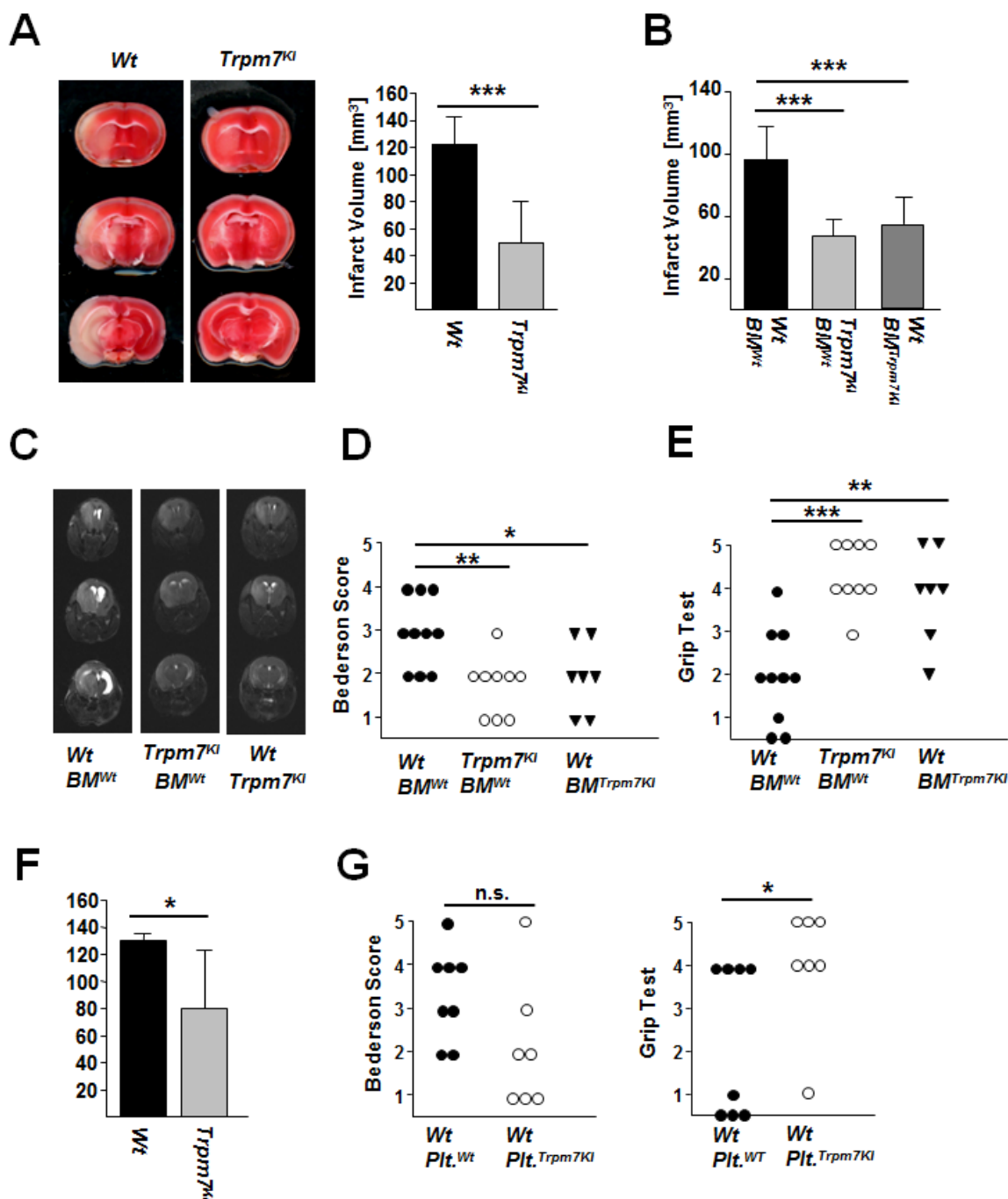


Figure 3-29: *Trpm7*^{KI} mice are protected from cerebral ischemia. (A) Representative images of three corresponding coronal sections of *Wt* and *Trpm7*^{KI} mice stained with TTC 24 hours after tMCAO. Stroke volumes in *Wt* and *Trpm7*^{KI} mice are depicted. (B) In order to figure out if decreased vulnerability of neurons lacking the TRPM7 kinase activity or altered blood cell function leads to protection in *Trpm7*^{KI} animals, bone marrow chimeras were generated. Planimetric volumetry and corresponding magnetic resonance images (C) of tMCAO infarct volumes at day 1 after stroke are displayed. (D and E) Reduced ischemic brain damage translated in better functional outcome as measured with the Bederson score and the grip test. (F) Platelet transfusion experiment showed a protection of *Wt* mice transfused with *Trpm7*^{KI} platelets. Infarct volumes were measured 24 hours after tMCAO. (G) Bederson score and Grip test in *Wt* mice transfused with *Wt* platelets or *Trpm7*^{KI} platelets were assessed. * $p < 0.05$, ** $p < 0.01$, *** $p < 0.001$.

4 DISCUSSION

Platelet activation and aggregation are essential for preventing blood loss and for sealing wounds after vascular injury. However, under pathological conditions, uncontrolled platelet aggregation may lead to vessel occlusion or thromboembolism resulting in life threatening diseases such as myocardial infarction or stroke. Over the last decades several anti-thrombotic drugs such as aspirin, clopidogrel and integrin $\alpha\text{IIb}\beta\text{3}$ antagonists, have been used to prevent cardiovascular diseases. However, the use of these drugs is limited since they often lead to bleeding complications. Therefore, the comprehensive understanding of the signaling processes during platelet activation is essential for the development of novel, yet safe, anti-thrombotic therapies.

It is well established that the elevation of $[\text{Ca}^{2+}]_i$ is essential for platelet activation, firm adhesion and stable aggregation, as well as granule secretion. Furthermore, Mg^{2+} has also been proposed to play a role in regulating platelet activity. In this thesis, the functional crosstalk between two major Ca^{2+} channels Orai1 and TRPC6 was investigated by using genetic knockout mice. The results presented here show that Orai1-mediated SOCE enhances the enzymatic activity of PL isoforms and indirectly regulates TRPC6-mediated ROCE. In addition the role of TRPM7 kinase activity in the regulation of platelet activation was studied by using “kinase-dead” knockin mice. The loss of TRPM7 kinase activity was found to impair the enzymatic activity of PLC isoforms, thereby affecting Ca^{2+} mobilization and platelet activation. This signaling defect protected mice from arterial thrombosis and ischemic brain infarction.

4.1 Functional crosstalk between Orai1-mediated SOCE and TRPC6-mediated ROCE in mouse platelets

4.1.1 Orai1-mediated SOCE indirectly regulates TRPC6-mediated ROCE

The elevation of $[\text{Ca}^{2+}]_i$ is a critical step for several platelet functions, including integrin activation, aggregation and degranulation. In mouse platelets, it is established that the major Ca^{2+} entry routes are SOCE and ROCE.^{26,27} Orai1 is considered as the principal SOC channel in mouse platelets since in *Orai1*^{-/-} platelets TG-induced SOCE is almost completely abolished.²⁶ In addition, TRPC6 is suggested as an important channel for DAG-induced ROCE,^{27,78,187} since in *Trpc6*^{-/-} platelets OAG-triggered Ca^{2+} entry is significantly reduced.

Interestingly, in human platelets hTRPC6-induced Ca^{2+} influx was detected during TG treatment, indicating that hTRPC6 may be part of the *store-operated macromolecular* (SOM)

complex.^{155,172} Furthermore, hTRPC6 was suggested to directly interact with hTRPC1 and hOrai1 and form heterodimers.^{89,188} However, hTRPC6 and hOrai3 were found to dissociate from the SOM complex and to interact with hTRPC3 when the platelets were stimulated with OAG.⁸⁹ Taken together, these findings lead to the proposal that in human platelets TRPC and Orai isoforms can form heterodimers, and depending on the interacting proteins TRPC isoforms can either regulate SOCE or ROCE.^{60,172} DAG may activate heterodimers of TRPC6 with TRPC3 which subsequently trigger ROCE, while heterodimers of TRPC6 with Orai1 may be regulated by STIM1 and enhance SOCE during platelet activation. In agreement with a supportive role of TRPC6 in SOCE, the results presented here showed that TG-mediated SOCE was further reduced in *Orai1*^{-/-}/*Trpc6*^{-/-} platelets as compared to *Orai1*^{-/-} platelets (Figure 3-1), demonstrating that during SOCE TRPC6 activity is enhanced. However, this enhanced TRPC6 activity has a minor contribution to SOCE in mouse platelets, since this physiological function of TRPC6 was only detectable in the absence of Orai1.

Recent studies showed that TG-induced SOCE is normal in *Trpc6*^{-/-} platelets and DAG-mediated ROCE is not influenced in *Orai1*^{-/-} platelets.²⁷ The TRPC6 blocker LOE-908, a non-selective cation channel inhibitor, also did not influence SOCE in human platelets while it specifically blocked OAG-mediated Ca²⁺ entry.¹⁸⁹ These results suggested that Orai1 and TRPC6 function independently of each other in human platelets, although an indirect crosstalk between these two channels may exist. In this study, a hypothesis was proposed that during TG-induced SOCE DAG is produced to activate TRPC6, which subsequently contributes additional Ca²⁺ influx to SOCE.

There are two routes to generate DAG in platelets: PLD and PLC pathways. PLD can hydrolyze PC to PA and choline.¹⁹⁰ Thereafter, PA-phosphohydrolase converts PA to DAG and inorganic phosphate during platelet activation.¹⁹¹ PLD activity is regulated by phospholipids (PIP₂, PIP₃), PKC, Ca²⁺ and other factors.¹⁹² It has been shown that depletion of intracellular Ca²⁺ stores by BAPTA or inhibition of extracellular Ca²⁺ entry with EGTA lead to the inhibition of PLD activity,¹⁹² indicating that store release and Ca²⁺ influx are involved in the regulation of PLD function. The present results here showed that in *Orai1*^{-/-} and *Wt* platelets the release of Ca²⁺ from the store is similar. However, upon store release, a strong reduction of PLD activity was observed in *Orai1*^{-/-} platelets (Figure 3-3 B). Interestingly, *Stim1*^{-/-} platelets also showed a strong reduction of PLD activity after TG-induced store release and SOCE, similarly to *Orai1*^{-/-} platelets (data not shown). Taken together, it can be speculated that the Orai1/STIM1 complex may coordinate subcellular localization or enzymatic activity of PLD upon store release and SOCE. The results here also provide the first evidence that Orai1-mediated SOCE can modulate PLD activity in mouse platelets (Figure 3-3 A and B), which may further activate DAG-mediated ROCE. In line with this finding, the application of the PLD blocker FIPI was shown to reduce TG-mediated SOCE in

mouse platelets (Figure 3-3 A). The second pathway leading to DAG production is through PLC activation, independently of Ca^{2+} store release or Ca^{2+} entry. The treatment with the PLC blocker U73122 was found to inhibit TG-induced SOCE in mouse (Figure 3-3 A) and human platelets.¹⁹³ Furthermore, *Orai1*^{-/-} platelets displayed lower enzymatic activity of PLC compared to *Wt* platelets (Figure 3-3 C). Altogether, it can be concluded that Orai1-mediated SOCE enhances the enzymatic activity of phospholipases, thereby increasing $[\text{DAG}]_i$ and activating TRPC6-mediated Ca^{2+} entry.

Earlier, it was found that TG-mediated SOCE strongly enhances the release of the second wave mediator TxA_2 in human platelets.¹⁷² TxA_2 activates the TP receptor and subsequently enhances PLC β activity. Consistent with the results in human platelets, TG stimulation led to strong TxA_2 production in *Wt* platelets; however in *Orai1*^{-/-} and *Orai1*^{-/-}/*Trpc6*^{-/-} platelets, TxA_2 secretion was severely impaired (Figure 3-5). This indicates that Orai1-mediated SOCE plays a central role in amplifying TxA_2 -TP-PLC β -induced IP_3 and DAG production, confirming the regulating role of Orai1-mediated SOCE in TRPC6-mediated ROCE.

Altogether, a model of a functional crosstalk between Orai1 and TRPC6 can be proposed: Orai1-mediated SOCE can enhance PLC and PLD activity, and TxA_2 production as well, which further enhances PLC activity via the TP receptor. Enhanced PLC and PLD activity subsequently leads to DAG production and induces TRPC6-mediated ROCE (Figure 4-1).

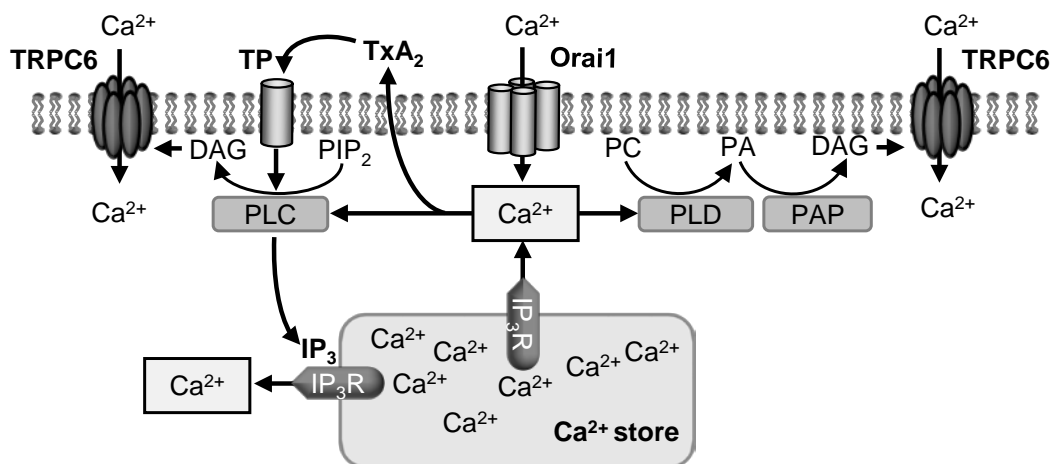


Figure 4-1: Proposed model of TRPC6 activation by Orai1 and PLs. Orai1-mediated SOCE regulates TRPC6-mediated ROCE indirectly in platelets. The details are described in the text (Picture is taken from: Chen *et al.*, *J Thromb Haemost* 2014).¹⁶⁹

Although Orai1-mediated SOCE can induce DAG production and indirectly regulates TRPC6 activation, it is important to note that this effect is strongly dependent on the stimulating compound. When Orai1 is selectively activated by TG, TRPC6 function is strongly dependent on Orai1-dependent DAG production. However, when platelets are stimulated by receptor agonists, Orai1 function appears to be dispensable for TRPC6 activation (Figure 3-4 C and

D). These results demonstrate that the crosstalk between TRPC6 and Orai1 seems to play only a minor role under normal physiological conditions where receptor-operated DAG production is the dominant route in TRPC6 activation, which strongly regulates TRPC6 function independently from the Ca^{2+} store release or SOCE. However, Orai1-mediated DAG production may play an important role under pathological conditions, for example when Orai1 channel activity is abnormal or receptor-mediated activation of phospholipases is hampered. Recently, it was shown that Orai1 abundance on the platelet surface is higher in patients with acute myocardial infarction.¹⁹⁴ In patients with diabetes mellitus type 2, Orai1 expression in platelets was also increased.¹⁹⁵ Under these pathophysiological conditions, aberrant Orai1-mediated SOCE may also accelerate PLD/PLC-induced DAG production, which can further enhance TRPC6 activity thereby causing “ Ca^{2+} overload” in platelets. However, the functional consequence of Orai1 in the regulation of phospholipase activity and DAG-mediated ROCE requires further detailed analysis in human platelets under normal and pathophysiological conditions.

4.1.2 Orai1 together with TRPC6 regulates store content

Apart from increasing Ca^{2+} levels in the cytoplasm, SOCE was also proposed to facilitate Ca^{2+} refilling of the store through SERCA.¹⁹⁶ In mammalian cells, the interaction between the SOM complex and SERCA isoforms led to the proposal of a model termed *calcium entry-calcium refilling coupling* (CERC) mechanism which is very efficient to pump Ca^{2+} back into the empty store during SOCE.¹⁹⁷ However, the detailed molecular mechanism of CERC in platelets is still not completely understood.

Earlier, it was shown that TG- and agonist-mediated Ca^{2+} store depletion is strongly altered in *Stim1*^{-/-} platelets indicating that STIM1 plays an important role in the regulation of the store content.⁵² Interestingly, the Ca^{2+} store content was also found to be reduced in *Orai1*^{-/-}/*Trpc6*^{-/-} platelets (Figure 3-2 B), but not in single knockouts of Orai1 or TRPC6; therefore both Ca^{2+} channels seem to be involved in refilling the stores. In human platelets, STIM1 binds to Orai1¹⁹⁸ and TRPC6.^{60,76} Moreover, an increased interaction between TRPC6 and SERCA2b was observed during SOCE.¹⁸⁸ Taking the results from human platelets and the recent findings in mouse platelets together, a model can be proposed that STIM1, Orai1, TRPC6 and SERCA2b may regulate CERC in platelets:

STIM1 seems to form a physical bridge between the DTS and the plasma membrane and to cluster Orai1 and TRPC6 in the plasma membrane. The physical interaction between STIM1 and TRPC6 does not regulate the channel activity of TRPC6, since OAG-mediated TRPC6 activation is normal in *Stim1*^{-/-} platelets.²⁷ During CERC, either Orai1 or TRPC6 may be activated to carry Ca^{2+} from the extracellular space into the empty store. Lack of either Orai1 or TRPC6 does not influence the CERC mechanism, since STIM1 can separately keep the

structure of CERC either with Orai1 or with TRPC6 and link the DTS close to the plasma membrane. When STIM1 function is deleted or STIM1 cannot be translocated to both Ca^{2+} channels, the physical interaction between the DTS and the plasma membrane is disrupted. Consequently, SERCA2b is not close enough to the Ca^{2+} channels so that the pumping Ca^{2+} back to the empty store is less effective and finally, the store content is reduced in platelets.

4.1.3 Enhanced ATP secretion in response to the GPCR agonists in *Orai1*^{-/-}/*Trpc6*^{-/-} platelets

Earlier, it was shown that in *Orai1*^{-/-} or *Trpc6*^{-/-} mutant mice GPCR-induced platelet activation and thrombus formation are unaltered,^{25,26} suggesting that neither Orai1 nor TRPC6 is essential for GPCR-induced platelet responses. In line with these findings, the present results here showed that GPCR-induced platelet activation and aggregation was unaltered in the absence of both Orai1 and TRPC6 channels (Figure 3-7 B and Figure 3-8). Moreover, thrombus formation under flow was even enhanced in *Orai1*^{-/-}/*Trpc6*^{-/-} platelets compared to *Orai1*^{-/-} (Figure 3-10 and Figure 3-11 A and B). These results suggest that an alternative signaling pathway may exist which compensates for the loss of both Ca^{2+} channels. Furthermore, ATP-secretion in response to thrombin and U46619 was found to be elevated in *Orai1*^{-/-}/*Trpc6*^{-/-} platelets compared to *Wt* or *Orai1*^{-/-} platelets (Figure 3-12 A) indicating that purinergic signaling pathways may compensate for the severe Ca^{2+} deficits in *Orai1*^{-/-}/*Trpc6*^{-/-} platelets *in vivo*, by enhancing Ca^{2+} influx through ATP-operated P2X₁ channels. The increased ATP-secretion was not due to the increased amount of ATP in the granules since high concentrations of thrombin induced normal ATP-secretion in *Orai1*^{-/-}/*Trpc6*^{-/-} platelets (Figure 3-12 A).

The ATP-activated P2X₁ Ca^{2+} channel plays a pivotal role in thrombus formation.^{87,199} It is important to note that the P2X₁ channel becomes desensitized by ADP in our standard experimental *in vitro* settings. Therefore the platelet aggregation assay was repeated in the presence of high doses of apyrase, which preserves P2X₁ channel function and blocks ADP-mediated Ca^{2+} responses. Our results showed that thrombin- and U46619-induced platelet aggregation responses were strongly enhanced in *Orai1*^{-/-}/*Trpc6*^{-/-} platelets, when the desensitization of P2X₁ channel was prevented (Figure 3-12 B). Altogether, it can be assumed that P2X₁ channel and purinergic signaling pathways seem to compensate for the severe Ca^{2+} deficits of *Orai1*^{-/-}/*Trpc6*^{-/-} platelets under *in vivo* conditions.

4.2 The role of the TRPM7 kinase in mouse platelets

4.2.1 Normal Mg²⁺ homeostasis and TRPM7 channel activity in *Trpm7^{Kl}* mice

TRPM7 belongs to the TRPM subfamily of TRP channels and has been found to be expressed in almost all cell types and to regulate many cellular processes including cell cycle, migration and other important functions.^{118,141-143} TRPM7 forms a Mg²⁺ and Ca²⁺ permeable channel and is considered to play an important role in controlling [Mg²⁺]_i. TRPM7 contains an intracellular Ser/Thr kinase domain at its C-terminus. Up to now, the role of this kinase domain in regulating Mg²⁺ homeostasis remains controversial. It has been reported that the heterozygous deletion of the TRPM7 kinase domain results in reduced Mg²⁺ concentrations in plasma, urine and bones.¹⁵⁵ In addition, the deletion of the TRPM7 kinase domain leads to impaired TRPM7 channel activity.¹⁵⁵ On the contrary, other studies reported that the kinase domain and channel domain function independently of each other.¹⁵⁶ Schmitz *et al.* suggested that the TRPM7 kinase domain is not essential for the activation of the channel domain, however it plays a role in modulating channel activity.¹²⁸ The results presented here show that the disruption of kinase activity in *Trpm7^{Kl}* mice did not lead to impaired channel activity (Figure 3-17 A) and did not influence both intracellular and extracellular Mg²⁺ homeostasis (Figure 3-17 B and C). These results demonstrate that the catalytic activity of the TRPM7 kinase is not essential for the channel domain to function normally.

4.2.2 The TRPM7 kinase regulates the enzymatic activity of phospholipase

TRPM7 bears a Ser/Thr kinase domain with multiple autophosphorylation sites at the C-terminus. Although it is suggested to play a role in diverse signaling pathways, only a limited number of endogenous substrates for the TRPM7 kinase has been identified up to now. Recently, it was demonstrated that the TRPM7 kinase directly binds to the C2 domain of PLC isoforms including PLCβ, PLCγ and PLCδ.¹³⁸ Further, Schmitz *et al.* reported that PLCγ2, an important regulator in ITAM-receptor-mediated Ca²⁺ signaling, can be phosphorylated by the TRPM7 kinase in a DT40 cell line.¹⁵⁴ They identified two phosphorylation sites for the TRPM7 kinase in PLCγ2: one is Ser1164 in the C2 domain; the other one is Thr1045 in the linker region preceding the C2 domain. Further, under hypomagnesian conditions, the mutation of Thr1045 in PLCγ2 lead to impaired Ca²⁺ mobilization. Taken together, these findings lead to the proposal that TRPM7 kinase may regulate the enzymatic activity of PLCγ2 and Ca²⁺ homeostasis. The present results here support this model.

In this study, *Trpm7^{Kl}* platelets displayed severely impaired integrin αIIbβ3 activation, P-selectin exposure and aggregation in response to GPVI stimulation, while in response to the

GPCR agonist thrombin only slightly reduced platelet activation and aggregation was observed at threshold concentrations (Figure 3-19 and Figure 3-20). Interestingly ATP and serotonin secretion from dense granules were also significantly reduced in *Trpm7^{Kl}* platelets after thrombin and CRP activation at threshold concentrations (Figure 3-22). This suggests that in *Trpm7^{Kl}* platelets activation of ATP-operated P2X₁ Ca²⁺ channel, ADP-induced P2Y₁/P2Y₁₂ receptors and the serotonin-activated 5HT_{2A} receptor are reduced during platelet activation and aggregation. Furthermore, IP₃ production upon CRP and threshold concentrations of thrombin stimulation was also impaired in *Trpm7^{Kl}* platelets (Figure 3-23 A), which demonstrated that the TRPM7 kinase activity can regulate the enzymatic activity of PLC isoforms, especially PLC γ 2, in mouse platelets. PLC isoforms hydrolyze PIP₂ into IP₃ and DAG. It is known that IP₃-mediated stimulation of the IP₃R on the intracellular store membrane leads to the release of Ca²⁺ from internal stores and induces subsequent SOCE through Orai1 channel, and that DAG can directly bind to the TRPC6 channel and induce ROCE. Therefore, changes of [Ca²⁺]_i were measured in response to different agonists. In line with the IP₃ production results, store release and Ca²⁺ influx in response to CRP were markedly reduced in *Trpm7^{Kl}* platelets. However, normal Ca²⁺ homeostasis was observed in *Trpm7^{Kl}* platelets when stimulated by the GPCR agonists thrombin, ADP or U46619 (Figure 3-23 B). These findings suggest that the TRPM7 kinase activity plays a minor role in GPCR-PLC β pathways or that its function is strongly compensated by other kinases. However, the enzymatic activity of the TRPM7 kinase is essential for the full activation PLC γ 2 downstream of GPVI.

It is well established that the GPVI-PLC γ 2 signaling cascade is mainly mediated by tyrosine phosphorylation events. To investigate whether the Ser/Thr phosphorylation activity of the TRPM7 kinase influences tyrosine phosphorylation of the GPVI-signaling cascade, the tyrosine phosphorylation events of the regulating molecules was analyzed. Neither global tyrosine phosphorylation, nor phospho-Syk^{Y525/526}, phospho-LAT^{Y191}, nor phospho-PLC γ 2^{Y759} were altered in *Trpm7^{Kl}* platelets after activation by GPVI, indicating that the TRPM7 kinase does not influence tyrosine phosphorylation events in the GPVI-signaling cascade. Therefore, it can be speculated that the TRPM7 kinase regulates PLC γ 2 directly by Ser/Thr phosphorylation, instead of influencing the tyrosine phosphorylation of the GPVI-signaling cascade and regulating PLC γ 2 indirectly.

In summary, a model for the role of the TRPM7 kinase in regulating PLC isoforms can be proposed. When platelets are activated by the GPVI-specific agonists, PLC γ 2 is recruited to the GPVI signalosome associated with LAT and subsequently becomes phosphorylated by the tyrosine kinase Syk. The enzymatic activity of PLC γ 2 is then further enhanced by the TRPM7 kinase-mediated Ser/Thr phosphorylation. Subsequently, PLC γ 2-mediated PIP₂

hydrolysis rapidly increases the levels of DAG and IP₃ in the cytosol and induces a strong activation of ROCE and SOCE, respectively (Figure 4-2).

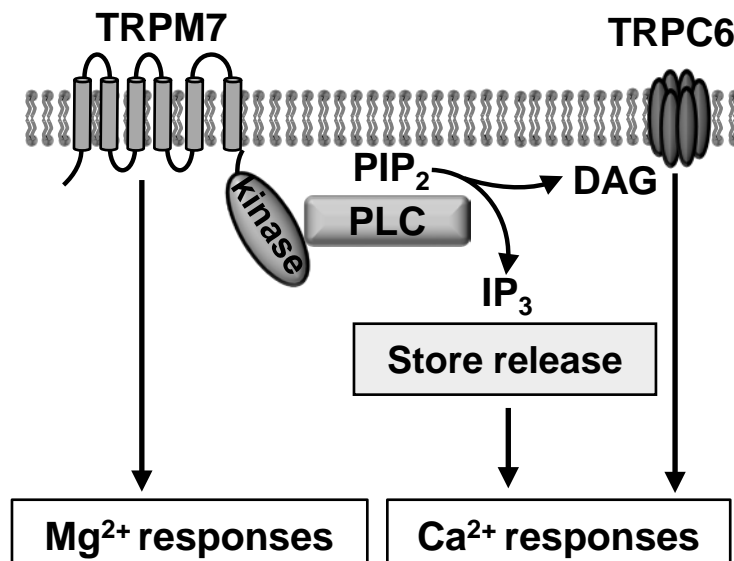


Figure 4-2: Proposed model of the TRPM7 kinase-mediated Ca²⁺ responses in GPVI signaling. The TRPM7 kinase regulates the Ser/Thr phosphorylation of PLC γ 2. PLC γ 2 activation subsequently induces the production of DAG and IP₃, which trigger ROCE and SOCE, respectively.

4.2.3 The TRPM7 kinase plays an important role in thrombosis, hemostasis and stroke

It has been shown that GPVI deficiency protects mice from pathological thrombus formation.¹⁷³ To investigate whether the severe GPVI signaling defects in *Trpm7*^{KI} platelets also influences thrombosis, *ex vivo* and *in vivo* thrombosis models were performed. Consistent with the *in vitro* results, *Trpm7*^{KI} platelets exhibited markedly reduced platelet adhesion and impaired three-dimensional thrombus formation on fibrillar collagen under flow conditions (Figure 3-26). This translated into impaired arterial thrombus growth after mechanical or chemical (20% FeCl₃) vessel injury *in vivo* (Figure 3-27). In addition, *Trpm7*^{KI} mice exhibited prolonged tail bleeding times (Figure 3-28), which is in line with the previous findings that GPVI-defects have such an effect.¹⁷³ Altogether, these findings demonstrate that the blockage of the TRPM7 kinase activity is sufficient to protect mice from arterial thrombosis. Therefore, the TRPM7 kinase might become a promising therapeutic target for the development of novel anti-thrombotics.

Recently, TRPM7 was suggested as a potential drug target in stroke.²⁰⁰ In the tMCAO model of ischemic stroke in mice, the expression of TRPM7 protein was found to be up-regulated in neurons.¹⁴⁶ Furthermore, the down-regulation of TRPM7 in the ischemic brain protects neuron from necrosis.^{147,148} It was proposed that the increased channel function of TRPM7

may induce aberrant Ca^{2+} influx, thereby enhancing neuronal cell death during stroke development. However, the role of the TRPM7 kinase domain in this process remained largely unclear. In this study, the significance of the TRPM7 kinase in the pathogenesis of acute ischemic brain infarction was assessed in the tMCAO model. The infarct volumes in *Trpm7^{Kl}* brains were dramatically reduced compared to *Wt* brains (Figure 3-29 A), demonstrating that the disruption of the TRPM7 kinase activity can protect mice from ischemic stroke. However, this protection may originate from the effect of the abolished the TRPM7 kinase activity in blood cells or in non-hematopoietic cells (i.e. cells of the vessel wall and brain), since the infarct volumes in both *Trpm7^{Kl}* animals substituted with *Wt* BM and *Wt* animals substituted with *Trpm7^{Kl}* BM were reduced compared to *Wt* control (Figure 3-29 B). Consistent with the observed platelet defects, animals transfused with *Trpm7^{Kl}* platelets developed significantly smaller brain infarcts compared to *Wt* controls (Figure 3-29 F), indicating that the abolished TRPM7 kinase activity is sufficient to protect mice from ischemic stroke. In summary, these findings suggest that the disruption of the TRPM7 kinase activity in bone marrow-derived cells, brain cells or vessel wall cells protects mice from ischemic stroke, indicating the TRPM7 kinase is also a potential drug target for treatment of ischemic stroke.

4.3 Concluding remarks

In this thesis the role of Ca^{2+} and Mg^{2+} channel proteins for platelet function was investigated by the use of genetically modified mice. The major findings are:

Functional crosstalk between Orai1-mediated SOCE and TRPC6-mediated ROCE in mouse platelets.

- Orai1-mediated SOCE enhances phospholipase activity thereby regulating TRPC6-mediated ROCE indirectly.
- Orai1 together with TRPC6 regulates intracellular Ca^{2+} store content and basal cytoplasmic Ca^{2+} levels.
- Orai1 and TRPC6 are not essential for GPCR-mediated platelet activation, aggregation and thrombus formation.
- Orai1 and TRPC6 double deficiency is compensated through a possible mechanism, involving enhanced ATP secretion, which may compensate for severe Ca^{2+} deficits.

Function of the TRPM7 kinase on mouse platelets.

- High extracellular Mg^{2+} levels lead to impaired Ca^{2+} influx, platelet activation, aggregation and thrombus formation under flow.
- The TRPM7 kinase activity is not required for TRPM7 channel activity and Mg^{2+} homeostasis.
- The TRPM7 kinase is required for GPVI-induced Ca^{2+} mobilization and platelet

activation.

- The TRPM7 kinase regulates PLC γ 2 by its Ser/Thr phosphorylation without influencing tyrosine phosphorylation events in the GPVI signaling cascade.
- The TRPM7 kinase is required for arterial thrombus growth and ischemic stroke.

4.4 Perspective

In this thesis, it was shown that Orai1-mediated SOCE indirectly regulates TRPC6-mediated ROCE via PLC and PLD. However, it remains to be answered how Orai1-mediated SOCE enhances PLC and PLD activity. Furthermore TRPC3 has also been proposed to be a DAG-operated ROC channel in platelets; it is therefore important to study whether Orai1-mediated SOCE also regulates TRPC3-mediated ROCE. Additionally, the compensation mechanism induced by Orai1 and TRPC6 double deficiency requires further investigation.

Although in a DT40 cell line several Ser/Thr phosphorylation sites in PLC γ 2 have been shown to be phosphorylated by the TRPM7 kinase, the evidence for the TRPM7 kinase phosphorylating PLC γ 2 in platelets are still needed. Further it needs to be answered to what extent the TRPM7 kinase regulates PLC β . In addition, to further understand the role of the whole TRPM7 protein on platelet function, TRPM7 knockout mice should be analyzed. Finally, mouse lines deficient in other Mg²⁺ transporters, like MagT1 and TRPM6, need to be analyzed to better understand the role of Mg²⁺ homeostasis in platelet physiology.

5 REFERENCES

- 1 Murray CJ, Lopez AD. Mortality by cause for eight regions of the world: Global Burden of Disease Study. *Lancet*. 1997; **349**: 1269-76.
- 2 Savage B, Almus-Jacobs F, Ruggeri ZM. Specific synergy of multiple substrate-receptor interactions in platelet thrombus formation under flow. *Cell*. 1998; **94**: 657-66.
- 3 Nieswandt B, Brakebusch C, Bergmeier W, Schulte V, Bouvard D, Mokhtari-Nejad R, Lindhout T, Heemskerk JW, Zirngibl H, Fassler R. Glycoprotein VI but not alpha2beta1 integrin is essential for platelet interaction with collagen. *Embo J*. 2001; **20**: 2120-30.
- 4 Furie BC, Furie B. Tissue factor pathway vs. collagen pathway for in vivo platelet activation. *Blood Cells Mol Dis*. 2006; **36**: 135-8.
- 5 Nieswandt B, Watson SP. Platelet-collagen interaction: is GPVI the central receptor? *Blood*. 2003; **102**: 449-61.
- 6 Herzog BH, Fu J, Wilson SJ, Hess PR, Sen A, McDaniel JM, Pan Y, Sheng M, Yago T, Silasi-Mansat R, McGee S, May F, Nieswandt B, Morris AJ, Lupu F, Coughlin SR, McEver RP, Chen H, Kahn ML, Xia L. Podoplanin maintains high endothelial venule integrity by interacting with platelet CLEC-2. *Nature*. 2013; **502**: 105-9.
- 7 May F, Hagedorn I, Pleines I, Bender M, Vogtle T, Eble J, Elvers M, Nieswandt B. CLEC-2 is an essential platelet-activating receptor in hemostasis and thrombosis. *Blood*. 2009; **114**: 3464-72.
- 8 Stegner D, Nieswandt B. Platelet receptor signaling in thrombus formation. *J Mol Med (Berl)*. 2011; **89**: 109-21.
- 9 Varga-Szabo D, Pleines I, Nieswandt B. Cell adhesion mechanisms in platelets. *Arterioscler Thromb Vasc Biol*. 2008; **28**: 403-12.
- 10 Watson SP, Auger JM, McCarty OJ, Pearce AC. GPVI and integrin alphaIIb beta3 signaling in platelets. *J Thromb Haemost*. 2005; **3**: 1752-62.
- 11 Ginsberg MH, Partridge A, Shattil SJ. Integrin regulation. *Curr Opin Cell Biol*. 2005; **17**: 509-16.
- 12 Savi P, Pflieger AM, Herbert JM. cAMP is not an important messenger for ADP-induced platelet aggregation. *Blood Coagul Fibrinolysis*. 1996; **7**: 249-52.
- 13 Offermanns S, Toombs CF, Hu YH, Simon MI. Defective platelet activation in G alpha(q)-deficient mice. *Nature*. 1997; **389**: 183-6.
- 14 Pleines I, Dutting S, Cherpokova D, Eckly A, Meyer I, Morowski M, Krohne G, Schulze

- H, Gachet C, Debili N, Brakebusch C, Nieswandt B. Defective tubulin organization and proplatelet formation in murine megakaryocytes lacking Rac1 and Cdc42. *Blood*. 2013; **122**: 3178-87.
- 15 Pleines I, Hagedorn I, Gupta S, May F, Chakarova L, van Hengel J, Offermanns S, Krohne G, Kleinschnitz C, Brakebusch C, Nieswandt B. Megakaryocyte-specific RhoA deficiency causes macrothrombocytopenia and defective platelet activation in hemostasis and thrombosis. *Blood*. 2012; **119**: 1054-63.
- 16 Pleines I, Eckly A, Elvers M, Hagedorn I, Eliautou S, Bender M, Wu X, Lanza F, Gachet C, Brakebusch C, Nieswandt B. Multiple alterations of platelet functions dominated by increased secretion in mice lacking Cdc42 in platelets. *Blood*. 2010; **115**: 3364-73.
- 17 Pleines I, Elvers M, Strehl A, Pozgajova M, Varga-Szabo D, May F, Chrostek-Grashoff A, Brakebusch C, Nieswandt B. Rac1 is essential for phospholipase C-gamma2 activation in platelets. *Pflugers Arch*. 2009; **457**: 1173-85.
- 18 Hirsch E, Bosco O, Tropel P, Laffargue M, Calvez R, Altruda F, Wymann M, Montrucchio G. Resistance to thromboembolism in PI3Kgamma-deficient mice. *Faseb J*. 2001; **15**: 2019-21.
- 19 Lian L, Wang Y, Draznin J, Eslin D, Bennett JS, Poncz M, Wu D, Abrams CS. The relative role of PLCbeta and PI3Kgamma in platelet activation. *Blood*. 2005; **106**: 110-7.
- 20 Daniel JL, Dangelmaier C, Jin J, Kim YB, Kunapuli SP. Role of intracellular signaling events in ADP-induced platelet aggregation. *Thromb Haemost*. 1999; **82**: 1322-6.
- 21 Yang J, Wu J, Kowalska MA, Dalvi A, Prevost N, O'Brien PJ, Manning D, Poncz M, Lucki I, Blendy JA, Brass LF. Loss of signaling through the G protein, Gz, results in abnormal platelet activation and altered responses to psychoactive drugs. *Proc Natl Acad Sci U S A*. 2000; **97**: 9984-9.
- 22 Nieswandt B, Bergmeier W, Schulte V, Rackebrandt K, Gessner JE, Zirngibl H. Expression and function of the mouse collagen receptor glycoprotein VI is strictly dependent on its association with the FcRgamma chain. *J Biol Chem*. 2000; **275**: 23998-4002.
- 23 Suzuki-Inoue K, Tulasne D, Shen Y, Bori-Sanz T, Inoue O, Jung SM, Moroi M, Andrews RK, Berndt MC, Watson SP. Association of Fyn and Lyn with the proline-rich domain of glycoprotein VI regulates intracellular signaling. *J Biol Chem*. 2002; **277**: 21561-6.
- 24 Locke D, Liu C, Peng X, Chen H, Kahn ML. Fc Rgamma -independent signaling by the platelet collagen receptor glycoprotein VI. *J Biol Chem*. 2003; **278**: 15441-8.
- 25 Suzuki-Inoue K, Fuller GL, Garcia A, Eble JA, Pohlmann S, Inoue O, Gartner TK,

- Hughan SC, Pearce AC, Laing GD, Theakston RD, Schweighoffer E, Zitzmann N, Morita T, Tybulewicz VL, Ozaki Y, Watson SP. A novel Syk-dependent mechanism of platelet activation by the C-type lectin receptor CLEC-2. *Blood*. 2006; **107**: 542-9.
- 26 Braun A, Varga-Szabo D, Kleinschnitz C, Pleines I, Bender M, Austinat M, Bosl M, Stoll G, Nieswandt B. Orai1 (CRACM1) is the platelet SOC channel and essential for pathological thrombus formation. *Blood*. 2009; **113**: 2056-63.
- 27 Ramanathan G, Gupta S, Thielmann I, Pleines I, Varga-Szabo D, May F, Mannhalter C, Dietrich A, Nieswandt B, Braun A. Defective diacylglycerol-induced Ca²⁺ entry but normal agonist-induced activation responses in TRPC6-deficient mouse platelets. *J Thromb Haemost*. 2012; **10**: 419-29.
- 28 Parekh AB, Putney JW, Jr. Store-operated calcium channels. *Physiol Rev*. 2005; **85**: 757-810.
- 29 Berridge MJ, Bootman MD, Roderick HL. Calcium signalling: dynamics, homeostasis and remodelling. *Nat Rev Mol Cell Biol*. 2003; **4**: 517-29.
- 30 Carafoli E. Calcium signaling: a tale for all seasons. *Proc Natl Acad Sci U S A*. 2002; **99**: 1115-22.
- 31 Pozzan T, Rizzuto R, Volpe P, Meldolesi J. Molecular and cellular physiology of intracellular calcium stores. *Physiol Rev*. 1994; **74**: 595-636.
- 32 Sorrentino V, Rizzuto R. Molecular genetics of Ca(2+) stores and intracellular Ca(2+) signalling. *Trends Pharmacol Sci*. 2001; **22**: 459-64.
- 33 Locke EG, Bonilla M, Liang L, Takita Y, Cunningham KW. A homolog of voltage-gated Ca(2+) channels stimulated by depletion of secretory Ca(2+) in yeast. *Mol Cell Biol*. 2000; **20**: 6686-94.
- 34 Partiseti M, Le Deist F, Hivroz C, Fischer A, Korn H, Choquet D. The calcium current activated by T cell receptor and store depletion in human lymphocytes is absent in a primary immunodeficiency. *J Biol Chem*. 1994; **269**: 32327-35.
- 35 Varga-Szabo D, Braun A, Nieswandt B. Calcium signaling in platelets. *J Thromb Haemost*. 2009; **7**: 1057-66.
- 36 Enouf J, Bredoux R, Papp B, Djaffar I, Lompre AM, Kieffer N, Gayet O, Clemetson K, Wuytack F, Rosa JP. Human platelets express the SERCA2-b isoform of Ca(2+)-transport ATPase. *Biochem J*. 1992; **286 (Pt 1)**: 135-40.
- 37 Bobe R, Bredoux R, Wuytack F, Quarck R, Kovacs T, Papp B, Corvazier E, Magnier C, Enouf J. The rat platelet 97-kDa Ca²⁺ATPase isoform is the sarcoendoplasmic reticulum Ca²⁺ATPase 3 protein. *J Biol Chem*. 1994; **269**: 1417-24.

-
- 38 Wuytack F, Papp B, Verboomen H, Raeymaekers L, Dode L, Bobe R, Enouf J, Bokkala S, Authi KS, Casteels R. A sarco/endoplasmic reticulum Ca(2+)-ATPase 3-type Ca²⁺ pump is expressed in platelets, in lymphoid cells, and in mast cells. *J Biol Chem*. 1994; **269**: 1410-6.
- 39 Cavallini L, Coassin M, Alexandre A. Two classes of agonist-sensitive Ca²⁺ stores in platelets, as identified by their differential sensitivity to 2,5-di-(tert-butyl)-1,4-benzohydroquinone and thapsigargin. *Biochem J*. 1995; **310 (Pt 2)**: 449-52.
- 40 Jardin I, Lopez JJ, Pariente JA, Salido GM, Rosado JA. Intracellular calcium release from human platelets: different messengers for multiple stores. *Trends Cardiovasc Med*. 2008; **18**: 57-61.
- 41 Taylor CW, da Fonseca PC, Morris EP. IP(3) receptors: the search for structure. *Trends in biochemical sciences*. 2004; **29**: 210-9.
- 42 Mountian II, Baba-Aissa F, Jonas JC, Humbert De S, Wuytack F, Parys JB. Expression of Ca(2+) Transport Genes in Platelets and Endothelial Cells in Hypertension. *Hypertension*. 2001; **37**: 135-41.
- 43 Braun A, Vogtle T, Varga-Szabo D, Nieswandt B. STIM and Orai in hemostasis and thrombosis. *Front Biosci (Landmark Ed)*. 2011; **16**: 2144-60.
- 44 Putney JW, Jr. A model for receptor-regulated calcium entry. *Cell Calcium*. 1986; **7**: 1-12.
- 45 Cheek TR, Thastrup O. Internal Ca²⁺ mobilization and secretion in bovine adrenal chromaffin cells. *Cell Calcium*. 1989; **10**: 213-21.
- 46 Ely JA, Ambroz C, Baukal AJ, Christensen SB, Balla T, Catt KJ. Relationship between agonist- and thapsigargin-sensitive calcium pools in adrenal glomerulosa cells. Thapsigargin-induced Ca²⁺ mobilization and entry. *J Biol Chem*. 1991; **266**: 18635-41.
- 47 Jackson TR, Patterson SI, Thastrup O, Hanley MR. A novel tumour promoter, thapsigargin, transiently increases cytoplasmic free Ca²⁺ without generation of inositol phosphates in NG115-401L neuronal cells. *Biochem J*. 1988; **253**: 81-6.
- 48 Kaneko Y, Tsukamoto A. Thapsigargin-induced persistent intracellular calcium pool depletion and apoptosis in human hepatoma cells. *Cancer Lett*. 1994; **79**: 147-55.
- 49 Zhang SL, Yu Y, Roos J, Kozak JA, Deerinck TJ, Ellisman MH, Stauderman KA, Cahalan MD. STIM1 is a Ca²⁺ sensor that activates CRAC channels and migrates from the Ca²⁺ store to the plasma membrane. *Nature*. 2005; **437**: 902-5.
- 50 Roos J, DiGregorio PJ, Yeromin AV, Ohlsen K, Lioudyno M, Zhang S, Safrina O, Kozak JA, Wagner SL, Cahalan MD, Velicelebi G, Stauderman KA. STIM1, an essential and

- conserved component of store-operated Ca^{2+} channel function. *J Cell Biol.* 2005; **169**: 435-45.
- 51 Grosse J, Braun A, Varga-Szabo D, Beyersdorf N, Schneider B, Zeitlmann L, Hanke P, Schropp P, Muhlstedt S, Zorn C, Huber M, Schmittwolf C, Jagla W, Yu P, Kerkau T, Schulze H, Nehls M, Nieswandt B. An EF hand mutation in Stim1 causes premature platelet activation and bleeding in mice. *J Clin Invest.* 2007; **117**: 3540-50.
- 52 Varga-Szabo D, Braun A, Kleinschnitz C, Bender M, Pleines I, Pham M, Renne T, Stoll G, Nieswandt B. The calcium sensor STIM1 is an essential mediator of arterial thrombosis and ischemic brain infarction. *J Exp Med.* 2008; **205**: 1583-91.
- 53 Baba Y, Nishida K, Fujii Y, Hirano T, Hikida M, Kurosaki T. Essential function for the calcium sensor STIM1 in mast cell activation and anaphylactic responses. *Nat Immunol.* 2008; **9**: 81-8.
- 54 Feske S, Gwack Y, Prakriya M, Srikanth S, Puppel SH, Tanasa B, Hogan PG, Lewis RS, Daly M, Rao A. A mutation in Orai1 causes immune deficiency by abrogating CRAC channel function. *Nature.* 2006; **441**: 179-85.
- 55 Vig M, Peinelt C, Beck A, Koomoa DL, Rabah D, Koblan-Huberson M, Kraft S, Turner H, Fleig A, Penner R, Kinet JP. CRACM1 is a plasma membrane protein essential for store-operated Ca^{2+} entry. *Science.* 2006; **312**: 1220-3.
- 56 Prakriya M, Feske S, Gwack Y, Srikanth S, Rao A, Hogan PG. Orai1 is an essential pore subunit of the CRAC channel. *Nature.* 2006; **443**: 230-3.
- 57 Yeromin AV, Zhang SL, Jiang W, Yu Y, Safrina O, Cahalan MD. Molecular identification of the CRAC channel by altered ion selectivity in a mutant of Orai. *Nature.* 2006; **443**: 226-9.
- 58 Vig M, Beck A, Billingsley JM, Lis A, Parvez S, Peinelt C, Koomoa DL, Soboloff J, Gill DL, Fleig A, Kinet JP, Penner R. CRACM1 multimers form the ion-selective pore of the CRAC channel. *Curr Biol.* 2006; **16**: 2073-9.
- 59 Zhang SL, Yeromin AV, Zhang XH, Yu Y, Safrina O, Penna A, Roos J, Stauderman KA, Cahalan MD. Genome-wide RNAi screen of Ca^{2+} influx identifies genes that regulate Ca^{2+} release-activated Ca^{2+} channel activity. *Proc Natl Acad Sci U S A.* 2006; **103**: 9357-62.
- 60 Luik RM, Wang B, Prakriya M, Wu MM, Lewis RS. Oligomerization of STIM1 couples ER calcium depletion to CRAC channel activation. *Nature.* 2008; **454**: 538-42.
- 61 Smyth JT, DeHaven WI, Bird GS, Putney JW, Jr. Role of the microtubule cytoskeleton in the function of the store-operated Ca^{2+} channel activator STIM1. *J Cell Sci.* 2007;

- 120**: 3762-71.
- 62 Wu MM, Buchanan J, Luik RM, Lewis RS. Ca²⁺ store depletion causes STIM1 to accumulate in ER regions closely associated with the plasma membrane. *J Cell Biol.* 2006; **174**: 803-13.
- 63 Luik RM, Wu MM, Buchanan J, Lewis RS. The elementary unit of store-operated Ca²⁺ entry: local activation of CRAC channels by STIM1 at ER-plasma membrane junctions. *J Cell Biol.* 2006; **174**: 815-25.
- 64 Park CY, Hoover PJ, Mullins FM, Bachhawat P, Covington ED, Raunser S, Walz T, Garcia KC, Dolmetsch RE, Lewis RS. STIM1 clusters and activates CRAC channels via direct binding of a cytosolic domain to Orai1. *Cell.* 2009; **136**: 876-90.
- 65 Yuan JP, Zeng W, Dorwart MR, Choi YJ, Worley PF, Muallem S. SOAR and the polybasic STIM1 domains gate and regulate Orai channels. *Nat Cell Biol.* 2009; **11**: 337-43.
- 66 Lewis RS. Store-operated calcium channels: new perspectives on mechanism and function. *Cold Spring Harb Perspect Biol.* 2011; **3**.
- 67 Tolhurst G, Carter RN, Amisten S, Holdich JP, Erlinge D, Mahaut-Smith MP. Expression profiling and electrophysiological studies suggest a major role for Orai1 in the store-operated Ca²⁺ influx pathway of platelets and megakaryocytes. *Platelets.* 2008; **19**: 308-13.
- 68 Rosado JA, Brownlow SL, Sage SO. Endogenously expressed Trp1 is involved in store-mediated Ca²⁺ entry by conformational coupling in human platelets. *J Biol Chem.* 2002; **277**: 42157-63.
- 69 Berna-Erro A, Galan C, Dionisio N, Gomez LJ, Salido GM, Rosado JA. Capacitative and non-capacitative signaling complexes in human platelets. *Biochim Biophys Acta.* 2012; **1823**: 1242-51.
- 70 Varga-Szabo D, Authi KS, Braun A, Bender M, Ambily A, Hassock SR, Gudermann T, Dietrich A, Nieswandt B. Store-operated Ca²⁺ entry in platelets occurs independently of transient receptor potential (TRP) C1. *Pflugers Arch.* 2008; **457**: 377-87.
- 71 Elvers M, Stegner D, Hagedorn I, Kleinschnitz C, Braun A, Kuijpers ME, Boesl M, Chen Q, Heemskerk JW, Stoll G, Frohman MA, Nieswandt B. Impaired alpha(IIb)beta(3) integrin activation and shear-dependent thrombus formation in mice lacking phospholipase D1. *Sci Signal.* 2010; **3**: ra1.
- 72 Thielmann I, Stegner D, Kraft P, Hagedorn I, Krohne G, Kleinschnitz C, Stoll G, Nieswandt B. Redundant functions of phospholipases D1 and D2 in platelet alpha-

- granule release. *J Thromb Haemost.* 2012; **10**: 2361-72.
- 73 Merida I, Avila-Flores A, Merino E. Diacylglycerol kinases: at the hub of cell signalling. *Biochem J.* 2008; **409**: 1-18.
- 74 Stefanini L, Roden RC, Bergmeier W. CalDAG-GEFI is at the nexus of calcium-dependent platelet activation. *Blood.* 2009; **114**: 2506-14.
- 75 Hassock SR, Zhu MX, Trost C, Flockerzi V, Authi KS. Expression and role of TRPC proteins in human platelets: evidence that TRPC6 forms the store-independent calcium entry channel. *Blood.* 2002; **100**: 2801-11.
- 76 Carter RN, Tolhurst G, Walmsley G, Vizuete-Forster M, Miller N, Mahaut-Smith MP. Molecular and electrophysiological characterization of transient receptor potential ion channels in the primary murine megakaryocyte. *J Physiol.* 2006; **576**: 151-62.
- 77 Hofmann T, Obukhov AG, Schaefer M, Harteneck C, Gudermann T, Schultz G. Direct activation of human TRPC6 and TRPC3 channels by diacylglycerol. *Nature.* 1999; **397**: 259-63.
- 78 Harper MT, Londono JE, Quick K, Londono JC, Flockerzi V, Philipp SE, Birnbaumer L, Freichel M, Poole AW. Transient receptor potential channels function as a coincidence signal detector mediating phosphatidylserine exposure. *Sci Signal.* 2013; **6**: ra50.
- 79 Sun B, Li J, Okahara K, Kambayashi J. P2X1 purinoceptor in human platelets. Molecular cloning and functional characterization after heterologous expression. *J Biol Chem.* 1998; **273**: 11544-7.
- 80 Wang L, Ostberg O, Wihlborg AK, Brogren H, Jern S, Erlinge D. Quantification of ADP and ATP receptor expression in human platelets. *J Thromb Haemost.* 2003; **1**: 330-6.
- 81 Mahaut-Smith MP, Ennion SJ, Rolf MG, Evans RJ. ADP is not an agonist at P2X(1) receptors: evidence for separate receptors stimulated by ATP and ADP on human platelets. *Br J Pharmacol.* 2000; **131**: 108-14.
- 82 Hechler B, Lenain N, Marchese P, Vial C, Heim V, Freund M, Cazenave JP, Cattaneo M, Ruggeri ZM, Evans R, Gachet C. A role of the fast ATP-gated P2X1 cation channel in thrombosis of small arteries in vivo. *J Exp Med.* 2003; **198**: 661-7.
- 83 Oury C, Toth-Zsomboki E, Thys C, Tytgat J, Vermynen J, Hoylaerts MF. The ATP-gated P2X1 ion channel acts as a positive regulator of platelet responses to collagen. *Thromb Haemost.* 2001; **86**: 1264-71.
- 84 Rolf MG, Brearley CA, Mahaut-Smith MP. Platelet shape change evoked by selective activation of P2X1 purinoceptors with alpha,beta-methylene ATP. *Thromb Haemost.* 2001; **85**: 303-8.

- 85 Erhardt JA, Pillarisetti K, Toomey JR. Potentiation of platelet activation through the stimulation of P2X1 receptors. *J Thromb Haemost.* 2003; **1**: 2626-35.
- 86 Erhardt JA, Toomey JR, Douglas SA, Johns DG. P2X1 stimulation promotes thrombin receptor-mediated platelet aggregation. *J Thromb Haemost.* 2006; **4**: 882-90.
- 87 Oury C, Kuijpers MJ, Toth-Zsamboki E, Bonnefoy A, Danloy S, Vreys I, Feijge MA, De Vos R, Vermeylen J, Heemskerk JW, Hoylaerts MF. Overexpression of the platelet P2X1 ion channel in transgenic mice generates a novel prothrombotic phenotype. *Blood.* 2003; **101**: 3969-76.
- 88 Liao Y, Erxleben C, Yildirim E, Abramowitz J, Armstrong DL, Birnbaumer L. Orai proteins interact with TRPC channels and confer responsiveness to store depletion. *Proc Natl Acad Sci U S A.* 2007; **104**: 4682-7.
- 89 Jardin I, Gomez LJ, Salido GM, Rosado JA. Dynamic interaction of hTRPC6 with the Orai1-STIM1 complex or hTRPC3 mediates its role in capacitative or non-capacitative Ca(2+) entry pathways. *Biochem J.* 2009; **420**: 267-76.
- 90 DeHaven WI, Jones BF, Petranka JG, Smyth JT, Tomita T, Bird GS, Putney JW, Jr. TRPC channels function independently of STIM1 and Orai1. *J Physiol.* 2009; **587**: 2275-98.
- 91 Baumann O, Walz B, Somlyo AV, Somlyo AP. Electron probe microanalysis of calcium release and magnesium uptake by endoplasmic reticulum in bee photoreceptors. *Proc Natl Acad Sci U S A.* 1991; **88**: 741-4.
- 92 Kubota T, Shindo Y, Tokuno K, Komatsu H, Ogawa H, Kudo S, Kitamura Y, Suzuki K, Oka K. Mitochondria are intracellular magnesium stores: investigation by simultaneous fluorescent imagings in PC12 cells. *Biochim Biophys Acta.* 2005; **1744**: 19-28.
- 93 Hughes A, Tonks RS. Platelets, Magnesium, and Myocardial Infarction. *Lancet.* 1965; **1**: 1044-6.
- 94 Shechter M, Merz CN, Rude RK, Paul Labrador MJ, Meisel SR, Shah PK, Kaul S. Low intracellular magnesium levels promote platelet-dependent thrombosis in patients with coronary artery disease. *Am Heart J.* 2000; **140**: 212-8.
- 95 Rasmussen HS, McNair P, Goransson L, Balslov S, Larsen OG, Aurup P. Magnesium deficiency in patients with ischemic heart disease with and without acute myocardial infarction uncovered by an intravenous loading test. *Arch Intern Med.* 1988; **148**: 329-32.
- 96 Nadler JL, Malayan S, Luong H, Shaw S, Natarajan RD, Rude RK. Intracellular free magnesium deficiency plays a key role in increased platelet reactivity in type II diabetes

- mellitus. *Diabetes Care*. 1992; **15**: 835-41.
- 97 Lucas MJ, Leveno KJ, Cunningham FG. A comparison of magnesium sulfate with phenytoin for the prevention of eclampsia. *N Engl J Med*. 1995; **333**: 201-5.
- 98 Walser M. Magnesium metabolism. *Ergeb Physiol*. 1967; **59**: 185-296.
- 99 Geiger H, Wanner C. Magnesium in disease. *Clin Kidney J*. 2012; **5**: 25-38.
- 100 Jahnen-Dechent W, Ketteler M. Magnesium basics. *Clin Kidney J*. 2012; **5**: 3-14.
- 101 Elin RJ. Assessment of magnesium status for diagnosis and therapy. *Magnes Res*. 2010; **23**: S194-8.
- 102 Hughes A, Tonks RS. Magnesium, adenosine diphosphate and blood platelets. *Nature*. 1966; **210**: 106-7.
- 103 Heptinstall S. The use of a chelating ion-exchange resin to evaluate the effects of the extracellular calcium concentration on adenosine diphosphate induced aggregation of human blood platelets. *Thromb Haemost*. 1976; **36**: 208-20.
- 104 Canton R, Manzanares J, Alvarez E, Zaragoza F. In vitro and in vivo antiaggregant effects of magnesium halogenates. *Thromb Haemost*. 1987; **58**: 957-9.
- 105 Briel RC, Lippert TH, Zahradnik HP. [Changes in blood coagulation, thrombocyte function and vascular prostacyclin synthesis caused by magnesium sulfate]. *Geburtshilfe Frauenheilkd*. 1987; **47**: 332-6.
- 106 Hwang DL, Yen CF, Nadler JL. Effect of extracellular magnesium on platelet activation and intracellular calcium mobilization. *Am J Hypertens*. 1992; **5**: 700-6.
- 107 Iseri LT, French JH. Magnesium: nature's physiologic calcium blocker. *Am Heart J*. 1984; **108**: 188-93.
- 108 Hunter DR, Haworth RA, Southard JH. Relationship between configuration, function, and permeability in calcium-treated mitochondria. *J Biol Chem*. 1976; **251**: 5069-77.
- 109 Wolf FI, Di Francesco A, Covacci V, Cittadini A. Regulation of magnesium efflux from rat spleen lymphocytes. *Arch Biochem Biophys*. 1997; **344**: 397-403.
- 110 Gunther T, Vormann J. Na(+)-dependent Mg²⁺ efflux from Mg(2+)-loaded rat thymocytes and HL 60 cells. *Magnes Trace Elem*. 1990; **9**: 279-82.
- 111 Matsuura T, Kanayama Y, Inoue T, Takeda T, Morishima I. cAMP-induced changes of intracellular free Mg²⁺ levels in human erythrocytes. *Biochim Biophys Acta*. 1993; **1220**: 31-6.
- 112 Romani A, Scarpa A. Hormonal control of Mg²⁺ transport in the heart. *Nature*. 1990;

- 346**: 841-4.
- 113 Vormann J, Gunther T. Amiloride-sensitive net Mg²⁺ efflux from isolated perfused rat hearts. *Magnesium*. 1987; **6**: 220-4.
- 114 Romani A, Scarpa A. Norepinephrine evokes a marked Mg²⁺ efflux from liver cells. *FEBS Lett*. 1990; **269**: 37-40.
- 115 Gunther T, Vormann J. Mg²⁺ influx into Mg(2+)-depleted reticulocytes. *Magnesium Trace Elem*. 1991; **10**: 17-20.
- 116 Jakob A, Becker J, Schottli G, Fritzsche G. Alpha 1-adrenergic stimulation causes Mg²⁺ release from perfused rat liver. *FEBS Lett*. 1989; **246**: 127-30.
- 117 Quamme GA. Molecular identification of ancient and modern mammalian magnesium transporters. *Am J Physiol Cell Physiol*. 2010; **298**: 407-29.
- 118 Nadler MJ, Hermosura MC, Inabe K, Perraud AL, Zhu Q, Stokes AJ, Kurosaki T, Kinoshita JP, Penner R, Scharenberg AM, Fleig A. LTRPC7 is a Mg.ATP-regulated divalent cation channel required for cell viability. *Nature*. 2001; **411**: 590-5.
- 119 Schlingmann KP, Weber S, Peters M, Niemann Nejsum L, Vitzthum H, Klingel K, Kratz M, Haddad E, Ristoff E, Dinour D, Syrrou M, Nielsen S, Sassen M, Waldegger S, Seyberth HW, Konrad M. Hypomagnesemia with secondary hypocalcemia is caused by mutations in TRPM6, a new member of the TRPM gene family. *Nat Genet*. 2002; **31**: 166-70.
- 120 Chubanov V, Waldegger S, Mederos y Schnitzler M, Vitzthum H, Sassen MC, Seyberth HW, Konrad M, Gudermann T. Disruption of TRPM6/TRPM7 complex formation by a mutation in the TRPM6 gene causes hypomagnesemia with secondary hypocalcemia. *Proc Natl Acad Sci U S A*. 2004; **101**: 2894-9.
- 121 Schlingmann KP, Waldegger S, Konrad M, Chubanov V, Gudermann T. TRPM6 and TRPM7--Gatekeepers of human magnesium metabolism. *Biochim Biophys Acta*. 2007; **1772**: 813-21.
- 122 Voets T, Nilius B, Hoefs S, van der Kemp AW, Droogmans G, Bindels RJ, Hoenderop JG. TRPM6 forms the Mg²⁺ influx channel involved in intestinal and renal Mg²⁺ absorption. *J Biol Chem*. 2004; **279**: 19-25.
- 123 Walder RY, Landau D, Meyer P, Shalev H, Tsolia M, Borochoy Z, Boettger MB, Beck GE, Englehardt RK, Carmi R, Sheffield VC. Mutation of TRPM6 causes familial hypomagnesemia with secondary hypocalcemia. *Nat Genet*. 2002; **31**: 171-4.
- 124 Walder RY, Yang B, Stokes JB, Kirby PA, Cao X, Shi P, Searby CC, Husted RF, Sheffield VC. Mice defective in *Trpm6* show embryonic mortality and neural tube

- defects. *Hum Mol Genet.* 2009; **18**: 4367-75.
- 125 Woudenberg-Vrenken TE, Sukinta A, van der Kemp AW, Bindels RJ, Hoenderop JG. Transient receptor potential melastatin 6 knockout mice are lethal whereas heterozygous deletion results in mild hypomagnesemia. *Nephron Physiol.* 2011; **117**: 11-9.
- 126 Chubanov V, Mederos y Schnitzler M, Meissner M, Schafer S, Abstiens K, Hofmann T, Gudermann T. Natural and synthetic modulators of SK (K(ca)²) potassium channels inhibit magnesium-dependent activity of the kinase-coupled cation channel TRPM7. *Br J Pharmacol.* 2012; **166**: 1357-76.
- 127 Runnels LW, Yue L, Clapham DE. TRP-PLIK, a bifunctional protein with kinase and ion channel activities. *Science.* 2001; **291**: 1043-7.
- 128 Schmitz C, Perraud AL, Johnson CO, Inabe K, Smith MK, Penner R, Kurosaki T, Fleig A, Scharenberg AM. Regulation of vertebrate cellular Mg²⁺ homeostasis by TRPM7. *Cell.* 2003; **114**: 191-200.
- 129 Jin J, Desai BN, Navarro B, Donovan A, Andrews NC, Clapham DE. Deletion of *Trpm7* disrupts embryonic development and thymopoiesis without altering Mg²⁺ homeostasis. *Science.* 2008; **322**: 756-60.
- 130 Chubanov V, Schlingmann KP, Waring J, Heinzinger J, Kaske S, Waldegger S, Mederos y Schnitzler M, Gudermann T. Hypomagnesemia with secondary hypocalcemia due to a missense mutation in the putative pore-forming region of TRPM6. *J Biol Chem.* 2007; **282**: 7656-67.
- 131 Topala CN, Groenestege WT, Thebault S, van den Berg D, Nilius B, Hoenderop JG, Bindels RJ. Molecular determinants of permeation through the cation channel TRPM6. *Cell Calcium.* 2007; **41**: 513-23.
- 132 van de Graaf SF, Bindels RJ, Hoenderop JG. Physiology of epithelial Ca²⁺ and Mg²⁺ transport. *Rev Physiol Biochem Pharmacol.* 2007; **158**: 77-160.
- 133 Li M, Jiang J, Yue L. Functional characterization of homo- and heteromeric channel kinases TRPM6 and TRPM7. *J Gen Physiol.* 2006; **127**: 525-37.
- 134 Li M, Du J, Jiang J, Ratzan W, Su LT, Runnels LW, Yue L. Molecular determinants of Mg²⁺ and Ca²⁺ permeability and pH sensitivity in TRPM6 and TRPM7. *J Biol Chem.* 2007; **282**: 25817-30.
- 135 Monteilh-Zoller MK, Hermosura MC, Nadler MJ, Scharenberg AM, Penner R, Fleig A. TRPM7 provides an ion channel mechanism for cellular entry of trace metal ions. *J Gen Physiol.* 2003; **121**: 49-60.

-
- 136 Penner R, Fleig A. The Mg²⁺ and Mg(2+)-nucleotide-regulated channel-kinase TRPM7. *Handb Exp Pharmacol*. 2007: 313-28.
- 137 Langeslag M, Clark K, Moolenaar WH, van Leeuwen FN, Jalink K. Activation of TRPM7 channels by phospholipase C-coupled receptor agonists. *J Biol Chem*. 2007; **282**: 232-9.
- 138 Runnels LW, Yue L, Clapham DE. The TRPM7 channel is inactivated by PIP(2) hydrolysis. *Nat Cell Biol*. 2002; **4**: 329-36.
- 139 Gwanyanya A, Sipido KR, Vereecke J, Mubagwa K. ATP and PIP₂ dependence of the magnesium-inhibited, TRPM7-like cation channel in cardiac myocytes. *Am J Physiol Cell Physiol*. 2006; **291**: 627-35.
- 140 Paravicini TM, Chubanov V, Gudermann T. TRPM7: a unique channel involved in magnesium homeostasis. *Int J Biochem Cell Biol*. 2012; **44**: 1381-4.
- 141 Hanano T, Hara Y, Shi J, Morita H, Umebayashi C, Mori E, Sumimoto H, Ito Y, Mori Y, Inoue R. Involvement of TRPM7 in cell growth as a spontaneously activated Ca²⁺ entry pathway in human retinoblastoma cells. *J Pharmacol Sci*. 2004; **95**: 403-19.
- 142 Elizondo MR, Arduini BL, Paulsen J, MacDonald EL, Sabel JL, Henion PD, Cornell RA, Parichy DM. Defective skeletogenesis with kidney stone formation in dwarf zebrafish mutant for *trpm7*. *Curr Biol*. 2005; **15**: 667-71.
- 143 Cai Z, Jitkaew S, Zhao J, Chiang HC, Choksi S, Liu J, Ward Y, Wu LG, Liu ZG. Plasma membrane translocation of trimerized MLKL protein is required for TNF-induced necroptosis. *Nat Cell Biol*. 2014; **16**: 55-65.
- 144 Jin J, Wu LJ, Jun J, Cheng X, Xu H, Andrews NC, Clapham DE. The channel kinase, TRPM7, is required for early embryonic development. *Proc Natl Acad Sci U S A*. 2012; **109**: E225-33.
- 145 Simard JM, Tarasov KV, Gerzanich V. Non-selective cation channels, transient receptor potential channels and ischemic stroke. *Biochim Biophys Acta*. 2007; **1772**: 947-57.
- 146 Jiang H, Tian SL, Zeng Y, Li LL, Shi J. TrkA pathway(s) is involved in regulation of TRPM7 expression in hippocampal neurons subjected to ischemic-reperfusion and oxygen-glucose deprivation. *Brain Res Bull*. 2008; **76**: 124-30.
- 147 Aarts M, Iihara K, Wei WL, Xiong ZG, Arundine M, Cerwinski W, MacDonald JF, Tymianski M. A key role for TRPM7 channels in anoxic neuronal death. *Cell*. 2003; **115**: 863-77.
- 148 Sun HS, Jackson MF, Martin LJ, Jansen K, Teves L, Cui H, Kiyonaka S, Mori Y, Jones M, Forder JP, Golde TE, Orser BA, Macdonald JF, Tymianski M. Suppression of

- hippocampal TRPM7 protein prevents delayed neuronal death in brain ischemia. *Nat Neurosci.* 2009; **12**: 1300-7.
- 149 Aarts MM, Tymianski M. TRPM7 and ischemic CNS injury. *Neuroscientist.* 2005; **11**: 116-23.
- 150 Clark K, Middelbeek J, Morrice NA, Figdor CG, Lasonder E, van Leeuwen FN. Massive autophosphorylation of the Ser/Thr-rich domain controls protein kinase activity of TRPM6 and TRPM7. *PLoS One.* 2008; **3**: e1876.
- 151 Dorovkov MV, Ryazanov AG. Phosphorylation of annexin I by TRPM7 channel-kinase. *J Biol Chem.* 2004; **279**: 50643-6.
- 152 Clark K, Middelbeek J, Lasonder E, Dulyaninova NG, Morrice NA, Ryazanov AG, Bresnick AR, Figdor CG, van Leeuwen FN. TRPM7 regulates myosin IIA filament stability and protein localization by heavy chain phosphorylation. *Journal of molecular biology.* 2008; **378**: 790-803.
- 153 Perraud AL, Zhao X, Ryazanov AG, Schmitz C. The channel-kinase TRPM7 regulates phosphorylation of the translational factor eEF2 via eEF2-k. *Cell Signal.* 2011; **23**: 586-93.
- 154 Deason-Towne F, Perraud AL, Schmitz C. Identification of Ser/Thr phosphorylation sites in the C2-domain of phospholipase C gamma2 (PLCgamma2) using TRPM7-kinase. *Cell Signal.* 2012; **24**: 2070-5.
- 155 Ryazanova LV, Rondon LJ, Zierler S, Hu Z, Galli J, Yamaguchi TP, Mazur A, Fleig A, Ryazanov AG. TRPM7 is essential for Mg(2+) homeostasis in mammals. *Nat Commun.* 2010; **1**: 109.
- 156 Matsushita M, Kozak JA, Shimizu Y, McLachlin DT, Yamaguchi H, Wei FY, Tomizawa K, Matsui H, Chait BT, Cahalan MD, Nairn AC. Channel function is dissociated from the intrinsic kinase activity and autophosphorylation of TRPM7/ChaK1. *J Biol Chem.* 2005; **280**: 20793-803.
- 157 Nieswandt B, Schulte V, Bergmeier W, Mokhtari-Nejad R, Rackebrandt K, Cazenave JP, Ohlmann P, Gachet C, Zirngibl H. Long-term antithrombotic protection by in vivo depletion of platelet glycoprotein VI in mice. *J Exp Med.* 2001; **193**: 459-69.
- 158 Bergmeier W, Schulte V, Brockhoff G, Bier U, Zirngibl H, Nieswandt B. Flow cytometric detection of activated mouse integrin alphaIIb beta3 with a novel monoclonal antibody. *Cytometry.* 2002; **48**: 80-6.
- 159 Nieswandt B, Bergmeier W, Rackebrandt K, Gessner JE, Zirngibl H. Identification of critical antigen-specific mechanisms in the development of immune thrombocytopenic

- purpura in mice. *Blood*. 2000; **96**: 2520-7.
- 160 Dietrich A, Mederos YSM, Gollasch M, Gross V, Storch U, Dubrovskaja G, Obst M, Yildirim E, Salanova B, Kalwa H, Essin K, Pinkenburg O, Luft FC, Gudermann T, Birnbaumer L. Increased vascular smooth muscle contractility in TRPC6^{-/-} mice. *Mol Cell Biol*. 2005; **25**: 6980-9.
- 161 Vig M, DeHaven WI, Bird GS, Billingsley JM, Wang H, Rao PE, Hutchings AB, Jouvin MH, Putney JW, Kinet JP. Defective mast cell effector functions in mice lacking the CRACM1 pore subunit of store-operated calcium release-activated calcium channels. *Nat Immunol*. 2008; **9**: 89-96.
- 162 Dirnagl U. Bench to bedside: the quest for quality in experimental stroke research. *J Cereb Blood Flow Metab*. 2006; **26**: 1465-78.
- 163 Kleinschnitz C, Pozgajova M, Pham M, Bendszus M, Nieswandt B, Stoll G. Targeting platelets in acute experimental stroke: impact of glycoprotein Ib, VI, and IIb/IIIa blockade on infarct size, functional outcome, and intracranial bleeding. *Circulation*. 2007; **115**: 2323-30.
- 164 Bederson JB, Pitts LH, Germano SM, Nishimura MC, Davis RL, Bartkowski HM. Evaluation of 2,3,5-triphenyltetrazolium chloride as a stain for detection and quantification of experimental cerebral infarction in rats. *Stroke*. 1986; **17**: 1304-8.
- 165 Moran PM, Higgins LS, Cordell B, Moser PC. Age-related learning deficits in transgenic mice expressing the 751-amino acid isoform of human beta-amyloid precursor protein. *Proc Natl Acad Sci U S A*. 1995; **92**: 5341-5.
- 166 Kleinschnitz C, Kraft P, Dreykluft A, Hagedorn I, Gobel K, Schuhmann MK, Langhauser F, Helluy X, Schwarz T, Bittner S, Mayer CT, Brede M, Varallyay C, Pham M, Bendszus M, Jakob P, Magnus T, Meuth SG, Iwakura Y, Zerneck A, Sparwasser T, Nieswandt B, Stoll G, Wiendl H. Regulatory T cells are strong promoters of acute ischemic stroke in mice by inducing dysfunction of the cerebral microvasculature. *Blood*. 2013; **121**: 679-91.
- 167 Morowski M, Vogtle T, Kraft P, Kleinschnitz C, Stoll G, Nieswandt B. Only severe thrombocytopenia results in bleeding and defective thrombus formation in mice. *Blood*. 2013; **121**: 4938-47.
- 168 Jardin I, Redondo PC, Salido GM, Rosado JA. Phosphatidylinositol 4,5-bisphosphate enhances store-operated calcium entry through hTRPC6 channel in human platelets. *Biochim Biophys Acta*. 2008; **1783**: 84-97.
- 169 Chen W, Thielmann I, Gupta S, Subramanian H, Stegner D, van Kruchten R, Dietrich A,

- Gambaryan S, Heemskerk JW, Hermanns HM, Nieswandt B, Braun A. Orai1-induced store-operated Ca²⁺ entry enhances phospholipase activity and modulates canonical transient receptor potential channel 6 function in murine platelets. *J Thromb Haemost.* 2014; **12**: 528-39.
- 170 Mogami H, Lloyd Mills C, Gallacher DV. Phospholipase C inhibitor, U73122, releases intracellular Ca²⁺, potentiates Ins(1,4,5)P₃-mediated Ca²⁺ release and directly activates ion channels in mouse pancreatic acinar cells. *Biochem J.* 1997; **324 (Pt 2)**: 645-51.
- 171 Stegner D, Thielmann I, Kraft P, Frohman MA, Stoll G, Nieswandt B. Pharmacological inhibition of phospholipase D protects mice from occlusive thrombus formation and ischemic stroke--brief report. *Arterioscler Thromb Vasc Biol.* 2013; **33**: 2212-7.
- 172 Malcolm KC, Fitzpatrick FA. Indirect actions of thapsigargin on human platelets: activation of eicosanoid biosynthesis and cellular signaling pathways. *J Pharmacol Exp Ther.* 1992; **260**: 1244-9.
- 173 Bender M, Hagedorn I, Nieswandt B. Genetic and antibody-induced glycoprotein VI deficiency equally protects mice from mechanically and FeCl₃ -induced thrombosis. *J Thromb Haemost.* 2011; **9**: 1423-6.
- 174 Zwaal RF, Schroit AJ. Pathophysiologic implications of membrane phospholipid asymmetry in blood cells. *Blood.* 1997; **89**: 1121-32.
- 175 Heemskerk JW, Kuijpers MJ, Munnix IC, Siljander PR. Platelet collagen receptors and coagulation. A characteristic platelet response as possible target for antithrombotic treatment. *Trends Cardiovasc Med.* 2005; **15**: 86-92.
- 176 Heemskerk JW, Mattheij NJ, Cosemans JM. Platelet-based coagulation: different populations, different functions. *J Thromb Haemost.* 2013; **11**: 2-16.
- 177 Clark K, Middelbeek J, Dorovkov MV, Figdor CG, Ryazanov AG, Lasonder E, van Leeuwen FN. The alpha-kinases TRPM6 and TRPM7, but not eEF-2 kinase, phosphorylate the assembly domain of myosin IIA, IIB and IIC. *FEBS Lett.* 2008; **582**: 2993-7.
- 178 Romani A. Regulation of magnesium homeostasis and transport in mammalian cells. *Arch Biochem Biophys.* 2007; **458**: 90-102.
- 179 Romani AM. Cellular magnesium homeostasis. *Arch Biochem Biophys.* 2011; **512**: 1-23.
- 180 Watson SP, Herbert JM, Pollitt AY. GPVI and CLEC-2 in hemostasis and vascular integrity. *J Thromb Haemost.* 2010; **8**: 1456-67.
- 181 Balagopalan L, Coussens NP, Sherman E, Samelson LE, Sommers CL. The LAT story:

- a tale of cooperativity, coordination, and choreography. *Cold Spring Harb Perspect Biol.* 2010; **2**: a005512.
- 182 Zhang J, Billingsley ML, Kincaid RL, Siraganian RP. Phosphorylation of Syk activation loop tyrosines is essential for Syk function. An in vivo study using a specific anti-Syk activation loop phosphotyrosine antibody. *J Biol Chem.* 2000; **275**: 35442-7.
- 183 Finney BA, Schweighoffer E, Navarro-Nunez L, Benezech C, Barone F, Hughes CE, Langan SA, Lowe KL, Pollitt AY, Mourao-Sa D, Sheardown S, Nash GB, Smithers N, Reis e Sousa C, Tybulewicz VL, Watson SP. CLEC-2 and Syk in the megakaryocytic/platelet lineage are essential for development. *Blood.* 2012; **119**: 1747-56.
- 184 Judd BA, Myung PS, Oberfell A, Myers EE, Cheng AM, Watson SP, Pear WS, Allman D, Shattil SJ, Koretzky GA. Differential requirement for LAT and SLP-76 in GPVI versus T cell receptor signaling. *J Exp Med.* 2002; **195**: 705-17.
- 185 Lopez AD, Mathers CD, Ezzati M, Jamison DT, Murray CJ. Global and regional burden of disease and risk factors, 2001: systematic analysis of population health data. *Lancet.* 2006; **367**: 1747-57.
- 186 Stoll G, Kleinschnitz C, Nieswandt B. Molecular mechanisms of thrombus formation in ischemic stroke: novel insights and targets for treatment. *Blood.* 2008; **112**: 3555-62.
- 187 Authi KS. TRP channels in platelet function. *Handb Exp Pharmacol.* 2007: 425-43.
- 188 Redondo PC, Jardin I, Lopez JJ, Salido GM, Rosado JA. Intracellular Ca²⁺ store depletion induces the formation of macromolecular complexes involving hTRPC1, hTRPC6, the type II IP₃ receptor and SERCA3 in human platelets. *Biochim Biophys Acta.* 2008; **1783**: 1163-76.
- 189 Harper MT, Poole AW. Protein kinase C θ negatively regulates store-independent Ca²⁺ entry and phosphatidylserine exposure downstream of glycoprotein VI in platelets. *J Biol Chem.* 2010; **285**: 19865-73.
- 190 McDermott M, Wakelam MJ, Morris AJ. Phospholipase D. *Biochemistry and cell biology = Biochimie et biologie cellulaire.* 2004; **82**: 225-53.
- 191 Holmsen H, Hindenes JO, Fukami M. Glycerophospholipid metabolism: back to the future. *Thrombosis research.* 1992; **67**: 313-23.
- 192 Vorland M, Thorsen VA, Holmsen H. Phospholipase D in platelets and other cells. *Platelets.* 2008; **19**: 582-94.
- 193 Heemskerk JW, Farndale RW, Sage SO. Effects of U73122 and U73343 on human platelet calcium signalling and protein tyrosine phosphorylation. *Biochim Biophys Acta.*

- 1997; **1355**: 81-8.
- 194 Tolios A, Gatidis S, Munzer P, Liu G, Towhid ST, Karathanos A, Tavlaki E, Geisler T, Seizer P, May AE, Bigalke B, Borst O, Gawaz M, Lang F. Increased platelet Ca²⁺ channel Orai1 expression upon platelet activation and in patients with acute myocardial infarction. *Thromb Haemost.* 2013; **110**: 386-9.
- 195 Zbidi H, Lopez JJ, Amor NB, Bartegi A, Salido GM, Rosado JA. Enhanced expression of STIM1/Orai1 and TRPC3 in platelets from patients with type 2 diabetes mellitus. *Blood Cells Mol Dis.* 2009; **43**: 211-3.
- 196 Alonso MT, Manjarres IM, Garcia-Sancho J. Privileged coupling between Ca(2+) entry through plasma membrane store-operated Ca(2+) channels and the endoplasmic reticulum Ca(2+) pump. *Molecular and cellular endocrinology.* 2012; **353**: 37-44.
- 197 Manjarres IM, Alonso MT, Garcia-Sancho J. Calcium entry-calcium refilling (CECR) coupling between store-operated Ca(2+) entry and sarco/endoplasmic reticulum Ca(2+)-ATPase. *Cell Calcium.* 2011; **49**: 153-61.
- 198 Jardin I, Lopez JJ, Salido GM, Rosado JA. Orai1 mediates the interaction between STIM1 and hTRPC1 and regulates the mode of activation of hTRPC1-forming Ca²⁺ channels. *J Biol Chem.* 2008; **283**: 25296-304.
- 199 Mahaut-Smith MP, Jones S, Evans RJ. The P2X1 receptor and platelet function. *Purinergic Signal.* 2011; **7**: 341-56.
- 200 Bae CY, Sun HS. TRPM7 in cerebral ischemia and potential target for drug development in stroke. *Acta Pharmacol Sin.* 2011; **32**: 725-33.

6 APPENDIX

6.1 Abbreviation

α	alpha
β	beta
δ	delta
γ	gamma
μ	micro
AA	Amino acid
AC	Adenylyl cyclase
ACD	Acid-citrate-dextrose
ADP	Adenosine diphosphate
APS	Ammonium peroxodisulfate
ATP	Adenosine triphosphate
BM	Bone marrow
BSA	Bovine serum albumin
Ca^{2+}	Calcium
$^{\circ}\text{C}$	Degree Celsius
$[\text{Ca}^{2+}]_i$	Intracellular Ca^{2+} concentration
cAMP	Cyclic adenosine monophosphate
CCE	Capacitive calcium entry
CERC	Calcium entry-calcium refilling coupling
CLEC-2	C-type lectin-like receptor 2
CRAC	Calcium release activated calcium
CRP	Collagen-related peptide
CVX	Convulxin
DAG	Diacylglycerol
DIC	Differential interference contrast
DTS	Dense tubular system
ECM	Extracellular matrix
ELISA	Enzyme-linked immunosorbent assay
ER	Endoplasmic reticulum
ES	Embryonic stem
et al.	et alteri
FACS	Fluorescence-activated cell sorting
FcR	Fc receptor
FeCl_3	Ferric(III)chloride
FITC	Fluorescein isothiocyanate
FIPI	5-fluoro-2-indolyl des-chlorohalopemide
FSC	Forward scatter
g	Gram
GP	Glycoprotein

GPCR	G protein-coupled receptors
h	Hour(s); human
H ₂ O	Water
HEPES	4-(2-hydroxyethyl)-1-piperazineethanesulfonic acid
HSH	Hypomagnesaemia with secondary hypocalcemia
Ig	Immunoglobulin
IFI	Integrated fluorescence intensity
IP ₃	Inositol-1,4,5-trisphosphate
IP ₃ R	IP ₃ receptor
ITAM	Immunoreceptor tyrosine-based activation motif
L	Liter
LAT	Linker of activated T cells
M	Molar
MFI	Mean fluorescence intensity
min	Minute(s)
MRI	Magnetic resonance imaging
mL	Milliliter
mm ²	Square millimeter
NaCl	Sodium chloride
NCX	Na ⁺ /Ca ²⁺ exchanger
OAG	1-oleoyl-2-acetyl-sn-glycerol
OGD	Oxygen and glucose deprivation
PA	Phosphatidic acid
PAR	Protease-activated receptor
PC	Phosphatidylcholine
PCR	Polymerase chain reaction
PE	Phycoerythrin
PGI ₂	Prostacyclin
PH	Pleckstrin homology
PI3K	Phosphatidylinositol 3-kinase
PIP ₂	Phosphatidylinositol-4,5-bisphosphate
PIP ₃	Phosphatidylinositol-3,4,5-triphosphate
PKC	Protein kinase C
PL	Phospholipase
PM	Plasma membrane
PMCA	Plasma membrane Ca ²⁺ ATPase
PRP	Platelet rich plasma
PS	Phosphatidylserine
Rho	Ras homolog gene family
Rho-GEF	Rho-specific guanine nucleotide exchange factor
ROC	Receptor-operated calcium
ROCE	Receptor-operated calcium entry
RT	Room temperature; in case of RT-PCR, RT indicates reverse transcription

s	Second(s)
SCID	Severe combined immune deficiency
SD	Standard deviation
SDS	Sodium dodecyl sulfate
Ser/Thr	Serine/Threonine
SERCA	Sarcoplasmic/endoplasmic reticulum Ca ²⁺ ATPase
SFK	Src- family kinase
SLP-76	SH2 domain containing leukocyte protein of 76 kDa
SOC	Store-operated calcium
SOCE	Store-operated calcium entry
SOM	Store-operated macromolecular
SR	Sarcoplasmic reticulum
STIM	Stromal interaction molecule
Syk	Spleen tyrosine kinase
TAE	TRIS acetate EDTA buffer
TBS	TRIS-buffered saline
TE	TRIS EDTA buffer
TF	Tissue factor
TG	Thapsigargin
tMCAO	Transient middle cerebral artery occlusion
TMB	3,3',5,5'-tetramethylbenzidine
TP	Thromboxane A ₂ receptor
TRIS	Tris(hydroxymethyl)aminomethane
TRP	Transient receptor potential
TRPC	Canonical transient receptor potential channel
TRPM	Transient receptor potential melastatin-like
TTC	2,3,5-triphenyltetrazolium chloride
TxA ₂	Thromboxane A ₂
TxB ₂	Thromboxane B ₂
U	Units
U73122	1-[6-(((17β)-3-Methoxyestra-1,3,5[10]-trien-17-yl)amino)hexyl]-1H-pyrrole-2,5-dione
vWF	von Willebrand factor

6.2 Curriculum vitae

Name	Wenchun Chen
Date of birth	May 30th, 1984
Place of birth	Fujian, China
Nationality	China

Education

2010 - now	PhD student in the group of Prof. Dr. Bernhard Nieswandt, Chair of Experimental Biomedicine, University Hospital and Rudolf Virchow Center for Experimental Biomedicine, Julius-Maximilians-Universität Würzburg
2007 - 2010	Master of Molecular Neurobiology Key Laboratory of Brain Functional Genomics, Ministry of Education East China Normal University, Shanghai, China
2003 - 2007	Bachelor of Biotechnology at Heilongjiang University, China
1991 - 2003	Primary, Secondary and High School in Zhangzhou, Fujian, China

Würzburg, July 2014

6.3 Publications

6.3.1 Original articles

1. **Chen W**, Thielmann I, Gupta S, Subramanian H, Stegner D, Kruchten R. van, Dietrich A, Gambaryan S, Heemskerk J, Hermanns H, Nieswandt B, Braun A. Orai1-induced store-operated calcium entry enhances phospholipase activity and modulates TRPC6 function in murine platelets. *J Thromb Haemost.* 2014; 12: 528-539.

2. Braun A, **Chen W**, Kraft P, Chubanov V, Morowski M, Stritt S, Zierler S, Gotru SK, Gupta S, Hermanns H, Stoll G, Schmitz C, Gudermann T, Nieswandt B. TRPM7 kinase controls calcium responses in arterial thrombosis and stroke. (in preparation)

6.3.2 Posters

58th Annual Meeting of the Society of Thrombosis and Haemostasis Research, February 2014, Vienna, Austria. **“Phospholipase-mediated crosstalk between Orai1 and TRPC6 in murine platelets”**

SCI, 8th International Symposium, the Graduate School of Life Science, University of Würzburg, Würzburg, Germany, October 2013. **“Orai1-induced store-operated calcium entry enhances phospholipase activity and modulates TRPC6 function in murine platelets”**

XXIVth Congress of the International Society on Thrombosis and Hemostasis, Amsterdam, The Netherlands, July 2013. **“Redundant functions of TRPC6 and Orai1 in murine platelets”**

EPOS, 7th International Symposium, the Graduate School of Life Science, University of Würzburg, Würzburg, Germany, October 2012. **“Dual role of TRPM7 in magnesium and calcium homeostasis in platelets”**

Bio Bang, 6th International Symposium, the Graduate School of Life Science, University of Würzburg, Würzburg, Germany, October 2011. **“Analysis of platelet function in mice lacking N-BAR domain proteins Bin1 and Bin3”**

6.4 Acknowledgement

The work presented here was performed at the Chair of Experimental Biomedicine, Rudolf Virchow Center for Experimental Biomedicine, University of Würzburg, in the group of Prof. Dr. Bernhard Nieswandt.

During the period of my PhD work (November 2010 - June 2014), many people helped and supported me. Therefore I would like to thank the following people:

- My primary supervisor, Prof. Dr. Bernhard Nieswandt for allowing me to perform my PhD work in his laboratory, for his great ideas, useful advice and support. I would like to thank him as well for allowing me to present my work at various international conferences.
- My supervisory committee, Prof. Dr. Manfred Gessler and Prof. Dr. Guido Stoll for kind support and scientific advice, and for reviewing my thesis.
- Prof. Dr. Stephan Kissler for giving me valuable suggestions and sharing his lentiviral vectors.
- Dr. Attila Braun for his great idea, close team work and support throughout my work and his carefully reading my thesis.
- Prof. Dr. Thomas Gudermann and Dr. Vladimir Chubanov for providing *Trpm7^{KI}* mice and measuring TRPM7 channel activity.
- Prof. Dr. Alexander Dietrich for providing *Trpc6^{-/-}* mice.
- Prof. Dr. Guido Stoll, Dr. Peter Kraft and their team for performing the stroke experiments.
- Martina Morowski and Ina Thielmann for performing in vivo experiments and Ina Thielmann also for the PLD assay in Orai1 and TRPC6 double knock-out project.
- Prof. Dr. Johan Heemskerk and Dr. David Stegner for the support in Orai1 and TRPC6 double knock-out project
- Dr. Heike Hermanns, Dr. Shuchi Gupta, Simon Stritt, Deya Cherpokova and Sanjeev K. Gotru for their effort and support in TRPM7 "kinase-dead" project.
- All of the technical assistants and animal caretakers for providing an excellent working basis.
- All proofreaders, especially Dr. Timo Vögtle.

- All of the members of AG Nieswandt for their kind help, the useful discussions and for the good atmosphere in the group.
- Finally, I would like to thank my family and my friends for their understanding, encourage and endless support.

6.5 Affidavit

I hereby confirm that my thesis entitled “Studies on the role of calcium channels and the kinase domain of *transient receptor potential melastatin-like 7* (TRPM7) in platelet function” is the results of my own work. I did not receive any help or support from commercial consultants. All sources and/or materials applied are listed and specified in the thesis.

Furthermore, I confirm that this thesis has not been submitted as part of another examination process neither in identical nor in similar form.

Würzburg, July 2014 _____

Eidesstattliche Erklärung

Hiermit erkläre ich an Eides statt, die Dissertation „Studien über die Rolle von Calcium Kanälen und der Kinase Dömane von *transient receptor potential melastatin-like 7* (TRPM7) für die Thrombozytenfunktion“ eigenständig, d.h. insbesondere selbständig und ohne Hilfe eines kommerziellen Promotionsberaters, angefertigt und keine anderen als die von mir angegebenen Quellen und Hilfsmittel verwendet zu haben.

Ich erkläre außerdem, dass die Dissertation weder in gleicher noch in ähnlicher Form bereits in einem anderen Prüfungsverfahren vorgelegen hat.

Würzburg, Juli 2014 _____